Macromolecular modification of the cell wall of Gram-negative bacteria leading to antibiotic resistance and formation of outer membrane vesicles

Inaugural Dissertation
submitted to the
Faculty of Medicine
in partial fulfillment of the requirements
for the PhD-Degree
of the Faculties of Veterinary Medicine and Medicine
of the Justus Liebig University Giessen

by
Gwozdzinski, Konrad
of
Lodz, Poland

Giessen 2017

From the Institute of Medical Microbiology
Director: Prof. Dr. Trinad Chakraborty
of the Faculty of Medicine of the Justus Liebig University Giessen

First Supervisor and Committee Member:	Prof. Trinad Chakraborty
Second Supervisor and Committee Member:	Prof. Albrecht Bindereif
Committee Members:	Prof. Martin Diener
	Prof. Magdalena Huber

Date of Doctoral Defense: 16.04.2018

Table of Contents

Page

Abstract

Membrane remodeling occurring in Gram-negative bacteria is a fundamental process involved in many aspects of bacterial physiology. Bacteria have evolved a variety of membrane modifications, e.g., outer membrane vesicles (OMVs), nanotubular membrane structures, lipopolysaccharide alteration, allowing them to better cope with a constantly changing, often hostile, environment. The overall goal of this dissertation was to investigate the influence of the macromolecular modification of the cell wall of Gram-negative bacteria on the development of antibiotic resistance and formation of outer membrane vesicles. One section of this work examines the phenomenon of the bacterial OMVs with respect to the mechanism underlying their formation and their contribution to antibiotic resistance. This research showed that all of the investigated opportunistic pathogens including *Acinetobacter baumannii*, *Citrobacter freundii*, *Enterobacter* sp., *Escherichia coli* and *Serratia marcescens* were able to continuously release vesicles into the surrounding milieu during *in vitro* growth. I validated that OMVs constitute an ubiquitous secretion system that may play a pivotal role in the transmission of enzymatically active compounds (e.g., active β-lactamases), antibiotic resistance genes (e.g., KPC-2), and overall bacterial survival. However, the general mechanism underlying OMV formation still needs to be understood. Here, I demonstrated that the hemolysin F gene (*hlyF*), a putative virulence factor associated with highly virulent strains of avian pathogenic *E. coli* and neonatal meningitis *E. coli*, is involved in OMV formation. Overexpression of *hlyF* increased OMV production in *E. coli* and the presence of the truncated version of this gene led to a hypovesiculation phenotype. Therefore, *hlyF* appears to be part of a natural biological switch, regulating the vesiculation process in Gram-negative bacteria. Furthermore, I demonstrated that some clinical isolates of *C. freundii* may release OMVs acting as vehicles for transferring antibiotic resistance genes over longer distances. Field emission scanning electron microscopy (FE-SEM) and transmission electron microscopy (TEM) visualized the shedding of DNA-containing OMVs. Exposure to OMVs derived from the carbapenemase gene KPC-2-containing donor cells resulted in gene transfer to *E. coli*. The second section of this work, focused on the modification of lipopolysaccharide (LPS), mediated by the plasmid-borne *mcr-1* gene, leading to colistin resistance in *Enterobacteriaceae*. I established a methodology for purification of a full-length MCR-1 and showed an *in vitro* activity of this enzyme for catalyzing phosphoethanolamine (pEtN) hydrolysis from a lipid substrate. Lastly, I discovered that an optimized level of Ca^{2+} is required for the functionality of the *mcr-1*-mediated resistance. With this, I was able to develop a novel calcium-enhanced medium for the improved

determination of Colistin resistance and the detection of *mcr-1*-producing *Enterobacteriaceae*. The medium devised here has been patented and a related patent application examining conditions associated with MCR-1 activity is ongoing.

Zusammenfassung

Modifikationen der Struktur der Membranen Gram-negativer Bakterien sind ein fundamentaler Prozess, der in vielen Aspekten der Bakterienphysiologie relevant ist. Bakterien haben eine Vielzahl von Membranmodifikationen entwickelt, wie z. B. äußere Membranvesikel (OMV), nanotubuläre Membranstrukturen und Lipopolysaccharid-Veränderung, die ihnen erlauben, mit einer ständig wechselnden und oft feindlichen Umwelt zurecht zu kommen. Das Ziel dieser Dissertation war es, den Einfluss der makromolekularen Zellwandmodifikation auf die Entwicklung der Antibiotikaresistenzen und die Bildung von äußeren Membranvesikeln von Gram-negativen Bakterien zu untersuchen. Ein Teil dieser Arbeit untersucht das Phänomen der bakteriellen OMV im Hinblick auf den Mechanismus, der ihrer Entstehung zugrunde liegt, und ihren Beitrag zur Antibiotikaresistenz. Diese Untersuchungen zeigten, dass alle getesteten opportunistischen Krankheitserreger, einschließlich *Acinetobacter baumannii*, *Citrobacter freundii*, *Enterobacter* sp., *Escherichia coli* und *Serratia marcescens* während des Wachstums *in vitro* kontinuierlich Vesikel in das umgebende Milieu freisetzen konnten. Ich konnte zeigen, dass OMV ein allgegenwärtiges Sekretionssystem darstellen, welches eine Schlüsselrolle bei der Übertragung von enzymatisch aktiven Verbindungen (z. B. aktiven β-Lactamasen), Antibiotikaresistenzgenen (z. B. KPC-2) und dem gesamten bakteriellen Überleben spielen kann. Der allgemeine Mechanismus der OMV-Bildung muss jedoch noch verstanden werden. Hier konnte ich zeigen, dass das Hämolysin F Gen (*hlyF*), ein mutmaßlicher Virulenzfaktor, der mit hochvirulenten Stämmen von aviären *E. coli* und neonatalen Meningitis *E. coli* assoziiert ist, an der OMV-Bildung beteiligt ist. Die Überexpression von *hlyF* erhöhte die OMV-Produktion in *E. coli* und die Anwesenheit der verkürzten Version dieses Gens führte zu einem Hypovesikulations-Phänotyp. Daher scheint *hlyF* Teil eines natürlichen biologischen Regulators zu sein, der den Vesikulationsprozess bei Gram-negativen Bakterien steuert. Darüber hinaus habe ich gezeigt, dass einige klinische Isolate von *C. freundii* OMV als Vehikel für die Übertragung von Antibiotikaresistenzgenen über längere Distanzen fungieren können. Die Feldemissions-Rasterelektronenmikroskopie (FE-REM) und die Transmissions-elektronenmikroskopie (TEM) visualisierten die Freisetzung von DNA-haltigen OMV. Die Exposition gegenüber OMV, die aus den Carbapenemase Gen KPC-2-enthaltenden Spenderzellen stammen, führte zu einem Gentransfer in *E. coli*. Der zweite Teil dieser Arbeit konzentrierte sich auf die Modifikation des Lipopolysaccharids (LPS), verursacht durch das Plasmid-getragene *mcr-1*-Gen, was zu einer Colistinresistenz in *Enterobacteriaceae* führte. Ich etablierte eine Methode zur Aufreinigung eines vollständigen MCR-1 Proteins und zeigte eine

in vitro Aktivität dieses Enzyms als Katalysator der Phosphoethanolamin (pEtN)-Hydrolyse eines Lipidsubstrats. Schließlich entdeckte ich, dass für die Funktionalität des *mcr-1*-vermittelten Widerstands ein optimiertes Niveau von Ca^{2+} erforderlich ist. Damit konnte ich ein neuartiges Calcium-supplementiertes Medium zur verbesserten Bestimmung der Colistin-Resistenz und der Identifizierung von *mcr-1*-produzierenden *Enterobacteriaceae* entwickeln. Das hier entwickelte Medium wurde patentiert, eine ähnliche Patentanmeldung ist geplant, die die hiermit verbundenen Zusammenhänge der MCR-1-Aktivität untersucht.

Patents & Publications

Parts of this work have been published in the following patents literature and manuscripts:

- Chakraborty T., **Gwozdzinski K**., Falgenhauer F., Imirzalioglu C. (2017). Erfindung betreffend Detektion und Quantifizierung von Colistin-Resistenz bei Gram-negativen Bakterien. European reference No. EP17173895. Germany. Submitted to the European Patent Office

- Chakraborty T., **Gwozdzinski K**., Falgenhauer F., Imirzalioglu C. (2017). A novel EGTA-based method to differentiate between mobile colistin resistance (MCR) and intrinsic/adaptive colistin resistance. Germany. Submitted to the German Patent Office

- **Gwozdzinski K**., Azarderakhsh S., Imirzalioglu C., Falgenhauer L., Chakraborty T. (2018). An improved medium for colistin susceptibility testing. J Clin Microbiol., Accepted

Abbreviations

List of abbreviations

Amp	Ampicillin
BMD	Broth microdilution
bp	Base pair
BSA	Bovine serum albumin
$CaCl_2$	Calcium chloride
Cam	Chloramphenicol
cAMPs	Cationic antimicrobial peptides
CE-MHB	Cation-enhanced mueller hinton broth
CLSI	Clinical and Laboratory Standards Institute
Da	Dalton
ddH_2O	Distilled deionized water
DNA	Deoxyribonucleic acid
DNAse	Deoxyribonuclease
DTT	Dithiothreitol
EDTA	Ethylenediaminetetraacetic acid
EPS	Extracellular polymeric substances
ER	Endoplasmic reticulum
EUCAST	European Committee on Antimicrobial Susceptibility Testing
FA	Formaldehyde
FBS	Fetal bovine serum
FE-SEM	Field-emission scanning electron microscopy
GA	Glutaraldehyde
GES	Guanidinium thiocyanate solution
GFP	Green fluorecent protein
HeLa cells	Human cervical cancer cells
HEPES	4-(2-hydroxyethyl)-1-piperazineethanesulfonic acid
HGT	Horizontal gene transfer
hlyF	Hemolysin F
HPLC	High pressure liquid chromatography
IM	Inner membrane
IPTG	Isopropyl -D-1-thiogalactopyranoside
Km	Kanamycin
KPC-2	*Klebsiella pneumoniae* carbapenemase 2
LB	Luria broth
LPS	Lipopolysaccharide
MALDI-TOF-MS	Matrix-assisted laser desorption/ionization time-of-flight mass spectrometry

mcr-1	mobilized colistin resistance gene 1
MEM	Minimum essential media
MIC	Minimum inhibitory concentration
MHB	Mueller hinton broth
mRNA	Messenger ribonucleic acid
MS	Mass spectrometry
MSC	Multiple cloning site
MVs	Membrane vesicles
MW	Molecular weight
NMR	Nuclear magnetic resonance
NP	Nucleoprotein
NSAF	Normalized spectral abundance factor
OD	Optical density
OM	Outer membrane
OMP	Outer membrane protein
OMV	Outer membrane vesicle
PBP	Penicillin-binding protein
PBS	Phosphate buffered saline
PCR	Polymerase chain reaction
PDB	Protein data bank
pEtN	Phosphoethanolamine
PG	Peptidoglycan
PL	Phospholipid
Pm	Polymyxin
PQS	Pseudomonas quinolone signal
PVDF membrane	Polyvinylidene fluoride membrane
RNA	Ribonucleic acid
RT	Room temperature
S1-PFGE	S1 nuclease digestion followed by Pulsed-field Gel Electrophoresis
SDS-PAGE	Sodium dodecyl sulfate polyacrylamide gel electrophoresis
SEM	Scanning electron microscope
TBE buffer	Tris-borate-EDTA buffer
TC	Transconjugant
TCS	Two-component system
TEM	Transmission electron microscope
TM	Transmembrane
Tris	Tris(hydroxymethyl)aminomethane
WCL	Whole cell lysate
WT	Wild type

1 Introduction

1.1 Gram-negative pathogens studied in the thesis

Gram-negative bacteria are characterized by their cell envelopes, which are composed of inner and outer membranes that are separated by the periplasm containing peptidoglycan (Needham & Trent 2013). They are prevalent globally, in almost all environments that support life. The Proteobacteria are a major group of Gram-negative bacteria, comprising a wide variety of pathogens, such as *Acinetobacter*, *Escherichia*, *Salmonella*, *Neisseria*, *Vibrio*, *Helicobacter*, *Yersinia* and many other noteworthy genera. Bacteria that are not pathogenic, but are present within the host e.g. as colonizers, are known as commensal bacteria. In healthy individuals, commensal Gram-negative bacteria are involved in maintaining fitness and wellness, as they regulate colonization and eradication of pathogens as well as acquisition of nutrients (Kamada et al. 2013). In this PhD thesis, various clinical isolates of pathogens have been studied. Each of the investigated bacterial species, is shortly described below in this chapter. All bacteria used in the thesis are listed in Table 3.7.

Acinetobacter baumannii (*A. baumannii*) is an emerging and often multidrug-resistant, opportunistic, nosocomial pathogen that causes infections in immunocompromised and chronically ill individuals. *A. baumannii* is considered as causing a variety of severe nosocomial infections, including bacteremia, meningitis, wound infections, urinary tract infections, skin and soft tissue infections and ventilator-associated pneumonia, which represents the most important disease caused by this bacterium (Dijkshoorn et al. 2007). In recent years, increasing numbers of *A. baumannii* outbreaks have been reported by hospitals and long-term care facilities all over the Europe (Jones et al. 2015). Even though the increasing global importance of *A. baumannii* as a nosocomial pathogen, still little is known about the virulence factors responsible for its pathogenesis. *A. baumannii* exhibits several pathogenic traits, including biofilm formation, serum resistance, iron acquisition, adherence to and invasion of host cells and formation of outer membrane vesicles (OMVs) (Nho et al. 2015). However, specific virulence factors of this bacterium have not been fully determined.

Citrobacter freundii (*C. freundii*) is a clinically relevant opportunistic pathogen, member of family *Enterobacteriaceae* that has been associated with several nosocomial infections in immunocompromised patients. *C. freundii* related illnesses include respiratory tract infections, urinary tract infections, bloodstream infections and neonatal meningitis (Pepperell et al. 2002).

In recent years, *C. freundii* have demonstrated reduced susceptibility not only to traditional antibiotics such as ampicillin, carbenicillin, and cephalothin, but also to third-generation cephalosporins and carbapenems (Gaibani et al. 2013). In this thesis, the *Klebsiella pneumoniae* carbapenemase-2 (KPC-2) producing, multidrug-resistant *C. freundii* isolates have been investigated in the context of gene transfer mediated by outer membrane vesicles (OMVs).

Enterobacter sp. is a rod-shaped bacterium that belongs to the family of *Enterobacteriaceae*. Bacteria of this genus are ubiquitous in nature. They are found in the intestinal tracts of animals and plants resulting in their wide distribution in soil, water, and sewage. A number of strains of *Enterobacter* are pathogenic and cause opportunistic infections in immunocompromised individuals. *Enterobacter* can cause a variety of conditions, ranging from bacteremia and eye and skin infections to urinary tract infections, pneumonia and meningitis (Davin-Regli & Pagès 2015).

Escherichia coli (*E. coli*) is a facultatively anaerobic, rod-shaped bacterium that is generally found in the lower intestine of warm-blooded organisms. *E. coli* is the most widely studied prokaryotic model organism for investigating molecular and cellular processes, including membranes remodeling. Nevertheless, *E. coli* is not only laboratory workhorse, but it can also be a highly versatile and frequently lethal pathogen. A number of different *E. coli* strains cause various intestinal and extraintestinal illnesses by means of different virulence factors affecting a wide range of the host cell activities (Kaper et al. 2004). The various pathotypes of *E. coli* include intestinal pathogens: enteropathogenic *E. coli* (EPEC), enterohaemorrhagic *E. coli* (EHEC), enterotoxigenic *E. coli* (ETEC), enteroaggregative *E. coli* (EAEC), enteroinvasive *E. coli* (EIEC), diffusely adherent *E. coli* (DAEC) and extraintestinal pathogen, comprising uropathogenic *E. coli* (UPEC) and meningitis and sepsis-associated *E. coli* (MNEC).

Serratia marcescens (*S. marcescens*) is an opportunistic Gram-negative pathogen that causes infections in patients with compromised host defense mechanisms. *S. marcescens* cause a broad range of hospital-acquired infections, including respiratory tract infections, urinary tract infections, meningitis, pneumonia, conjunctivitis wound and eye infections and septicaemia that can progress into sepsis. The major factors for sepsis caused by *S. marcescens* are hospitalization, placement of intravenous catheters, intraperitoneal and urinary catheters as well as previous instrumentation of the respiratory tract. An important characteristic of *S. marcescens* is its ability to produce beta-lactamase enzymes (AmpC- Betalactamases), which confers resistance to the broad spectrum beta lactam antibiotics (Panigraphy 2015).

In general, this research represents a comprehensive examination of the selected Gram-negative bacterial species with respect to their ability to cell wall remodeling that leads to antibiotic resistance and vesicle formation. All of the isolates investigated here are widespread pathogens that constitute a common and well-known health issue worldwide.

1.2 Cell envelope of Gram-negative bacteria

In order to discuss the modification of bacterial cell wall, it is necessary to be familiar with the architecture of the Gram-negative envelope where all changes originate (Figure 1.1). The cell wall is composed of the outer and inner membranes separated by a periplasm, which contains a thin layer of peptidoglycan (PG) (Needham & Trent 2013). The outer membrane consists of phospholipids in the inner leaflet and the glycolipid lipopolysaccharide (LPS) anchored to the outer leaflet. Integral components of the outer bilayer are the β-barrel outer membrane proteins (OMPs), called porins that form nonspecific channels to allow translocation of small hydrophilic molecules across the membrane. LPS is composed of three main domains: the lipid A, the core oligosaccharide and the O antigen. Lipid A consists of a phosphorylated glucosamine disaccharide unit with fatty acyl chains that bind the LPS to the outer membrane and act as a scaffold for the assembly of the negatively charged core domain and the O-antigen subunit (Raetz et al. 2007). Divalent cations cross-bridge adjacent lipopolysaccharide molecules are preventing the electrostatic repulsion between the negatively charged entities. These lateral interactions stabilize the integrity of the outer membrane and provide the barrier against the environment by limiting the permeability of different agents through the membrane (Wu et al. 2013). In addition, LPS serves as an important defense system due to the fact that gram-negative bacteria can alter LPS structure to resist killing by cationic antimicrobial peptides (cAMPs) and to evade the host innate immune system (Chen & Groisman 2013). The murein (peptidoglycan) sacculus is the shape-determining component of the cell envelope located between outer and inner membranes. It protects the cell from rupture due to osmotic and mechanical stresses (Vollmer & Bertsche 2008). Lipoproteins Pal and Lpp are covalently bound to murein layer and together with inner membrane proteins TolA, TolQ, TolR and a periplasmic protein TolB maintain the envelope integrity by cross-linking all cell wall layers (Cascales et al. 2002).

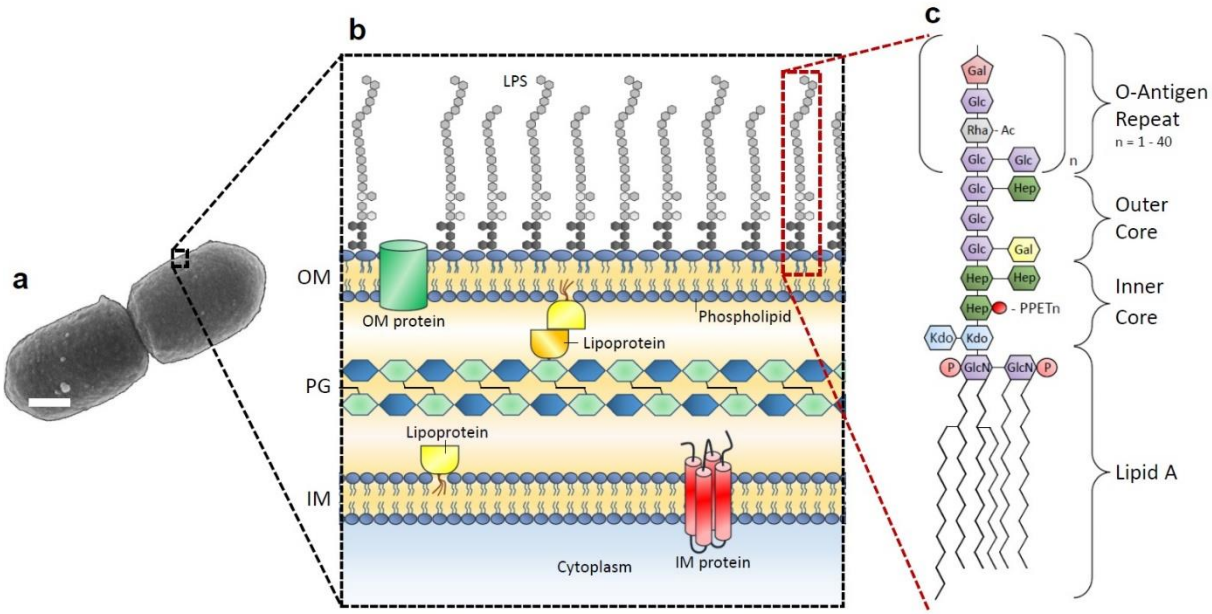

Figure 1.1 **The cell wall of Gram-negative bacteria. (A)** A field-emission scanning electron microscope image of an *Escherichia coli* cell (scale bar of 200 nm). **(B)** A schematic cross-section of the Gram-negative cell wall, showing the typical inner and outer membranes (IM, OM) that are separated by the periplasm layer, which contains peptidoglycan molecules (PG). The outer leaflet of the outer membrane consists of lipopolysaccharide (LPS), which is bound to the membrane by the lipid A domain. The inner leaflet of the outer membrane and the complete inner membrane contain only phospholipids. In both bilayers can be embedded a range of different types of membrane protein. **(C)** The LPS macromolecule is composed of three major domains: lipid A, the inner and outer core oligosaccharides, and a polymeric O-antigen subunit.

1.3 Cell membrane remodelling

Membrane remodeling is an essential part of many biological processes found in all domains of life and is achieved by the interplay between proteins and lipids (McMahon & Gallop 2005). Modification of cell membranes occurs largely through two processes, first is a membrane fission where one membrane divides into two and second is a membrane fusion where two membranes assemble together to form one (Tan & Ramamurthi 2013). The discovery of the soluble NSF attachment protein receptor (SNARE) as well as the dynamin protein family and endosomal sorting complex for transport (ESCRT) have led to a better understanding of the mechanisms that regulate membrane fusion and fission in eukaryotes (Figure 1.2). In contrast to eukaryotes, in prokaryotes the specific protein complexes responsible for cell wall remodeling remain still elusive, mainly because the factors that may possibly mediate these modification events are likely essential for bacterial viability. The primary role of SNARE proteins is to mediate the fusion of vesicles with their target membrane bound compartments,

whereas ESCRT protein complexes facilitate a unique mode of membrane changes resulting in membranes bending and budding (Schuh & Audhya 2014; Ungar & Hughson 2003). Additionally, other well-studied eukaryotic molecules involved in membrane modification are Bin-amphiphysin-Rvs (BAR) domain proteins. They play key roles in many cellular processes including clathrin -dependent and -independent endocytosis, cytokinesis as well as T-tubule morphogenesis. It is believed that the BAR proteins can be curved to various degrees, and therefore generate either positive or negative curvature of membranes (Davtyan et al. 2016). However, there are still many factors that regulate and participate in membrane remodeling that need to be understood.

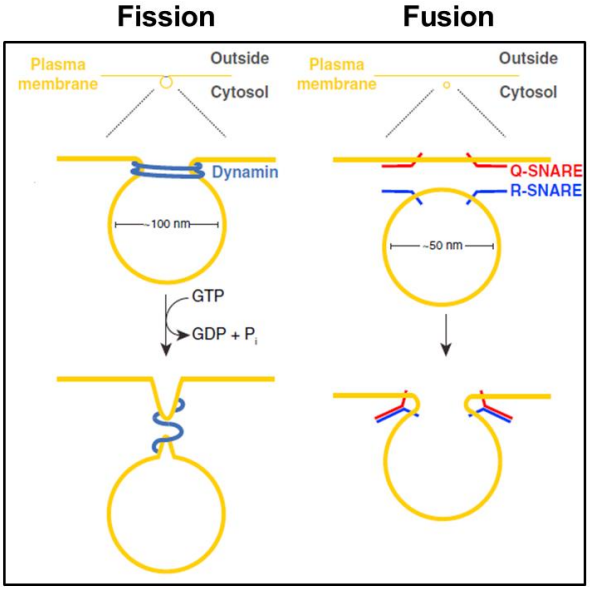

Figure 1.2 **Membrane modification events in prokaryotes and eukaryotes.** Dynamin protein assembles at the neck of an endocytic vesicle as it bulges out from the plasma membrane. GTP hydrolysis allows for the constriction of dynamin, and membrane scission. During exocytosis, R-SNARE proteins are anchored in the vesicular membrane and interact with Q-SNARES in order to form a stable cis-SNARE complex that drives membrane fusion. Lipid bilayers are depicted in yellow; Dynamin marked in blue. Figure modified from (Tan & Ramamurthi 2013).

1.3.1 Modification of the bacterial membranes

The cell wall of Gram-negative bacteria is the first protective barrier against the stressors of the surrounding environment. Bacteria have the ability to alter the structure of their envelope in respond to stress effectors by displaying a variety of surface antigens, changing LPS composition, releasing outer membrane vesicles, producing capsule structures surrounding the bacteria or forming nanotubes between cells (Mashburn-Warren & Whiteley 2006; Li et al. 2012; Pande et al. 2015; Schembri et al. 2004) (Figure 1.3). In other words, the bacterial cell

wall is highly dynamic and undergoes reorganization as a result of changes in milieu. One way to remodel the envelope and adapt to stressors, such as the increased concentration of cationic antimicrobial peptides (cAMPs) are LPS modifications. Most LPS modifications occur on the lipid A portion of the molecule and include the addition of aminoarabinose moieties, phosphoethanolamine moieties as well as phosphorylation, deacylation and acylation events (Needham & Trent 2013). Changes in LPS lead to decreased affinity between antimicrobial peptides and outer membrane by increasing overall net negative charge of bacterial cell wall. Another example of the cell wall remodeling is the production of outer membrane vesicle, which are nanometer-sized spherical structures released by various bacteria. Vesicles have diverse biological functions, including the delivery of numerous proteins and toxins. Therefore, they can help bacteria to accommodate to changing environmental factors. However, the exact mechanism of OMV biogenesis and, subsequently their contribution to biological processes has not been fully understood. In this thesis, I address the open questions regarding the molecular basis for the process of OMV formation and their biological functions. The release of OMV and its roles as well as resistance to cAMPs in the context of Gram-negative envelope modifications will be viewed in the next chapters.

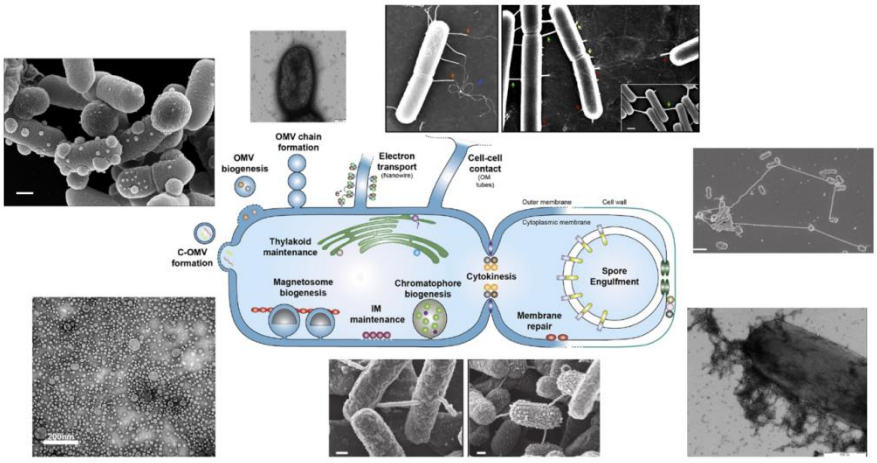

Figure 1.3 **The key membrane remodeling events occurring in bacteria.** Membrane modifications are fundamental biological processes including basic events such as bacterial cell division and growth, or more complex behaviours such as outer membrane vesicle and nanotube formation leading to exchange of intracellular compartments and intercellular communication. Images modified from (Pande et al. 2015; Bohuszewicz et al. 2016).

1.4 Vesiculation in Gram-negative bacteria

The release of outer membrane vesicles from bacteria is a process described almost 50 years ago (Chatterjee & Das 1967). OMVs are released constitutively during the normal growth of

Gram-negative as well as some Gram-positive bacteria. They are defined as spherical, bilayered, nanometer-sized proteophospholipids with an average diameter of 20–200 nm (Schwechheimer & Kuehn 2015). The protein composition of OMVs resemble the proteome of parental bacterial cell, therefore these small particles are composed of inner and outer membrane proteins, lipopolysaccharides, periplasmic proteins and other bacterial membrane components, which get locked in the bleb lumen during the formation process. Moreover, vesicles may contain cytoplasmic proteins, as well as DNA and RNA, however the mechanism underlying the export of cytoplasmic compartments into OMVs remains elusive (Kulp & Kuehn 2010; Kulkarni & Jagannadham 2014; Fulsundar et al. 2014).

1.4.1 Biogenesis of outer membrane vesicle (OMV)

Several models for OMV biogenesis have been proposed based on both experimental evidence as well as architectural features of the bacterial cell wall (Kulp & Kuehn 2010). However, the molecular mechanism leading to OMV formation is not known. It is clear that, there is no one mode of OMV shedding, but more likely multiple mechanisms are responsible for vesicles biogenesis (Roier et al. 2016). There are three main models that are deliberated within the scientific community. The first model suggests that an accumulation of peptidoglycan fragments and/or misfolded proteins in the periplasm initiates the process of bulging out and pinching off of the outer membrane, subsequently leading to OMV formation. Such accumulations can be caused by, for instance, defects in bacterial membrane synthesis or temperature stress (Kulp & Kuehn 2010; McBroom & Kuehn 2007). The second model proposes that relocation or loss of lipoproteins, which covalently link the outer membrane to the peptidoglycan layer, leads to a outer membrane protrusion, and thus triggers vesicle formation (McBroom et al. 2006). The third model is based on the structural changes of lipopolysaccharide that can induce the charge-charge repulsion among adjacent LPS molecules, leading to local deformation and budding of the bacterial cell wall. It is known that divalent cations cross-bridge the highly anionic LPS molecules and stabilise the whole outer membrane. Therefore, remodeling of LPS that leads to removal of Ca^{2+} and Mg^{2+} ions may contribute to increased vesicle formation (Elhenawy 2016; Kulkarni & Jagannadham 2014). In summary, it is currently unknown whether biogenesis of OMVs released by different Gram-negative bacteria is regulated by one unified, evolutionary conserved mechanism or each single bacterial species have their own special system to control vesiculation process.

1.4.2 Probably roles of OMVs

It is advantageous for Gram-negative bacteria to release vesicles, since the production of these large macromolecular complexes must be accompanied with a high fitness cost. Although the exact mode of OMV formation remains unknown, a number of studies have highlighted the miscellaneous biological roles for bacterial vesicles (Figure 1.4). OMVs have been implicated in many processes, which include the release of virulence factors, signaling between bacterial and eukaryotic cells, DNA transfer, antibacterial activity and immunomodulation of the host (Ellis & Kuehn 2010; McBroom et al. 2006; Renelli et al. 2004).

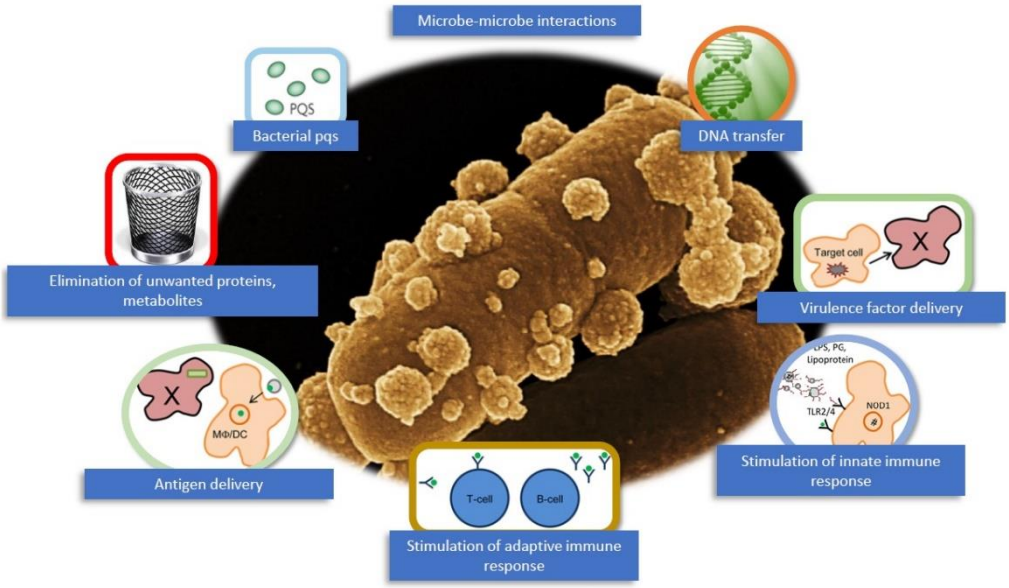

Figure 1.4 **The functions of outer membrane vesicles derived from Gram-negative bacteria.** OMVs can function in multiple mechanisms that promote bacterial survival and pathogenicity. They can provide an avenue to remove toxic compounds and unwanted metabolites, such as misfolded proteins, from bacterial lumen. OMVs can also contribute to dissemination of antibiotic resistance genes to recipient bacteria by serving as vehicles for delivery of plasmid DNA as well as they can carry hydrolysing enzymes that degrade antibiotics. Vesicles allows for interacting with host cells to mediate the delivery of various virulence factors, such as toxins. In addition, they can deliver diverse bacterial antigens to the host cells, which evoke inflammation. The FE-SEM image of bacterial cells releasing OMVs was taken as described in chapter 3.5.3.

OMVs provide a unique, long-distance mode for the secretion of proteins and virulence factors. They can act as vehicles for delivery of insoluble molecules and other cellular compartments that cannot be easily transported across the surrounding milieu (Bomberger et al. 2009). For instance, OMVs have been shown to be involved in horizontal gene transfer (HGT). Recently, the genetic transformation potential of outer membrane vesicles and nanotubes has been studied

in several bacterial species. A number of research groups have shown that OMVs contain genetic material (both plasmid and chromosomal DNA) and can facilitate the transfer of plasmid DNA to other recipients (Yaron et al. 2000; Rumbo et al. 2011; Renelli et al. 2004; Kadurugamuwa & Beveridge 1995; Fulsundar et al. 2014; Dorward et al. 1989; Pande et al. 2015). In this study, the involvement of vesicles in dissemination of resistance genes was investigated (see chapter 4.1.5 and 4.3). OMVs also contribute to defence of bacterial cells against antibacterial agents. The OMVs secreted by one bacterial species can provide protection to other bacterial species from the antibiotic stress. The presence of different peptidases, proteases and enzymes, such as β-lactamases has been observed in OMVs (Schaar et al. 2011). The OMV-mediated inactivation of antibiotics has been studied by (Ciofu et al. 2000). The contribution of vesicles to antibiotic resistance has been examined and described in chapter 4.1.4. OMVs are also known to play an important role in the biofilm formation. They were found to be involved in delivery of exopolysaccharides and the process of cell co-aggregation. It has been proposed that vesicles might act as a platform for connecting of proteins, exopolysaccharide molecules, DNA and the attachment surface, together with the bacterial cells. However, the detailed mechanism underlying the involvement of OMVs in biofilm formation is unknown (Kulkarni & Jagannadham 2014). Furthermore, the vesicles are involved in modulating the host immune response, since they contain the antigenic components, such as OM, PG and LPS (De et al. 1959). OMVs produced by *Salmonella* Typhimurium elicit proinflammatory responses in macrophages, induce dendritic cell maturation, enhance the expression of MHC class II molecules and also stimulate proinflammatory cytokine secretion and CD4+ T-cell activation (Alaniz et al. 2007). A proinflammatory response to vesicles has also been reported for other pathogens, including *Helicobacter pylori* or *Pseudomonas aeruginosa*. The epithelial cells exposed to *H. pylori* or *P. aeruginosa* OMVs induce the expression of cytokine IL-8 which is a strong activator for neutrophil and monocytes *in vivo* (Ellis & Kuehn 2010; Bauman & Kuehn 2006). The OMVs can also have an anti-inflammatory effect on the host cells and help bacteria to evade the host immune system mechanisms. The vesicles derived from *Porphyromonas gingivalis* possess gingipain proteases that can degrade the membrane-bound CD14 receptors. The loss of LPS receptors results in a reduced immune response to *P. gingivalis* colonisation (Duncan et al. 2004). *Moraxella catarrhalis* OMVs contain outer membrane-bound superantigen *Moraxella* immunoglobulin D-binding protein (MID), which potentially delay the production of specific antibodies (Schwechheimer & Kuehn 2015). Despite ubiquitous nature of OMV production and their diverse biological capabilities, we understand very little about mechanistic aspects of OMV formation and their biological

functions. Given the promiscuous character of bacteria, the role of OMVs is probably even more varied than is presently appreciated.

1.4.3 Immunogenic and protective immune response of OMVs in an invertebrate larvae model

Due to fact that the composition of vesicle resembles the parental bacterial cell, OMVs are the source of active antigens, and therefore they have a strong immunogenic properties (Mitra et al. 2015). A number of studies have been performed to examine the immunogenicity and protective immune response of OMVs in vertebrate as well as invertebrate models. Invertebrates, like the greater wax moth larvae, *Galleria mellonella* (*G. mellonella*), have a sophisticated and effective immune system that fight against all microbial and parasitic pathogens. Unlike vertebrates that possess both innate and adaptive immune responses, invertebrates rely mostly on humoral and cellular defense system to protect themselves from various infections (Wu et al. 2014). Humoral defenses are generated by the synthesis of antimicrobial peptides (AMPs), the activation of cascades that regulate coagulation and melanization processes, and the production of reactive oxygen and nitrogen intermediates. Cellular defenses include hemocyte-mediated phagocytosis, encapsulation and nodule formation (Strand 2008). A number of insect species have been used to study innate immunity. One of the most popular insects for laboratory use are *G. mellonella* larvae, which have many advantages, including suitable sizes that make them easy to handle and they are easy to culture in the laboratory environment. Additionally, *G. mellonella* has a growth optimum at 37°C and they contain abundance of hemolymph, which makes it convenient for performing a different biochemical tests (Mukherjee et al. 2010).

In this thesis, OMVs derived from different Gram-negative bacteria were isolated and examined with regard to their ability to induce innate immune responses in *G. mellonella* model. The larvae priming experiments are described in chapter 4.4.3.

1.5 Vesiculation in Gram-positive bacteria

The release of spherical, membranous vesicles occurs not only in Gram-negative bacteria but is widely conserved across all prokaryotes and eukaryotes, including Gram-positive bacteria, archaea, parasites and fungi (Deatheragea & Cooksona 2012). Several research groups have reported that Gram-positive bacteria such as *Bacillus anthracis*, *Staphylococcus aureus* or *Listeria monocytogenes* also produce vesicles during their growth (Lee et al. 2009; Lee et al.

2013; Rivera et al. 2010). Figure 1.5 represents the cells of *L. monocytogenes* that secrete membrane vesicles (MVs). The size of MVs derived from Gram-positive bacteria has been found to be ranging from 50 to 150 nm in diameter, whereas proteomics studies revealed that they are rich in membrane lipids, cytosolic-associated proteins and different toxins. MVs are involved in different processes, including the delivery of many virulence-associated proteins to host cells. Vesicles from *Bacillus anthracis* have biologically active toxins, such as anthrolysin O (ALO) and they are capable of inducing a protective immune response in immunized mice (Rivera et al. 2010). MVs derived from *Staphylococcus* aureus can serve as a vehicle for virulence factors delivery and induce cytotoxicity effect in host cells (Gurung et al. 2011). Up to date, little is known about the mechanism underlying biogenesis of MVs derived from Gram-positive bacteria and their associations with host cell pathology. Further studies are required to understand all processes that link MV formation and bacterial pathogenic potential.

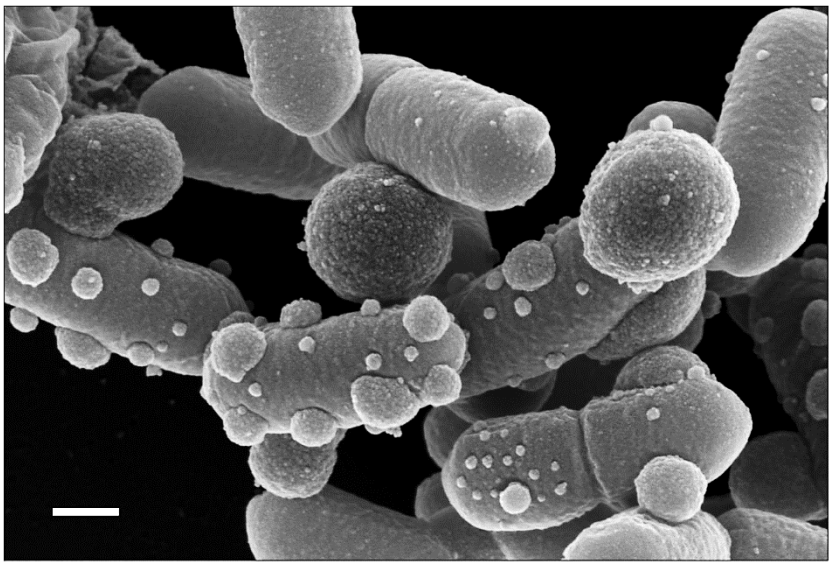

Figure 1.5 **Field-emission scanning electron microscopy image of Gram-positive bacteria cells and their vesicles.** The FE-SEM image of *Listeria monocytogenes* and their MVs being released from bacterial surface. The sample of *L. monocytogenes* was prepared as described in chapter 3.5.3. The scale bare 200 nm.

1.6 Antibiotics and resistance

The serendipitous discovery of the first antibiotic, penicillin made by Sir Alexander Fleming in 1928 was a major breakthrough in the history of medicine (Ligon 2004). Since then, antibiotics have represented almost the only effective treatment option for life-threatening illnesses caused by bacterial infections (Bernal et al. 2013). Nonetheless, their efficiency has been severely

compromised by misuse and over-use of antibiotic drugs, which have led to the appearance of bacteria resistant to many frequently used antibiotics.

There are three general categories of antibiotic resistance displayed by bacteria, such as intrinsic, acquired and adaptive (Alekshun & Levy 2007). Intrinsic resistance is related to the specific feature inherent to a bacterial species and every member of this species displays this resistance. For instance, Gram-negative bacteria can exhibit resistance to many antibiotics due to the presence of a modified lipopolysaccharide causing low permeability of outer membrane and functions as an extra barrier preventing the entry of drug into the cell. Moreover, many bacteria comprise efflux pumps that pump actively antibiotic molecules out of the cell, and thus decrease their concentration in the bacteria. Bacterial-acquired resistance to antibiotics is the consequence of the acquisition of new genetic material i.e. plasmids, integrons, transposons by horizontal gene transfer or mutations in chromosomal genes, leading to drug resistance. It provides selective advantages in the presence of antimicrobial drugs and can be transferred to daughter cells resulting in the appearance of antibiotic-resistant bacterial strains. In addition to intrinsic and acquired resistance to antibiotics, bacteria can develop an adaptive resistance, which involves a temporary increase in the ability of a microorganism to survive an antibiotic, as the result of alterations in gene and protein expression triggered by different environmental conditions The adaptive resistance is transient and typically reverts upon the elimination of the inducing condition (Olaitan, Morand & J.M. Rolain 2014).

In addition, the antibiotic resistance in bacteria can be caused by several mechanisms, which can be divided into three biochemical routes: first, those that minimize the absorption of the antibiotic as a consequence of poor penetration into the bacterium or of antibiotic efflux, second, those that alter the antibiotic target by chromosomal mutation or post-translational modification of the target and third, those that inactivate the drug by hydrolysis or modification (Blair et al. 2015) (Figure 1.6). In this thesis, the major events of bacterial membrane remodeling (i.e., formation of outer membrane vesicle and modification of lipopolysaccharides), which contribute to antibiotic resistance encountered in clinical practice have been investigated.

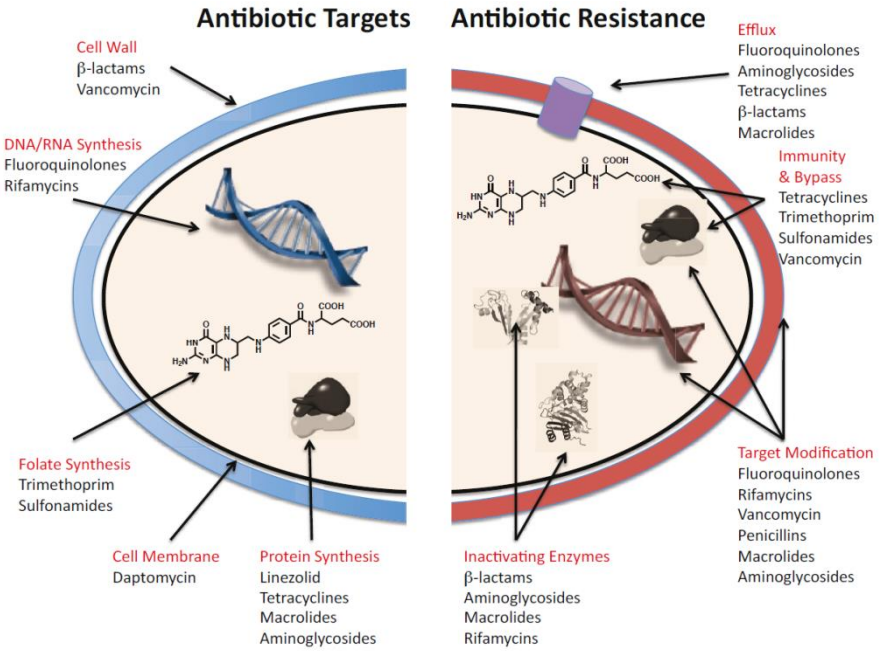

Figure 1.6 **The antibiotic target sites and molecular mechanisms of antibiotic resistance.** In general, antibiotics target five major sites: bacterial cell wall, cell membrane, protein synthesis, DNA and RNA synthesis, and folic acid metabolism. These targets are very different or even do not exist in eukaryotic cells, which means that many antibiotics are relatively nontoxic for human being. Resistance to antibiotics occurs through four general mechanisms: target modification; efflux pumps, immunity and bypass as well as enzymatic inactivation. Figure adapted from (Wright 2010).

1.6.1 Colistin and related peptide antibiotics

A rapid dissemination of multidrug-resistant *Enterobacteriaceae* combined with the paucity of novel antibiotics classes able to cope with them have led to the restoration of cationic antimicrobial peptides (cAMPs), i.e. colistin and polymyxin B as a precious addition to the current therapeutic armamentarium (Falagas et al. 2006; Conly & Johnston 2006; Magiorakos et al. 2011). Colistin (also known as polymyxin E) is an old class of cationic, cyclic, basic polypeptide antibiotics that was discovered in the late 1940s from the soil bacterium *Paenibacillus polymyxa* subsp. *colistinus* (Laurent Poirel, Aurélie Jayol 2017). Polymyxins contain five chemically different compounds (polymyxins A–E), but due to their high toxicity, only polymyxin B and polymyxin E have been approved to use in clinical practice (Conly & Johnston 2006; Falagas & Kasiakou 2005). Polymyxins consist of a mixture of D- and L -amino acids, a heptapeptide ring, 2,4-diaminobutyric acid and a fatty acid coupled with the peptide through an amide bond (Figure 1.7) (Hancock 1997). In analogy to polymyxin B, Colistin is active predominantly against gram-negative bacteria by interacting with anionic lipopolysaccharide molecules in the outer leaflet of the outer membrane. It competitively

displace divalent cations, like Ca^{2+} and Mg^{2+} from the phosphate groups of membrane lipids, thus causing an increase in the permeability of the cell membranes, leakage of intracellular contents and ultimately bacterial death (Hancock 1997).

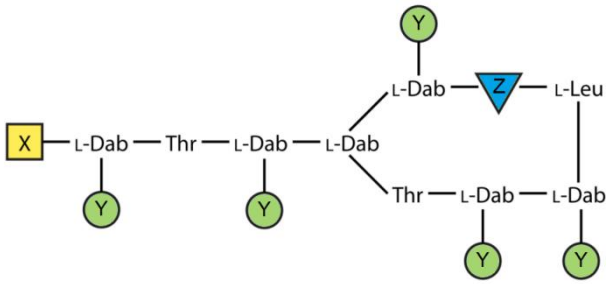

Figure 1.7 **The Schematic structures of a colistin and polymyxin B antibiotics.** Colistin and Polymyxin B are cationic polypeptides composed of a cyclic heptapeptide and a tripeptide side chain, which is acylated at the N terminal side by a fatty acid tail. X – Fatty acid residues; Y – NH_2 for colistin and polymyxin B; Z – D-Leu for colistin, D-Phe for polymyxin B. Figure modified from (Laurent Poirel, Aurélie Jayol 2017).

1.6.2 Intrinsic, adaptive and transferable resistance to colistin

Bacteria developed several mechanisms to protect themselves from exposure to cationic antimicrobial peptides (cAMPs). These strategies include intrinsic, adaptive and transferable resistance mechanisms (Munita et al. 2016). Intrinsic resistance to colistin is mediated by modification of lipopolysaccharide with amino sugars or overexpression of outer membrane proteins. In *Serratia marcescens* and *Proteus mirabilis* resistance to polymyxins is associated with expression of the *eptB* gene or the arnBCADTEF operon resulting in addition of phosphoethanolamine (pEtN) or 4-amino-4-deoxy-L-arabinose (L-Ara4N) groups to the lipid A domain. Such modifications lead to a decreased affinity between polymyxins and the bacterial cell wall by increasing the net negative charge of LPS (Laurent Poirel, Aurélie Jayol 2017).

Adaptive resistance involves activation of LPS-modifying operons by mutations in two-component sensing systems (TCSs) such as PmrA/PmrB and PhoP/phoQ or expression of efflux pumps (Olaitan, Morand & J.-M. Rolain 2014). In several genera of the *Enterobacteriaceae*, such as *Enterobacter*, *Escherichia*, *Klebsiella* and *Salmonella*, the adaptive resistance to colistin is mediated by modification of LPS with L-Ara4N and pEtN groups (Raetz et al. 2007). A number of genes and operons play a role in mediating resistance to polymyxins. The *pmrC* gene, *pmrE* gene, pmrHFIJKLM operon encode for enzymes that are directly responsible for LPS modifications. The *mgrB* gene is involved in negative regulation

of PhoP/phoQ system. Besides, the colistin resistance regulator (*crrAB*) is associated with the regulation of the PmrAB two-component system (Olaitan, Morand & J. M. Rolain 2014). Figure 1.8 represents known regulatory pathways for modifications of lipopolysaccharides.

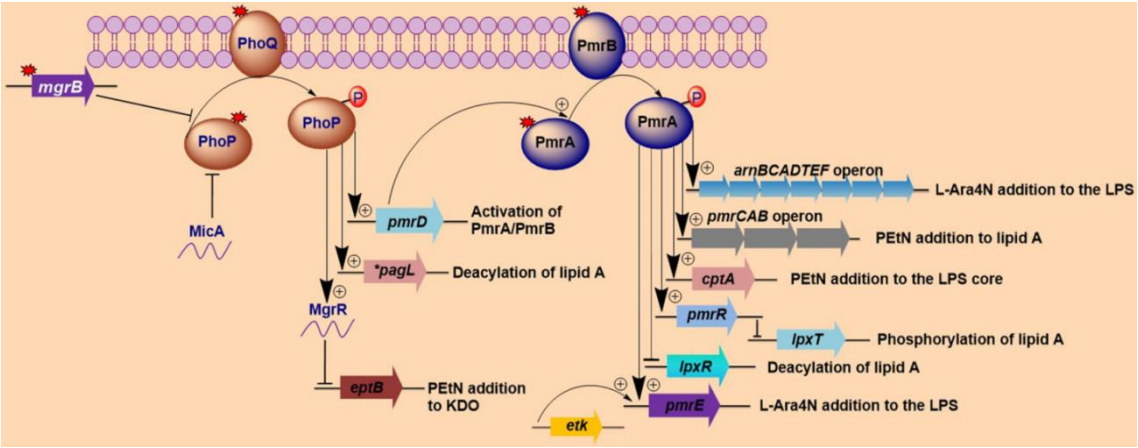

Figure 1.8 **Regulation pathways of lipopolysaccharide modifications in Gram-negative bacteria.** In *Escherichia coli*, MicA and MgrB cause negative feedback on the *phoP/phoQ* regulatory system, whereas mutations in *mgrB* or *phoP/phoQ* (marked as a red-colored asterisk) usually lead to the induction of the *phoP/phoQ* two-component system (TCS). In *Salmonella* sp., the induction of TCS activates: *pagL* gene resulting in deacylation of lipid A, *pmrD* gene leading to activation of *pmrA* and additionally, *eptB* is repressed by the activation of MgrR. Moreover, in *Klebsiella pneumoniae*, the *phoP/phoQ* regulatory system activates directly the arnBCADTEF operon. All these changes in LPS structure mediate resistance to polymyxin. Figure adapted from (Olaitan, Morand & J. M. Rolain 2014).

Chromosomal mutations are heritable vertically and generally considered non-transferable by mobile genetic elements. However, in the late 2015 Liu et al. reported an existence of a plasmid-mediated, colistin resistance conferring gene, named *mcr-1* in animal and human isolates that can be transmitted by horizontal gene transfer (HGT) (Liu et al. 2016). This first identified plasmid-borne mechanism of polymyxin resistance is mediated by phosphoethanolamine transferase-like enzyme (MCR-1). MCR-1 catalyzes transfer of pEtN group onto the glucosamine-disaccharide of lipid A at the outer leaflet of the bacterial outer membrane, and therefore confers colistin resistance (Figure 1.9). The detailed characterization of the mobile colistin resistance is presented in chapter 4.5.

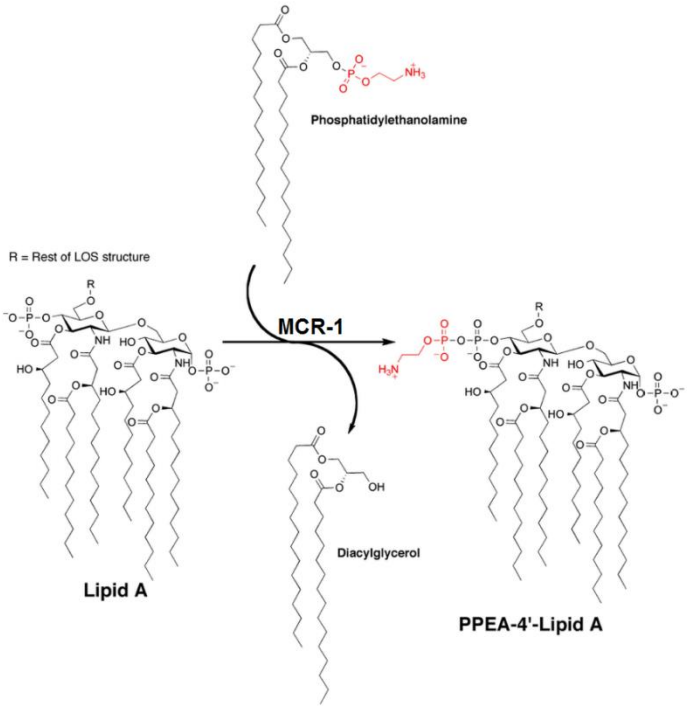

Figure 1.9 **Reaction catalyzed by MCR-1 enzyme.** MCR-1 catalyses transfer of phosphoethanolamine group from a phosphatidylethanolamine donor substrate onto the 1′ or 4′ position of lipid A domain. Figure modified from (Anandan, Evans, Condic-Jurkic, O'Mara, John, Phillips, G. A. Jarvis, et al. 2017)

2 Thesis objectives

The aim of this thesis was to investigate the molecular basis for remodeling of the cell envelope of Gram-negative bacteria and its impacts on bacterial abilities to develop resistance to antibiotics and the release of outer membrane vesicles.

Specific Aims:

- The development and optimization of a protocol for isolating bacterial outer membrane vesicles.
- The investigation of the OMV formation from different Gram-negative bacterial species with an emphasis on the mechanism of vesicle biogenesis, its regulation and the immunogenic properties of bacterial blebs.
- The examination of the vesicles potential ability to transfer genetic material (including antibiotic resistance determinants) to other bacteria.
- Studying the role of LPS remodeling mediated by MCR-1 in resistance development towards cationic antimicrobial peptides (cAMPs).
- The analysis of the conditions required for functionality of the mobile colistin resistance (*mcr-1*).
- The examination of the involvement of MCR-1 in production of OMV.

3 Materials and Methods

3.1 Materials

3.1.1 Instruments

Equipment used in this thesis is listed in Table 3.1, Appendix A.

3.1.2 Consumables

Consumables used in this thesis are listed in Table 3.2, Appendix A.

3.1.3 Chemicals

Chemicals used in this thesis are listed in Table 3.3, Appendix A.

3.1.4 Enzymes

Enzymes used in this thesis are listed in Table 3.4, Appendix A.

3.1.5 Kits

Kits used in this thesis are listed in Table 3.5, Appendix A.

3.1.6 Buffers, media and solutions

Buffers, media and solutions used in this thesis and their composition are listed in Table 3.6, Appendix A.

3.1.7 Bacterial strains and isolates

Strains, isolates and plasmids used in this study are listed in Table 3.7.

Table 3.7 Bacterial strains, isolates and plasmids used in this dissertation.

Bacterial isolate and strains	**Description**	**Source**
A. baumannii 10	Clinical isolate; Köln outbreak	Institute collection
A. baumannii 13-B9879	Clinical isolate; Bonn outbreak	Institute collection
A. baumannii 25	Clinical isolate; Köln outbreak	Institute collection
A. baumannii 65	Clinical isolate; Kiel outbreak	Institute collection
A. baumannii ATCC 17978	Clinical isolate	ATCC collection
A. lwoffii	Clinical isolate	Institute collection
C. freundii 08698	Clinical isolate; IncN plasmid::bla_{KPC-2}	Institute collection
Enterobacter 247	Clinical isolate	Institute collection
E. coli BL21 DE3 GOLD	Competent cells (High Efficiency)	NEB, Cambrige, UK
E. coli DH10β	Competent cells (High Efficiency)	NEB, Cambrige, UK
E. coli DH5α	Competent cells (High Efficiency)	NEB, Cambrige, UK
E. coli H16	Clinical isolate; ColV plasmid::Δ*hlyF*	Institute collection
E. coli H76	Clinical isolate; ColV plasmid::*hlyF*	Institute collection
E. coli H8	Clinical isolate; ColV plasmid::*hlyF*	Institute collection
E. coli J53	A derivative of *E. coli* K-12, resistant to sodium azide	Institute collection
L. monocytogenes EGD-e	Wild type isolate	Institute collection
S. marcescens 2099	Clinical isolate	Institute collection
S. marcescens 2126	Clinical isolate	Institute collection
S. marcescens 273255	Clinical isolate	Institute collection
Various *E. coli* and *K. pneumoniae*	*Mcr-1*-producing as well as colistin susceptible isolates, For detailed description, see Appendix A, Table A-1	Institute collection
Plasmids	**Description**	**Source**
pUC19	Insert: *hlyF* gene; *mcr-1* gene	This study
pET-28a	Insert: *mcr-1*	This study
pAc5.1/V5-HisA	Insert: EGFP-LC3 gene fusion	Institute collection
pJBA27	Insert: EGFP, pUC18 backbone	Institute collection
p002	*Mcr-1* encoding plasmid of *E. coli* 002	Institute collection
p002::Δ*mcr-1*	*Mcr-1* deletion mutant of p002	This study

3.2 Bacterial techniques

3.2.1 Bacterial growth conditions

Bacteria were grown overnight at 37°C with shaking at 180 rpm in Lysogeny broth (LB) (BD Bioscience, Heidelberg, Germany) media unless otherwise noted. The composition of LB broth is described in Table 3.6. For short-term storage, bacteria were plating out on a LB agar plates supplemented with a proper antibiotic, followed by overnight incubation at 37°C. LB plates were prepared using the same recipe for LB with the addition of 15 g agar per liter of broth. The antibiotic concentrations used are as follows: ampicillin (100 mg/L), cefotaxime (2 mg/L), colistin (2 mg/L), kanamycin (30 mg/L). For long-term storage, bacterial cultures were prepared

by mixing an overnight culture with 60% (v/v) glycerol in LB medium at ration 1:1. The cultures were stored in a cryovials at -80°C or in liquid nitrogen.

3.2.2 DNA purification and quantification

Plasmids DNA were isolated using either the Mini plasmid isolation kit (Sigma-Aldrich, Germany) or Maxi plasmid isolation kit (Qiagen, Germany) according to the manufacturer's protocol. For Maxi plasmid isolation kit, 100 – 500 ml of an overnight culture of bacteria harboring plasmid DNA was centrifuged at 6000 rpm for 20 min at 4°C to harvest bacterial cells. The pellets were resuspended in 10 ml of P1 buffer (resuspension buffer) containing RNase, mixed with 10 ml of P2 buffer (lysis buffer) by inverting each tube 4-6 times and incubated for 5 min at RT. Afterwards, 10 ml of P3 buffer (neutralization buffer) was added to the lysate, mixed by inverting 4-6 times, then incubated on ice for 20 min and followed by centrifugation at 13000 rpm for 30 min at 4°C. Afterwards, the QIA filter column was washed with 10 ml of QBT buffer (equilibration buffer) and the lysate was filtered through the HiSpeed column. Next, the column was washed two times with 30 ml of QC buffer (wash buffer) to remove contaminants; the flow-through was discarded. Then, plasmid DNA was eluted with 15 ml of QF buffer (elution buffer), precipitated with 9.5 ml of ice cold isopropanol and incubated for 1 h at -20°C. Plasmid DNA was centrifuged at 6000 rpm for 1 h at 4°C, washed twice with 5 ml of 70% ethanol, air-dried and dissolved in 100 ml of TE buffer. Isolated plasmid DNA was stored at 4 or -80°C. For Mini plasmid isolation kit, 3 ml of an overnight bacterial culture was pelleted by centrifugation (6000 rpm, 5 min) and completely resuspend with 200 µl of the resuspension solution, followed by lysis with 200 µl of the lysis solution. Cell debris was precipitated by adding 350 µl of the neutralization/binding solution. Next, the cell debris was pelleted by centrifuging (12000 rpm, 10 min) and then the cleared lysate was transferred to the column and again centrifuged at 12,000 rpm 1 min. Afterwards, the column was washed with 750 µl of the wash solution and the plasmid DNA was eluted with 100 µl of the elution solution. DNA was stored at 4 or -80°C. The concentration of plasmid DNA was measured by Nanodrop (Thermo Scientific, Waltham, USA) according to the manufacturer's protocol. For quantification of OMV-associated DNA, vesicles were treated with DNase I (Thermo Scientific, USA) to hydrolyze surface-associated and free DNA. DNase I pretreated OMVs were then lysed with GES solution (5 M guanidinium thiocyanate, 100 mM EDTA, 0.5% (v/v) Sarkosyl) to release DNA from OMVs, and then DNA was purified by the use of a PCR product

purification kit (Stratec molecular, Birkenfeld, Germany). Purified vesicle DNA was quantified using the The Qubit® 2.0 Fluorometer (Life technologies, USA).

3.2.3 Agarose gel electrophoresis

1% agarose gels were prepared and run according to standard procedures (Sambrook, J., Russell, D.W. & Laboratory. 2012). The agarose gel was prepared by dissolving agarose in 1x TBE buffer supplemented with 5 mg/L of ethidium bromide (Thermo Scientific, USA). The tray containing gel was placed in an electrophoresis apparatus (construction of the institute) filled with 1x TBE buffer. The DNA samples were mixed with loading buffer and loaded into the wells of the gel. Electrophoresis was performed at 150V, 250 mA for 1 h. Sizes of DNA-fragments were estimated by using a 1-kb plus DNA marker (Thermo Scientific, USA). The agarose gel was then visualized using the gel imaging system (Bio-Rad, Hercules, USA).

3.2.4 S1 nuclease digestion followed by pulsed-field gel electrophoresis (S1-PFGE)

To detect and estimate the sizes of bacterial plasmids, S1 nuclease digestion followed by pulsed-field gel electrophoresis (S1-PFGE) was performed as described previously (Barton et al. 1995). Briefly, the agarose-embedded total cellular DNA was incubated with lysis buffer (1M NaCl, 100 mM EDTA, 50 mM Tris-HCl (pH 7.6), 0.5% N-lauroylsarcosine) supplemented with lysozyme for 3 hours at 55°C. Gel plugs were washed 5 times with TE buffer and milli-q water followed by S1 nuclease digestion for 2 hours at 37°C. Digested plugs were applied to wells in 1% agarose gel. Electrophoresis was conducted using a CHEF-DRIVE III apparatus (Bio-Rad, USA) in 0.5 x Tris–borate–ethylene diamine tetra-acetic acid (TBE) buffer; conditions were 6 V, with 1 s–25 s pulses for 18 hrs. Patterns were normalized using the molecular weight marker (PFGE Lambda or Low range Marker, Thermo Scientific, USA).

3.2.5 Preparation of chemically competent cells

Chemically competent bacteria were prepared according to (Sambrook, J., Russell, D.W. & Laboratory. 2012) with some modification. An overnight bacterial culture was diluted 1:50 in LB medium and grown until an OD_{600} of 0.4 was reached. The Cells were incubated on ice for 20 min prior to centrifugation at 4000 x g at 4°C for 10 min. The supernatant was discarded and pellets were re-suspended in 17 ml ice-cold CCMB80 buffer and incubated on ice for 10 min. Afterwards, cells were harvested by centrifugation as previously described and resuspended in

4.2 ml ice-cold CCMB80 buffer. 200 µl aliquots were frozen down in liquid nitrogen and stored at -80°C.

3.2.6 Transformation of chemically competent cells

Plasmids were transformed by using the heat shock method according to standard protocols (Sambrook, J., Russell, D.W. & Laboratory. 2012). 5 µl of DNA (50-100 ng) were added to 200 µl of competent cells and incubated on ice for 30 min. Cells were then heat shocked at 42°C for 90 seconds followed by incubation on ice for 10 min. 750 µl pre-warmed SOC medium was added and cells were incubated at 37°C for 1 h, with shaking 250 rpm. Bacteria were spread onto LB plates containing a proper antibiotic and incubated overnight at 37°C.

3.2.7 Construction of expressing vectors

The sequences of the primers are shown in Table 3.8

Construction of pUC19 vector expressing *hlyF* gene

The *hly*F gene was PCR amplified from the *E. coli* V76 by using primers hlyF_F and hlyF_R. The resulting amplicon was digested with XbaI and HindIII, and the *hlyF*-containing fragment ligated to a multiple cloning site (MCS) of XbaI/HindIII digested pUC19 plasmid. The resultant plasmids pUC19::*hlyF* was transformed into *E. coli* DH10β.

Construction of pUC19 vector expressing *mcr-1* gene

pUC19::*mcr-1* was constructed by PCR amplifying *mcr-1* gene using as a template *E. coli* V163 and oligonucleotide primers mcr-1_F and mcr-1_R. The resulting amplicon was digested with SalI and EcoRI enzymes, and then the *mcr-1*-containing fragment was ligated to MCS of Sal1/EcoR1 digested pUC19 plasmid. Finally, *E. coli* DH10β were transformed using constructed plasmid.

Construction of *mcr-1* and *mcr-1*$_{\Delta 1\text{-}214}$ genes for purification

To construct plasmid pET-28a::*mcr-1* and pET-28a::*mcr-1*$_{\Delta 1\text{-}214}$, DNA fragments encoding complete or truncated *mcr-1* genes and pET-28-a backbone were amplified by PCR from plasmids p002 and pET28-a, respectively, with a 15 bp overhang for each fragment. The pairs of primers: *mcr-1*_pET28_F, *mcr-1*_pET28_R and *mcr-1*$_{\Delta 1\text{-}214}$_F, *mcr-1*$_{\Delta 1\text{-}214}$_R were used to amplify *mcr-1* and *mcr-1*$_{\Delta 1\text{-}214}$ genes, and pairs of primers pET28a_F, pET28a_R and pET28a_forΔ_F, pET28a_forΔ_R were used to amplify pET28-a backbone. A Gibson assembly cloning kit (New England Biolabs, UK) was then used for assembly of the fragments.

To clone *hlyF* and *mcr-1* genes, the translational coupling strategy was used. This approach is based on controlling the translation rate of an upstream protein coding sequence by the translation rate of a downstream protein coding sequence. In this case, the translational coupling occurs when there is an overlap between open reading frames of *lacZ* and *hlyF* or *lacZ* and *mcr-1* genes (Figure 3.1).

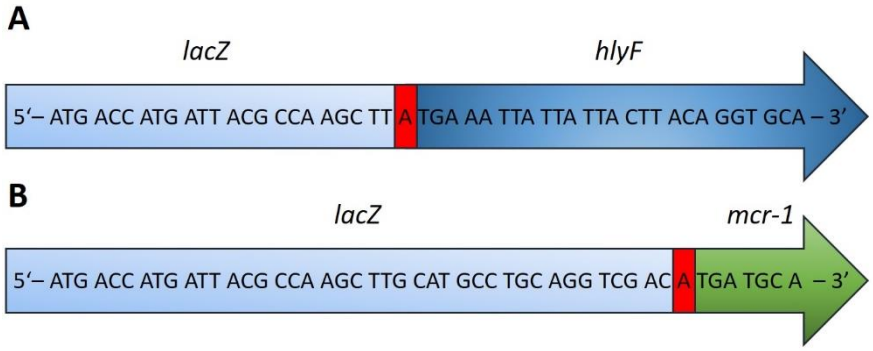

Figure 3.1 **A Schematic representation of translational coupling strategy for cloning *hlyF* and *mcr-1* genes.** Translational coupling is defined as the codependence of translation efficiency of neighboring genes, which are encoded by the same polycistronic mRNA. It occurs when two open reading frames (in this case, *lacZ-hlyF* and *lacZ-mcr-1*) consist of overlapping stop and start codons (marked in red). It can help to sustain a stable ratio between proteins expressed from the same operon. The genes *hlyF* and *mcr-1* were cloned into pUC19 plasmid with inducible promoter by restriction digestion technique.

Table 3.8 Oligonucleotides used in this work.

Primer name	Sequence (5'->3')	Annealing temp. [C]
hlyF_F	GCGCGCAAGCTTATGAAATTATTATTACTTACAGGTGC	51.3
hlyF_R	GCGCGCTCTAGATTATTTAAAATCAACTTCCATTTGTTG	49.8
mcr-1_pUC19_F	GCGCGCGTCGACATGATGCAGCATACTTCTGTGT	62
mcr-1_ pUC19_R	GCGCGCGAATTCTCAGCGGATGAATGCGGTGC	64
mcr-1_pET28_F	CTTTAAGAAGGAGATATACCATGATGCAGCATACTTCTGTGTGG	68.2
mcr-1_pET28_R	CAGTGGTGGTGGTGGTGGTGGCGGATGAATGCGGTGCG	68.2
pET28a_F	CACCACCACCACCACCACTG	70.2
pET28a_R	GGTATATCTCCTTCTTAAAGTTAAACAAAATTATTTCTAGAGGGGAA TTGTTATC	70.2
mcr-1Δ1-214_F	TGGTGCCGCGCGGCAGCCATGCGCCAAAAGATACCATTTATCAC	65.1
mcr-1Δ1-214_R	GCCCCAAGGGGTTATGCTAGTCAGCGGATGAATGCGGTG	65.1
pET28a_forΔ_F	CTAGCATAACCCCTTGGG	63
pET28a_forΔ_R	ATGGCTGCCGCGCGGCAC	63

3.2.8 Plasmid mutagenesis

To remove the *mcr-1* gene (1626 bp) from IncX4 plasmid (36502 bp), the mutagenesis strategy based on RecA-independent recombination activity of *E. coli* K12 DH5α was performed.

Briefly, plasmid amplification was performed in a way that resulting fragments did not include *mcr-1* gene. PCR amplicons were transformed into highly competent *E. coli* 5α (New England Biolabs, Ipswich, USA), followed by the assembly of three PCR fragments. Plasmids were maintained by addition of 2 mg/L colistin sulfate salt (Sigma-Aldrich) or 30 mg/L of kanamycin (Sigma-Aldrich) to the broth. The created constructs were sequenced to verify proper assembly of the plasmids and to except unexpected mutations induced by DNA polymerase. The sequences of used PCR primers are listed in Table 3.9. The map of wild type p002 and p002::Δ*mcr-1* are depicted in Figure A-1; see Appendix C . The plasmid sequences of p002 and p002::Δ*mcr-1* are available in Genbank under the accession numbers MF381176 and MF381175, respectively.

Table 3.9 The nucleotide sequences of the primers used for deletion of *mcr-1* gene from IncX4 plasmid p002.

Primer	Sequence 5'→3'	Annealing temp. [C]
Δ*mcr-1*_Fragment1_FOR	ttccatcttcaacagatctctgattcgaaacc	60
Δ*mcr-1*_Fragment1_REV	ttgtctgttttcgaaaagattatcgtggattgt	60
Δ*mcr-1*_Fragment2_FOR	gtttataacaatccacgataatcttttcgaaaacagaca	60.2
Δ*mcr-1*_Fragment2_REV	tatttttgagtagtttctctttctccctgtatttttttccaaacccacc	60.2
Δ*mcr-1*_Fragment3_FOR	ggaaaaaatacagggagaaagagaaactactcaaaaaataaacggtggga	62.5
Δ*mcr-1*_Fragment3_REV	tgggctgtggtttcgaatcagagatctgttga	62.5

3.2.9 DNA sequencing, assembly and annotation

For sequencing of plasmid DNA derived from *C. freundii*, the bacterial DNA was isolated from the overnight culture using the PureLink Genomic DNA isolation kit (Thermo Scientific, USA) according to instructions of the manufacturer. DNA sequencing libraries were prepared using the Nextera® XT kit (Illumina, San Diego, USA). Paired-end sequencing with a read-length of 300 bp was performed using the Illumina MiSeq platform (Illumina, San Diego, USA). The sequences from each isolate were separately assembled de novo with SPAdes - St. Petersburg genome assembler or by using CLC Genomics Workbench and genome was annotated by GenDB (St. Petersburg Academic University, St. Petersburg, Russia (Nurk et al. 2013); QIAGEN Bioinformatics, Hilden, Germany and University of Giessen, Giessen, Germany for SPAdes, CLC Genomic and GenDB, respectively). The genetic map of the resulting contigs was generated with MAUVE software. For sequence of p002, a long-read single-molecule real-time (SMRT) sequencing (Pacific Biosciences, MenloPark, CA, USA) supplemented with short read sequencing using the Illumina platform was performed, as described earlier (Falgenhauer et al. 2017). For sequencing of p002::Δ*mcr-1*, plasmid DNA was isolated using the Qiagen Plasmid Maxi Kit (Qiagen, Hilden, Germany) following the manufacturer's instructions. A

Nextera XT library of the plasmid (Illumina, San Diego, USA) was sequenced on a NextSeq 500 platform using 2x150 bp runs. Raw data was assembled using SPAdes and comparison of pV002 with pV002::Δ*mcr-1* was performed using blastn.

3.2.10 Antibiotic susceptibility testing

The minimum inhibitory concentration (MIC) was determined by Broth microdilution (BMD) and E-test. The BMD with cation-adjusted Mueller-Hinton broth (Sigma Aldrich, Germany) was performed according to the Clinical and Laboratory Standards Institute (CLSI) recommendations (Eucast 2016). Colistin was tested over a range of dilution (0,16-256 mg/L). Due to lack of breakpoints for polymyxins for *Enterobacteriaceae* according to CLSI, I used the breakpoint values of the European Committee on Antimicrobial Susceptibility Testing (EUCAST) for reference. Enterobacterial isolates with colistin MICs <2 μg/mL were categorized as susceptible; those with MICs >2 μg/mL were categorized as resistant. As recommended by CLSI, microdilution method was performed in plain polystyrene microplate (Thermo Scientific, USA). For E-test method, the susceptibility to colistin was determined in accordance with the manufacturer's instructions (Liofilchem, Roseto degli Abruzzi, Italy). The MIC was read where growth inhibition intersected the antibiotic strip. When small colonies grew within the area of inhibition or a haze of growth occurred around the MIC end-point, the highest MIC intersection was noted.

3.3 Protein techniques

3.3.1 MCR-1 expression and purification

A starter inoculum was prepared by adding a single colony into 20 mL of LB medium containing 30 mg/ml of kanamycin antibiotic and grown at 37°C overnight at 180 rpm. The overnight culture was subculture into 1L of freshly prepared LB medium and incubated at 37°C in a shaking incubator set at 180 rpm until the OD_{600} reached 0.6. MCR-1 expression was induced by the addition of isopropyl β-D-1-thiogalactopyranoside (IPTG) (Sigma-Aldrich, St. Louis, USA) to a final concentration of 1 mM. After 3 hours of post-induction incubation, cells were harvested at 7000 rpm for 30 min at 4°C. The pelleted cells were resuspended in Phosphate-buffered saline (PBS) (Merck Millipore, Germany) and protease inhibitor cocktail was added (bimake.com, Houston, USA). Lysis was performed using a Mixer Mill MM 400 (Retsch GmbH, Haan, Germany). The lysate was centrifuged at 10,000 x g for 10 min at 4°C to remove the non-lysed cells. Membranes were pelleted by further centrifugation of the

supernatant at 100,000 x g for 1 hour using an L8-60M ultracentrifuge (Beckman Coulter, Brea, USA). The pelleted membrane fraction was resuspended in 1 mL of the lysis buffer (20 mM sodium phosphate pH 7.4, 500 mM NaCl, 10 mM imidazole, 1% n-Dodecyl β-D-maltoside (DDM) (Sigma-Aldrich, USA)). The mixture was then sonicated by B-12 Cell Disruptor (Branson Sonic Power Company, St. Louis, USA) and centrifuged at 40,000 x g for 10 min. The resultant supernatant containing the MCR-1 solubilized in DDM detergent micelles was filtered using an 0.22 μm syringe filter (Merck Millipore, Darmstadt, Germany) and applied onto a HisTrap HP 5ml affinity chromtagraphy column (GE Healthcare, Chicago, USA) equilibrated with binding buffer (20 mM sodium phosphate pH 7.4, 500 mM NaCl, 5 mM imidazole and 0.023 % DDM) using an ÅKTApurifier FPLC system (GE Healthcare, USA). The unbound protein was washed from the column with binding buffer until the absorbance at 280 nm reached a stable baseline value. The bound MCR-1 was eluted from the column using an increasing gradient of elution buffer (20 mM sodium phosphate pH 7.4, 500 mM NaCl, 500 mM imidazole, 0.023 % DDM). A peak corresponding to MCR-1 eluted between 40 % and 50 % elution buffer. The collected eluent fractions were pooled and applied onto a PD-10 desalting column (GE Healthcare, USA), equilibrated in 20 mM sodium phosphate pH 7.5, 500 mM sodium chloride and 0.023 % DDM. The final purified MCR-1 protein was resuspended in phosphate-buffered saline (PBS) containing 0.023% DDM. Then, SDS polyacrylamide gel electrophoresis (SDS-PAGE) was performed to assess the purity of the eluted peak fractions. Fractions of pure protein were pooled and concentrated using a 10 kDa molecular weight cut off centrifugal filter unit (Amicon Ultra-15, ultracel 10K, Merck Millipore, Germany) to 5 mg/mL as determined by the Bradford protein assay (Thermo Scientific, USA).

3.3.2 Outer membrane vesicles and whole cell fraction isolation

OMVs were isolated from bacterial liquid cultures as previously described (Kadurugamuwa & Beveridge 1995) with some modifications. Briefly, 10 ml of an overnight culture was used to inoculate 1 L of LB broth containing a proper antibiotic. Bacterial culture was grown at 37°C with shaking 180 rpm to the beginning of stationary phase. Cells were removed by centrifugation at 6,000 x g at 4°C for 30 min (Sorvall, Newtown, USA) and the culture supernatant was filtrated through a Stericup bottle top vacuum filter (0.2 μm size; Merck, USA). The supernatants were concentrated via a 100-kDa tangential filtration concentration unit (Pall Corporation, USA) or cross-flow filtration system (Spectrum labs, USA). The retentate was filtered through a 0.22 μm pore size, PVDF syringe filter (Merck, Germany) to remove the

remaining bacteria. OMVs were pelleted from the concentrates by ultracentrifugation at 100,000 x g for 3 hours at 4°C (Beckman Instruments, Canada; SW 40 Ti rotor). The pelleted OMVs were resuspended in PBS and once again filtered through 0.22 µm pore size syringe filters (Merck, USA). The absence of viable cells in OMVs suspensions was determined by spreading aliquots on LB agar plates to test for bacterial growth. Additionally, crude vesicles were purified on OptiPrep gradients according to method adapted from Susanne J. Bauman (Bauman & Kuehn 2006). The vesicles were stored at -80°C until further use. The whole cell lysate fraction was isolated from bacterial overnight culture. Cells were harvested by centrifugation at 13 200 x g for 5 min and re-suspended in 50 µl of two-times concentrated sample loading buffer. Samples were stored at - 80°C.

3.3.3 Protein Quantification

The protein concentration was determined according to the Bradford assay (Bio-Rad, USA) or β-Lactamase enzymes activity by using Nitrocefin (Thermo Scientific, USA). For Bradford assay, 10 µl pf protein sample was mixed with 200 µl of Bradford dye reagent (Bio-Rad, UK) and the mixture was incubated at room temperature for 5 min followed by the absorbance measurement at 595 nm. Samples were measured in triplicate and compared with a standard curve plotted using serial dilutions of bovine serum albumin (BSA). For spectrophotometric assay, the β-Lactamase activity of proteins was measured by the ability of the enzyme to hydrolyze the β-lactam Nitrocefin, leading to a change in absorbance from OD_{390} to OD_{486}. Enzyme activity was directly proportional to the intensity of Nitrocefin color.

3.3.4 Sodium dodecyl sulfate polyacrylamide gel electrophoresis (SDS-PAGE)

Proteins were resolved by SDS-PAGE method using polyacrylamide gels prepared according to Table 3.10. Resolving gel was prepared using a protean gel casting apparatus (Biometra, Goettingen, Germany) and allowed to polymerize at RT. Afterwards, the stacking gel was poured on top of resolving gel and a comb was inserted to allow the formation of sample wells. Once polymerized, the protein gel was assembled in the electrophoresis chamber filled with 1x SDS running buffer. Protein samples were denatured in 2x protein loading buffer for 10 min at 95°C, cooled on ice and loaded onto the gel. Protein Marker was loaded alongside the samples and electrophoresis was performed at 150 V for 90 min.

Table 3.10 Composition of stacking and resolving gels.

Component (10ml)	8% Resolving	10% Resolving	12% Resolving	5,7% Stacking
MQ water	4.6	3.8	3.2	5.95 ml
Tris HCl (pH 8.8; 1.5 M)	2,6 ml	2,6 ml	2,6 ml	
Tris HCl (pH 6.8; 0.5 M)				2.5 ml
30% Polyacrylamide	2.6 ml	3.4 ml	4 ml	1.34 ml
10% SDS	100 µl	100 µl	100 µl	100 µl
10% APS*	100 µl	100 µl	100 µl	100 µl
TEMED	10 µl	10 µl	10 µl	10 µl

*APS and TEMED were added right before use.

3.3.5 Vesicles-mediated transformation

Transformation experiments were performed using *E. coli* J53 (plasmid-free) as a recipient strain and outer membrane vesicles harvested from bacterial culture as donor molecules. The overnight culture of *E. coli* J53 was subcultured to fresh LB medium and incubated at 37°C at 180 rpm until optical density at 600 nm reached 0.4. Bacterial culture was mixed with purified vesicles, which have been pretreated with DNase I enzyme. The mixtures were then incubated at 37°C for 18 hours with shaking (100 rpm). Control experiments were carried out without vesicles or with 1 µg purified plasmid DNA. The bacterial cells that had acquired antibiotic resistance were selected on LB agar supplemented with a proper antibiotic and 200 mg/L of sodium azide. The plates were incubated for 48 h at 37°C and evaluated by colony counting. The antibiotic-resistant isolates were screened for the presence of the resistance gene by PCR. The size of transferred plasmid was evaluated by S1 nuclease digestion followed by pulsed-field gel electrophoresis (PFGE) as described in chapter 3.2.4.

3.3.6 Mass spectrometry analysis

For identification vesicular proteins, an Orbitrap Velos Pro mass spectrometer (Thermo Scientific, USA) was used. An ultimate nanoRSLC-HPLC system (Thermo Scientific, USA) was equipped with a nano C18 RP column and connected to the mass spectrometer through a nanospray ion source. 5 µL of the tryptic digest were injected onto a C18 column. Automated trapping and desalting of the sample was performed at a flowrate of 6 µL/min using water/0.05% formic acid as solvent. Separation of the tryptic peptides was attained with the following gradient of water/0.045% formic acid (solvent A) and 80% acetonitrile/0.05% formic acid (solvent B) at a flow rate of 300 nL/min: holding 4% B for five minutes, followed by a linear gradient to 45%B within 30 minutes and linear increase to 95% solvent B in additional 5 minutes. The column was connected to a stainless steel nanoemitter (Thermo Scientific, USA)

and the eluent sprayed directly to the heated capillary of the mass spectrometer using a potential of 2300 V. A survey scan with a resolution of 60000 within the Orbitrap mass analyzer was combined with at least three data-dependent MS/MS scans with dynamic exclusion for 25 s either using CID with the linear ion-trap or using HCD and orbitrap detection at a resolution of 7500. The analysis of data was done using Proteome Discoverer (Thermo Scientific, USA) with SEQUEST and MASCOT (version 2.2; Matrix science) search engines using a user defined database comprising the sequence of the protein of interest.

For analysis of lipid A fractions, an Ultraflex I TOF/TOF mass spectrometer (Bruker Daltonics, Bremen) equipped with a nitrogen laser and a LIFT-MS/MS facility was used. The instrument was operated in the positive-ion reflectron mode using 2.5-dihydroxybenzoic acid and methylendiphosphonic acid as matrix solution. Sum spectra consisting of 200-400 single spectra were acquired. For data processing and instrument control the Compass 1.1 software package consisting of FlexControl 2.4, FlexAnalysis 3.0 and BioTools 3.0 was used. External calibration was performed with a peptide standard (Bruker Daltonics).

3.3.7 Nuclear Magnetic Resonance (NMR) spectroscopy analysis

One- and two-dimensional 1H-NMR spectra were acquired on a Bruker AV600 spectrometer at temperatures between 280 and 310 K in DMSO-d6. Samples contained a 1-5 mM peptide antibiotic mixed with 0-300 mM calcium chloride dihydrate (Sigma Aldrich, Germany).

3.3.8 MCR-1 activity assay

The activity of MCR-1 was determined by using a substrate containing a fluorescent label, 1-acyl-2-{12-[(7-nitro-2-1,3- benzoxadiazol-4-yl)amino]dodecanoyl}-sn-glycero-3 phospho-ethanolamine (Acyl-NBD-PE) (Avanti Lipids, Alabaster, USA). To evaluate cleavage of pEtN group from acyl-NBD-PE catalyzed by MCR-1, 1µg of purified enzyme was added to 2µg of lipid substrate and incubated for 20 hours at RT. The reactions were applied to a TLC Silica gel 60 plate (Merck Millipore, Germany) and developed using ethyl acetate:methanol:water (7:2:1). The fluorescence signal on the plate was visualized in the Molecular Imager Gel Doc XR System (Bio-Rad, Hercules, USA). For confirmation of product formation (1-acyl-2-{12-[(7-nitro-2-1,3-benzoxadiazol-4-yl)amino]dodecanoyl}-sn-glycerol) the appropriate material was scraped off from the TLC plate and washed with methanol. The concentrated eluent was analyzed by mass spectrometry.

3.4 Cell culture techniques

Human cervical adenocarcinoma cells (HeLa) were used in this thesis. The eukaryotic cells were handled under a sterile laminar flow hood. Only sterile buffers, media, glassware, and consumables were used during working with cells.

3.4.1 Media and solution

Table 3.11 Media and solution used in this thesis.

DMEM	Dulbecco's Modified Eagle medium containing Earle's Salts, 1g/l D-glucose, L-glutamine and pyruvate
FBS	100% foetal bovine serum, inactivated at 56°C for 30 min
Freezing medium	90% FBS, 10% DMSO
HBSS	Hank's balanced salt solution without Ca^{2+}, Mg^{2+}, phenol red
NEA	100x non-essential amino acids
Opti-MEM	Reduced serum Eagle's minimum essential medium with HEPES, sodium bicarbonate, hypoxanthine, thymidine, sodium pyruvate, L-glutamine, trace elements and growth factors
PBS	Phosphate-buffered saline; without Ca^{2+} and Mg^{2+}
Trypsin/EDTA	1x trypsin/EDTA; 0.05%/0.02% (w/v) in PBS; without Ca^{2+} and Mg^{2+}

3.4.2 Culture of eukaryotic cells

Human cervical adenocarcinoma cells (HeLa) were maintained in 10 cm plates containing DMEM (Gibco, Thermo Scientific, USA) supplemented with 10% fetal bovine serum (FBS) at 37°C in a humid atmosphere of 5% CO_2. Cells were split every two to three days or whenever they attained 80–90% confluency. For splitting, the medium was removed and the cells were washed once with 4 ml of HBSS. To detach the adherent cells from the bottom of the plates, cells were incubated with 1.5 ml trypsin at 37°C in a CO_2-incubator for 3 min. The enzymatic reaction of trypsin was stopped by adding 1.5 ml of DMEM with 10% FBS, and the cells were then transferred into new cell culture plate containing the fresh medium. The total volume of medium in each petri dish was 10 ml. For storage, the detached cells were transferred into 15 ml tubes and centrifuged (700 rpm, 3 min, RT, Heraeus Megafuge 1.0 R centrifuge). The pellets were resuspended in freezing medium and placed into a 2 mL cryovials. The cells were either store at -80°C or in liquid nitrogen. To thaw frozen cells, cryovials were warmed up at 37°C and cells were transferred to a 10 ml dish containing 10 ml of fresh medium.

3.4.3 Transfection of eukaryotic cells

Cells were split approximately 18h prior to DNA transfections, and the confluency was between 60-75% at the time of transfection. For plasmid transfections, the cells (~$5x10^5$) were plated in 12-well plates and incubated at 37°C. Prior to transfection, the cells were washed three times with HBSS and the culture medium was changed to DMEM without FBS. HeLa cells were transfected with EGFP-LC3-plasmid. The plasmid DNA and lipofectamine 2000 were diluted in Opti-MEM medium and incubated for 5 min at RT (1 µg of plasmid DNA and 5 µl of lipofectamine 2000 per well). Diluted DNA and diluted lipofectamine were combined at a 1:1 ratio and incubated for 5 min at RT. The DNA-lipid complex was added to the cells and incubated at 37°C for 4h. Afterwards, fresh DMEM supplemented with 10% FBS was added and the cells were incubated for 24h.

3.4.4 Infection of eukaryotic cells

On the day of experiment, the HeLa cells were washed once with HBSS, the fresh DMEM medium was added and the cells were incubated at 37°C for 2h. Afterwards, the cells were washed carefully three times with prewarmed HBSS and the cells were kept in DMEM containing 0.5% FBS. The cells were then ready to be used for infection assays. For OMVs infections, the bacterial vesicles were prepared as described in chapter 3.3.5 and were added to the cells (1 or 3 µg of OMVs per well). The cell culture plates were incubated for 4 h at 37°C and 5% CO_2. The formation of autophagic vacuoles was observed by fluorescence microscopy (FM). Sample preparation for FM is described in chapter 3.5.1.

3.4.5 Immunoblotting

Following SDS-PAGE separation, protein sample were blotted onto a PVDF membrane for 1.5 hours at 72 mA by using an electroblotting apparatus (construction of the institute) in the presence of transfer buffer. Afterwards, membranes were blocked for one hour in blocking buffer (5 % milk powder in wash buffer). The membranes were then incubated with primary antibody followed by incubation with secondary antibody conjugated with horseradish peroxidase for overnight and 2 hours, respectively. Antibodies were diluted in blocking buffer. Then, the membranes were washed 3 times with TBST for 5 min per wash. The membranes were incubated with the enhanced chemiluminescence (ECL) detection system (Thermo Scientific, USA) for 1 min. Finally, the films were developed using a chemiluminescence imaging system (Syngene, Cambridge, UK).

3.5 Microscopic techniques

3.5.1 Fluorescence microscopy

For autophagy detection, the HeLa cells expressing GFP fused to LC3 gene were used to visualize the formation of autolysosomes observed as green puncta by fluorescence microscopy, BZ-8000K (Keyence, Neu-Isenburg, Germany). After the incubation of cells with OMVs, the culture medium was completely removed, and the cells were fixed with 500 µl of 3.7% formaldehyde in PBS for 10 min at RT. The coverslips were washed three times with PBS and were mounted on glass slides by using ProLong droplets with the cells facing down. The clear nail polish was used to seal the coverslips to the microscopic slides and then the samples were analyzed under the fluorescence microscope.

3.5.2 Transmission electron microscopy

The OMV or bacterial cell samples were applied on the formvar coated copper grids, negatively stained with 1% ammonium heptamolybdate or 1% uranyl acetate and subsequently decanted. Stained grids were allowed to air dry and then the samples were observed and imaged using a Zeiss EM900 transmission electron microscope (Carl Zeiss, Oberkochen, Germany). For ultrathin sectioning, the HeLa cells were seeded in a plastic chamber (Nunc Lab-Tek Chamber Slide system 2 wells, Permanox® slide) containing 2 ml of DMEM medium per well. After exposer to OMVs, the cells were rinsed with sodium cacodylate buffer (pH 7.4) and fixed with 2% glutaraldehyde in 0.1 M sodium cacodylate buffer for 1 h at room temperature, followed by post-fixation with 1% osmium tetroxide (OsO4) in 0.1 M sodium cacodylate buffer. The samples were then dehydrated in a graded series of ethanol (10%, 30%, 50%, 70%, 90% and twice 100%) for 10 min each and embedded in Epon resin (Pelco, USA) before ultrathin sections (70-100 nm) were applied to collodion-coated copper grids. The samples were then observed under Leo 912 transmission electron microscope (Carl Zeiss, Germany) at 80 kV accelerating voltage and combined with a TRS Sharpeye slow scan dual speed CCD camera (Albert Troendle Prototypentwicklung, Germany).

3.5.3 Field-emission scanning electron microscopy

The overnight bacterial culture was fixed with 5% formaldehyde and 1% glutaraldehyde in growth medium and dehydrated in a graded series of acetone (10%, 30%, 50%, 70%, 90% and twice 100%) on ice for 10 min each. Samples were then subjected to critical-point drying

apparatus with liquid CO_2 (CPD 030, Balzers, Liechtenstein). Dried samples were covered with a gold-palladium film by sputter coating (SCD 500, Balzers, Liechtenstein) before examination by field emission scanning electron microscope (FE-SEM) Zeiss Merlin (Carl Zeiss, Germany) with an accelerating voltage of 20 kV. Images were taken by the high efficiency SE2 detector. Contrast and brightness were adjusted by imageJ software.

3.6 *Galleria mellonella* infection assay

G. mellonella larvae were bred on an artificial diet containing 22% maize meal, 22% wheat germ, 17.5% bees wax, 11% dry yeast, 11% honey, and 11% glycerin at RT in darkness prior to infection. Bacterial inoculums were injected dorsolaterally into the hemocoel by using 1 ml hamilton syringe mounted on a microapplicator (Figure 3.2). After injection, larvae were incubated at 37°C in dark. Larvae were considered dead when they exhibited no movement in response to touch. No mortality of *G. mellonella* larvae was noted when they were injected with 0.85% sodium chloride solution. For cfu counting, infected *Galleria larvae* were homogenized in LB medium with 1% Triton X-100. Homogenates were plated onto LB agar plate and colonies were counted after incubation at 37°C for 24 h. For priming of *G. mellonella*, the larvae were injected with 3µg of bacterial OMV to trigger immune responses. 24 h after the administration of vesicles, different amount of various bacterial species were injected into each larva for determination of survival rates.

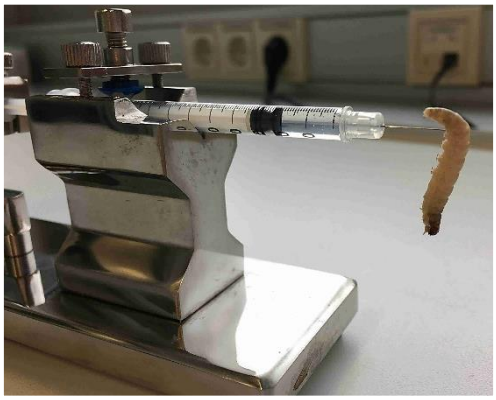

Figure 3.2 **Infection of *G. mellonella* larva with bacterial inoculum.** The larvae were infected by intrahemocoelic injection of bacterial inoculum through the last left pro-leg by using an injection apparatus. The survival rate of larvae was monitored for 7 days post bacterial challenge.

3.7 Bioinformatics tools used in this study

Cytoscape software (Institute for Systems Biology, USA) was used for visualizing protein-protein interaction networks and integrating these networks with annotation data. CBS Prediction Servers (Center for biological sequence analysis, Technical University of Denmark) including transmembrane helices prediction method based on a hidden Markov Model (TMHMM) was used to predict the presence of transmembrane helices in proteins of interest. The RaptorX structure prediction server (Källberg et al. 2012a) was used to predict tertiary structure of a protein sequence using known structure as a templates. The Pfam library of annotated protein domains (European Bioinformatics Institute, UK) was used to identify the domain architecture of analysed proteins. The Prosite and Myhits database (SIB Swiss Institute of Bioinformatics, Switzerland) were used to find the domains, families and functional sites within investigated proteins. The list of all bioinformatics tools used in this thesis is presented in Table 3.12.

Table 3.12 Bioinformatic softwares used in this study.

Software	Company
Brig	Open Source
Cytoscape	Institute for Systems Biology, USA
SeqBuilder	DNASTAR, USA
Easyfig	Beatson Microbial Genomics Lab.
EggNog 4.5 database	Embl, Germany
NEBcutter V2.0	New England Biolabs, UK
NEBuilder Assembly Tool	New England Biolabs, UK
Snapgene	GSL Biotech, USA

Construction of the protein - protein interaction network (PPIN)

To map the identified proteins of OMVs into the PPI network, all vesicular proteins were converted to gene symbols. Protein interaction data were gathered from the database of binary protein-protein interaction landscape of *Escherichia coli* (Rajagopala et al. 2014), which contains 2,234 high-quality PPIs among 1,269 proteins. Using the protein interaction data, the PPI networks for the vesicular proteins were constructed. The PPIN was visualized using Cytoscape software version 3.5.1 with self-interactions being removed prior to analysis.

3.8 Statistical analysis

The data were calculated and represented as mean +/- standard deviation (SD) from at least three independent trials. The statistical analysis toolkit included in the MS Excel 2016 (Microsoft, USA) package was used to test variances between experimental sets and

subsequently run the t-test. For all statistical operations $P < 0.05$ were considered as significant p-values. The graphs were plotted with Excel (Microsoft, USA) computer software.

4 Results

Section I

4.1 Isolation of outer membrane vesicles and their contribution to spread of bacterial intracellular constituents

4.1.1 Optimization of method for isolation of outer membrane vesicles

A main limitation in studying the OMVs is the great effort and the lack of standardization for already challenging procedures to isolate these nanometer-sized structures (Momen-Heravi et al. 2013). The current gold standard and most commonly used technique for OMVs purification is differential centrifugation and filtration, which involve a number of centrifugation, ultracentrifugation and filtration steps followed by quantification of vesicular proteins using e.g., Bradford assay and their quality control by electron microscopy. In this thesis, the outer membrane vesicles were isolated according to a previously described method with modifications (Kadurugamuwa & Beveridge 1995). I recommend this optimized protocol for everybody else as it results in a higher yield of bacterial blebs with greater purity and quantity.

The workflow of OMVs isolation used in this study is shown in Figure 4.1 and detailed described in chapter 3.3.2.

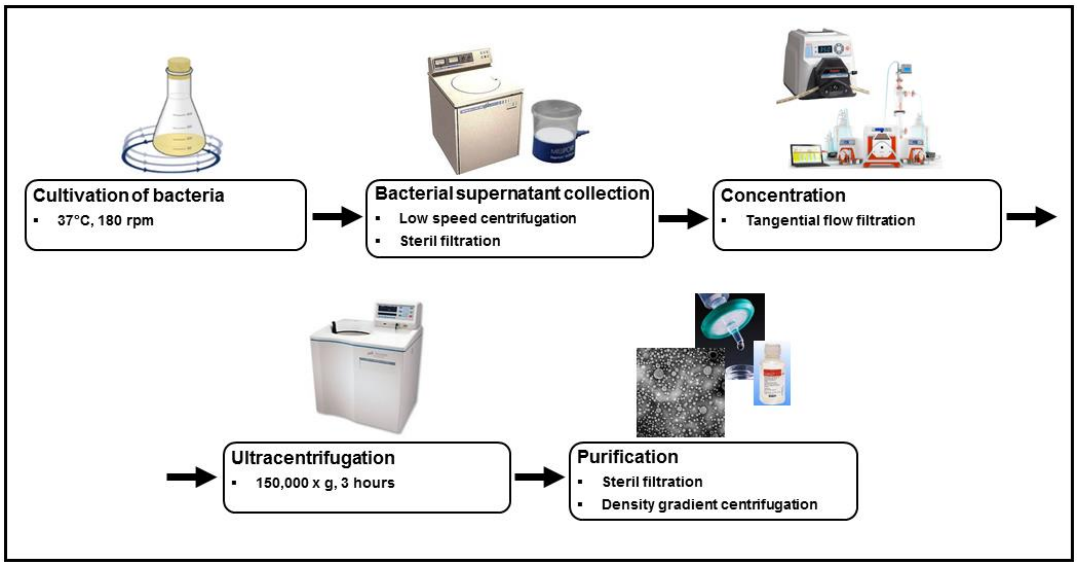

Figure 4.1 **Workflow of OMV isolation.** Vesicles purification protocol includes the following steps: Cultivation of bacterial isolates – the type of medium, incubation time and addition of antibiotics might influence the vesiculation rate and composition of OMVs; Removal of intact bacteria – low speed centrifugation followed by sterile filtration remove any residual bacterial cells; Concentration of the supernatant – ultrafiltration approach is usually used to preconcentrate the filtrate prior to ultracentrifugation; Purification – sterile filtration or density gradient centrifugation can by carried out to

remove any non-OMV-associated contaminants, such as flagella and pili structures. The final step should include the quantification of vesicular protein by e.g., Bradford assay and quality control assessed by electron microscopy. Additionally, the absence of viable bacteria is confirmed by plating out the aliquots of OMV samples onto LB agar plates to test bacterial growth.

In order to isolate bacterial vesicles, the OMVs were harvested from liquid culture after appropriately long incubation time. Too short cultivation results in very low OMVs yield, whereas too long bacterial growth leads to vesicles contamination through the broken membranes, debris and cytoplasmic proteins (Klimentová & Stulík 2015). Therefore, to keep possibly high vesicle yield and low impurity level, bacteria were grown until early-stationary phase. The next step in OMVs isolation included removal of intact bacteria by centrifuging at 6000 x g for 30 min at 4°C. The supernatant was further sterile filtrated through 0.22 μm, PVDF membrane (with low protein binding properties) to remove any residual cells. As a total amount of vesicles in the media is very low, a subsequent concentration step by e.g., ultrafiltration (UF) is very required and constitutes a crucial stage in OMVs purification. Supernatants were concentrated using two types of UF systems. Initially, the tangential flow filtration (TFF) device (Pall Corporation, USA), in which the solution flows through the system under gentle pressure in a parallel direction to the membrane was used (Figure 4.2A). Although, Pall TFF system exhibit highly predictable performance characteristics and yields, its throughput is very compromised, resulting in filtration speed only up to 1 L of culture per hour. Thus, I switched to cross-flow (CF) based filtration system (Spectrum Labs, USA), which has higher overall liquid removal rate compare to Pall TFF filtration (Figure 4.2B).

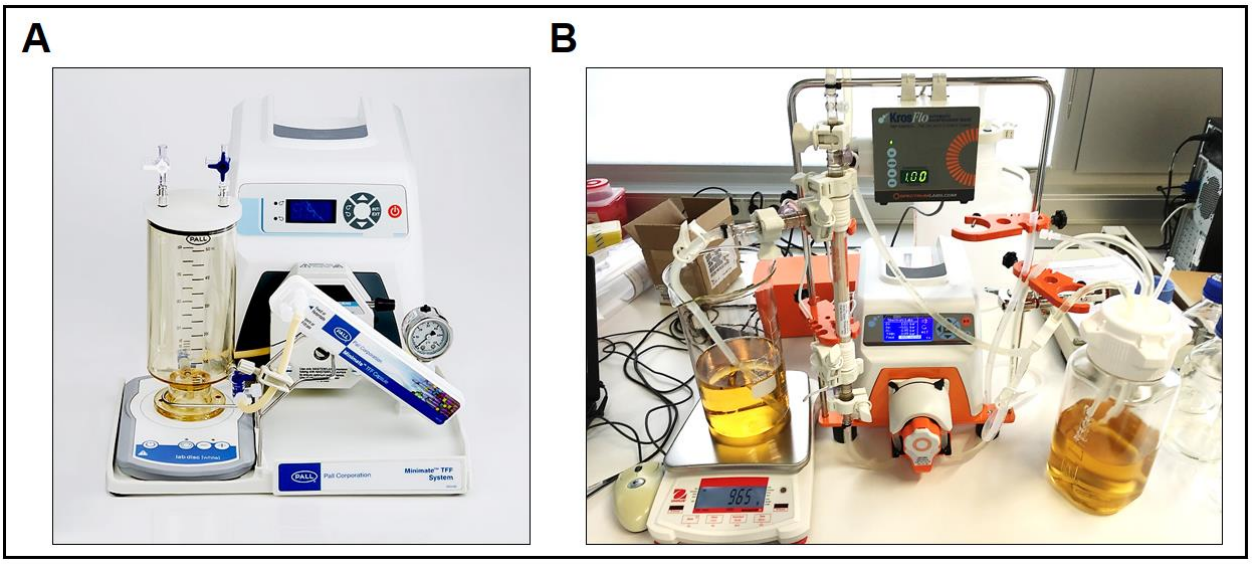

Figure 4.2 **Ultrafiltration devices used for OMVs isolation.** Ultrafiltration (UF) methods depend on the use of polymeric membranes with highly defined pores to separate molecules according to their size.

The tangential flow filtration (TFF) systems produced by Pall Corporation (A) and Spectrum Labs (B) were used**.** In UF process during OMVs isolation, a sterile filtrated bacterial supernatant was passed through a membrane with an appropriate molecular weight cut-off (100 kDa) to remove most of non-OMV-associated proteins and concentrate the OMVs-containing retentate prior to ultrafiltration.

By using Spectrum Labs filtration unit equipped with 100 kDa (molecular weight cut-off) hollow fiber membranes, proteins and other contaminants under 100 kDa were removed from supernatant and concentration time of 1 L of medium was reduced to approximately 10 min. The OMVs were afterwards pelleted from 50 times concentrated retentate by ultracentrifugation at 150,000 x g for 3 h at 4°C and resuspended in phosphate buffered saline. In order to exclude the other extracellular materials from the OMV preparations, it is extremely important to filter the retentate and then again pelleted crude vesicles through 0.22 μm syringe filter.

The protocol for OMVs isolation was optimized based on a very motile *Enterobacter* 247 isolate. To purify vesicles from highly flagellated bacteria and separate them from other contaminants including flagella, fimbria and pili, density gradient centrifugation (DGC) needs to be employed (Dauros Singorenko et al. 2017). OMVs are composed of lipids, and therefore their density is lower than that of flagella, pili and various soluble secreted proteins. The crude OMVs obtained after ultracentrifugation were mixed with high density OptiPrep solution, overlaid with step gradients of lower-density solutions and centrifuged 20 hours at 150,000 x g. Equal volume fractions were collected from the top of each gradient and analyzed by CBS SDS-PAGE and TEM microscopy (Figure 4.3). According to TEM micrographs, the purification technique utilizing DGC allowed for removing flagella-like contaminants. Optimized here method for isolation and purification of sufficient amounts of OMVs from bacterial cultures represents a pivotal step for the subsequent analyses.

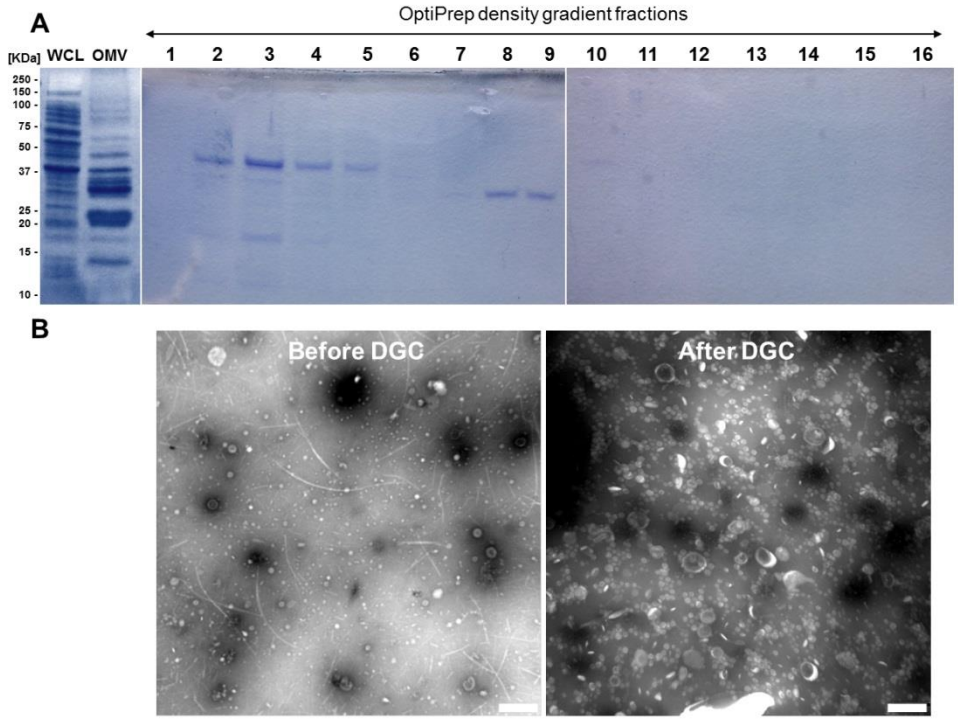

Figure 4.3 **Purification of OMVs derived from *Enterobacter* 247 by OptiPrep density gradient centrifugation (DGC).** OMVs were resuspended in 45% OptiPrep solution in 50 mM HEPES - 150mM NaCl, pH 6.8 and layered below OptiPrep density gradient (2 ml of 40%, 35%, 30%, 25% and 20% in HEPES) followed by centrifugation for 20 hours at 150,000 x g. Equal volume fractions (0.75 ml) were obtained sequentially from the top of each gradient and analyzed by Coomassie-stained SDS-PAGE **(A)** and TEM analysis **(B)** (fraction 3 shown). WCL - whole-cell lysate fraction, OMV - outer membrane vesicle fraction; Scale bar, 200 nm.

4.1.2 Involvement of the OMVs in antibiotic resistance

OMVs can mediate resistance to antibiotics through a diverse set of mechanisms. In some cases, they can serve as a vehicle for the transport of plasmids encoding antibiotic resistance. This mechanism of vesicles-mediated antibiotic resistance is discussed in chapter 4.3. In other cases, OMVs can carry active β-lactamases, and therefore provide protection against antibiotic-induced killing.

To detect the presence of active β-lactamase enzymes in OMVs, the chromogenic cephalosporin substrate Nitrocefin was used. OMVs derived from *Enterobacter* 247 and *E. coli* DH10β harboring pUC19 plasmid that encodes β-lactamase gene were mixed with Nitrocefin followed by spectrophotometric measurement (Figure 4.4A). The β-lactamase activity of vesicles was measured by the ability of the enzyme to hydrolyze the β-lactam Nitrocefin, leading to a change in absorbance from OD_{390} to OD_{486}. OMVs isolated from both *Enterobacter*

247 and *E. coli* carrying pUC19 were β-lactamase positive as Nitrocefin's color changed from yellow to red within 30 min.

To reveal whether vesicles derived from β-lactamase-producing bacteria can protect ampicillin-susceptible isolates, the *E. coli* DH10β (10^3 CFU/ml) was exposed to 10 μg of *Enterobacter* OMVs containing active β-lactamases, followed by streaking out the suspension onto LB agar plate supplemented with 100 mg/L of ampicillin. A significant increase in the number of CFU was noted for ampicillin-susceptible *E. coli* culture that had been preincubated with β-lactamase-carrying OMVs as compared to the control bacteria exposed to PBS (Figure 4.4B). Furthermore, when antibiotic-susceptible *E. coli* DH10β was incubated with β-lactamase-negative OMVs, bacteria were not able to grow on the ampicillin plate. The addition of vesicles in the absence of ampicillin did not interfere with bacterial growth (data not shown).

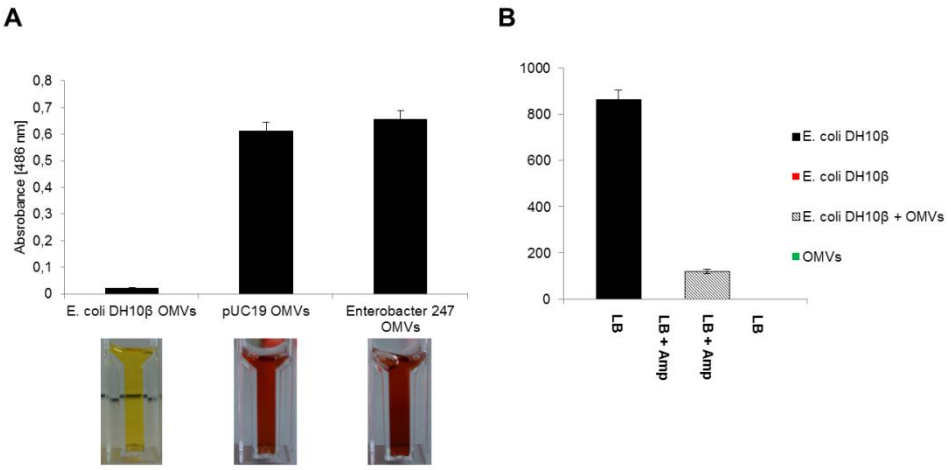

Figure 4.4 **OMVs-mediated protection against Ampicillin antibiotic. (A)** β-lactamase activity of bacterial OMVs was assessed by spectrophotometric assay using a chromogenic cephalosporin substrate (Nitrocefin, Thermo Scientific, USA). Nitrocefin has changed its color from yellow to red in the presence of active β-lactamases that are present inside outer membrane vesicles. **(B)** OMVs-mediated protection against Ampicillin-induced killing. Antibiotic-susceptible *E. coli* DH10β was protected against ampicillin in the presence of OMVs carrying β-lactamases, as determined by plating of the mixture of OMVs and bacteria onto LB agar plates supplemented with 100mg/L of ampicillin. Data are expressed as the mean value ± SEM of at least three independent experiments.

4.1.3 OMVs-mediated transfer of metabolites

To examine the ability of bacterial vesicles to mediate the exchange of cytoplasmic components, a pair of two amino-acid auxotrophs of *E. coli* was assembled. *E. coli* DH10β is auxotrophic for leucine (Leu), while strain of *E. coli* J53 is auxotrophic for methionine (Met) and proline (Pro). Therefore, both strains are unable to grow in the absence of an external supply

of either Leu or Pro and Met. Consequently, their growth in the coculture is indicative of the amino acid synthesis of the respective other strain. The scheme of the experimental setup for the analysis of the metabolites transfer mediated by OMVs is depicted in Figure 4.5A. Moreover, the cytoplasm of one partner in the pair of *E. coli* was labelled with a plasmid that encoded resistance to ampicillin (blaTEM-116) and constitutively expressed the enhanced green fluorescent protein (EGFP). The ability of OMVs to spread both green fluorescent protein and plasmid DNA encoding resistance to ampicillin was investigated. The transfer of EGFP was evaluated by observing via fluorescence microscopy the population of recipient *E. coli* J53 that have been preincubated with vesicles derived from donor *E. coli* DH10β cells and were able to fluoresce in green colour. A strong selection pressures for limiting resources was induced by culturing the autotrophs in M9 minimal medium. This experiment provided evidence for transfer of cytoplasmic protein mediated by OMVs, which was observed by a significant increase of EGFP-labelled *E. coli* J53 cells (Figure 4.5B). Additionally, in order to assess the transfer of plasmid DNA from OMVs to recipient cells, the mixture of donor-vesicles and recipient-*E. coli* J53 was plating out on ampicillin-containing plates after 1, 6 and 24 h of incubation. However, there was no indication for a transfer of plasmid DNA between cells under the given conditions, as not a single colony formed on the ampicillin-containing plates was detected.

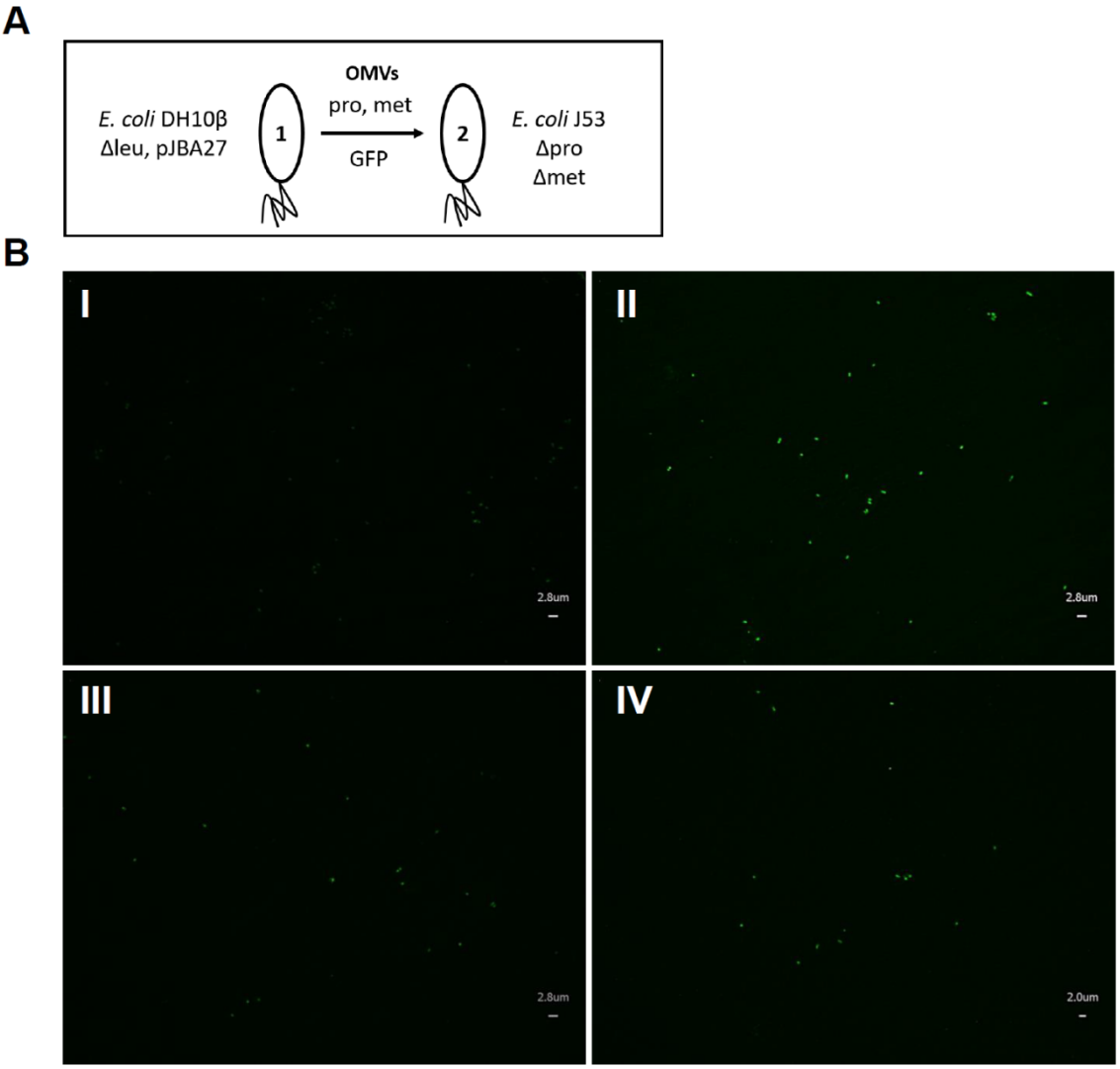

Figure 4.5 **Transfer of cytoplasmic marker mediated by outer membrane vesicles. (A)** A scheme of the experimental setup used for analysis of the OMV potential to transfer metabolites. **(B)** The outer membrane vesicles isolated from *E. coli* DH10β, ΔLeu were co-incubated with strain of *E. coli* J53, which is auxotrophic for Met and Pro. The donor of OMVs contained an EGFP-expressing plasmid that conferred resistance to the ampicillin antibiotic, while the recipient *E. coli* J53 was unlabeled and susceptible to ampicillin. Fluorescence pictures show *E. coli* J53 **(I)**, *E. coli* DH10β expressing EGFP **(II)** and the mixture of *E. coli* J53 preincubated with OMVs derived from *E. coli* DH10β harboring EGFP-pJBA27 plasmid **(III, IV)**. Exposure time, 0.5 s; Magnification, 600x; Scale bars, 2 and 2.8 μm.

4.2 *HlyF*-induced formation of outer membrane vesicles in *E. coli*

To date, a number of models for OMV biogenesis have been proposed (see chapter 1.4.1), yet the exact molecular mechanism leading to OMV formation and regulation remains unknown. By analyzing plasmid sequences of different highly virulent *E. coli* ST131 outbreak isolates, I found the strains that naturally harbor ColV plasmids encoding several virulence factors, such as iss, tsh, iroN, sitA, cavB, iutA as well as two variants of hemolysin F (*hlyF*) gene. The *hlyF* gene is mainly located on ColV plasmids and is epidemiologically associated to the most virulent strains of Avian Pathogenic *E. coli* (APEC) and Neonatal Meningitis *E. coli* (NMEC) (Morales et al. 2004; Johnson et al. 2006). An *in silico* analysis demonstrated that the *hlyF* gene would have a NAD-dependent epimerase/dehydratase activity and may therefore be involved in the remodeling of the bacterial outer membrane, triggering increased OMV formation. In this study, I examined two *E. coli* isolates that possess complete and naturally truncated *hlyF* genes in the context of their vesiculation capabilities and the involvement of *hlyF* in cell wall modification.

4.2.1 Comparative genomics reveals truncation in *hlyF* gene on ColV plasmid of *E. coli* H16 strain

Whole genome sequencing analysis of *E. coli* isolates collected from samples of clinically ill patients revealed two strains including *E. coli* H8 and *E. coli* H16 that harbour ColV plasmids. The ColV plasmids are known to encode for virulence genes and pathogenicity islands (PAIs), which are linked to the high virulence capability. Therefore, to detect such a conserved virulence gene cluster, I screened different virulence genes on ColV plasmids derived from these two strains. The analysis could identify a cluster of conserved virulence genes located on ColV plasmid of both the strains (Figure 4.6). In gene by gene comparative analysis between H8 and H16 strains, the *hlyF* gene of the *E. coli* H16 was observed to be truncated. Further nucleotide comparisons revealed loss of 231 nucleotides at the 5’ end of the gene.

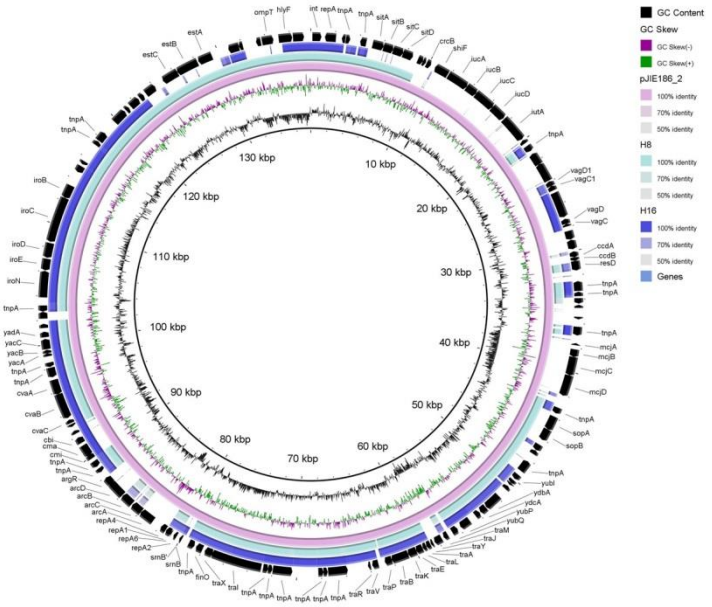

Figure 4.6 **The comparison of ColV plasmids present in *E. coli* H8 and H16.** The different rings represent (from inner to outer) deviation from average G+C content (ring 1), GC skew ((G2C)/(G+C); ring 2), pJIE186-2 reference plasmid (ring 3) and all genes and insertion elements, which are present on ColV plasmids isolated from *E. coli* H8 and H16 (rings 4 and 5, respectively). The map was generated by BLAST Ring Image Generator (BRIG) software. As a reference pJIE186-2 plasmid was used (Zong 2013).

4.2.2 The *E. coli* isolate carrying a complete *hlyF* exhibits a hypervesiculation phenotype compare to isolate with truncated version of the gene

The production of OMVs derived from the isolates of *E. coli* H8 expressing complete *hlyF* and *E. coli* H16 carrying a truncated version of this gene was accessed by quantification methods, including Bradford and β-lactamase activity assays. The protein concentration of OMVs determined by Bradford assay was 68.6 µg/L and 3.9 µg/L for *E. coli* H8 and H16, respectively (Figure 4.7A). The β-lactamase activity of vesicles amount to 1.4 and 0.4 for H8 and H16 (Figure 4.7B). Moreover, the vesicles were examined by transmission electron microscopy (TEM). Quantification of the OMVs revealed that the amount of bacterial blebs was significantly higher for the isolate expressing a full-length *hlyF* gene (Figure 4.7C). Together, these data indicated that an intact HlyF contributes to the overproduction of OMVs. Additionally, these results indicate that bacteria can not only overproduce, but also underproduce the outer membrane vesicles via modification of hemolysin F. Therefore, *hlyF* is the first virulence factor, which may serve as a natural biological switch that regulates vesiculation rate in bacteria, and consequently may contribute to the bacterial pathogenic properties.

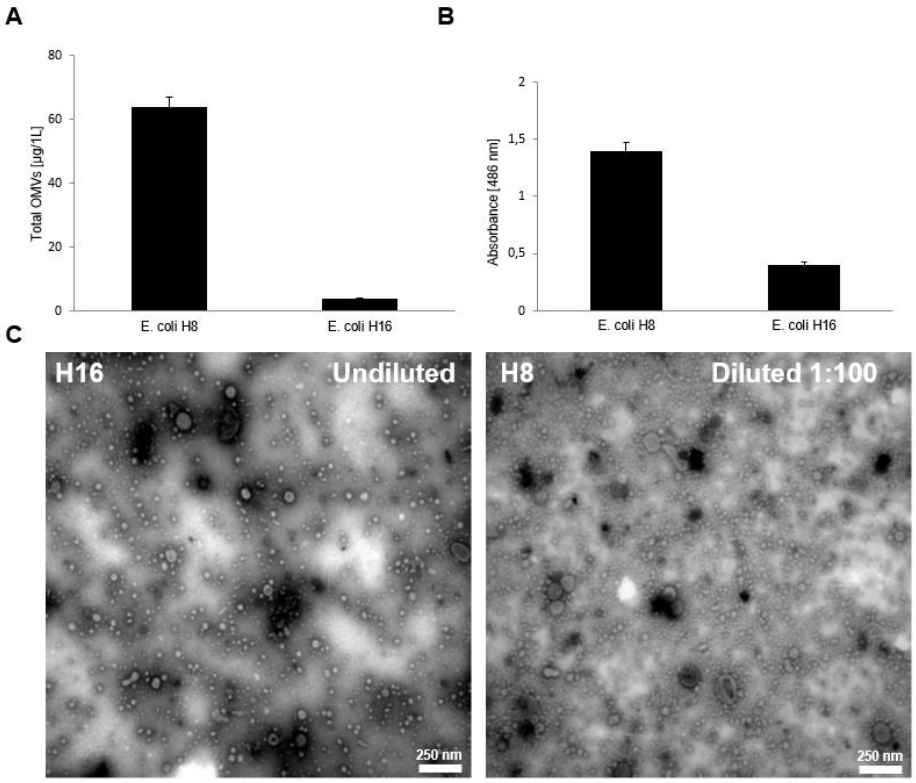

Figure 4.7 **The quantification of the OMV production derived from isolates of *E. coli* H8 and H16.** The OMVs were isolated from the bacterial culture by differential centrifugation and filtration steps followed by quantification using Bradford assay (A), β-lactamase activity test (B) and transmission electron microscopy (TEM) (C). All three quantification methods revealed that isolate of *E. coli* H8 harboring complete *hlyF* gene secreted significantly more OMVs compare to Δ*hlyF E. coli* H16. The outcomes (figure A and B) are presented as the mean ± SEM from three independent experiments.

4.2.3 Truncated *HlyF* lost an essential coenzyme NAD(P) binding site

BLAST analysis of a complete amino acid sequence of HlyF indicates strong similarity to the extended short-chain dehydrogenase/reductase (SDRs) that constitute a large NADB-Rossmann protein superfamily. This structural motif is found in enzymes including isomerases (e.g., glycosyl epimerases), lyases (e.g., glycosyl dehydratases) and some oxidoreductases (e.g., enzymes with both isomerase/dehydrogenase activities) (Kallberg et al. 2002; Kavanagh et al. 2008). A number of functionally defined SDRs play a role in LPS biosynthesis, such as WbpM and WbpK (Charter & Lam 1996) as well as carbohydrate, amino acid, and cofactor metabolism (Murase et al. 2016). Therefore, HlyF is likely to act as a fatty acyl CoA reductase or putative nucleoside-diphosphate-sugar (NDS) epimerase, and thus be involved in LPS synthesis or biogenesis of bacterial cell wall. An *in silico* analysis revealed the absence of 231 nucleotides at 5' end of *hlyF* gene in *E. coli* H16 (Figure 4.8). This mutation results in N-terminal deletion of 77 amino acids that leads to a loss of an essential coenzyme (NAD-(P)) binding site of HlyF

protein. As described above, vesiculation rate of *E. coli* H16 was significantly decreased compare to OMV levels released by *E. coli* H8 expressing a complete *hlyF* gene. Based on this data, it can be speculated that the loss of N-terminal part of HlyF including NAD-(P) binding site caused a defect in enzymatic activity, resulting in hypovesiculation mode of *E. coli* H16. These outcomes suggest that hemolysin F protein contributes to modulation of outer membrane vesicle formation and that the N-terminal domain is required for functional active this enzyme.

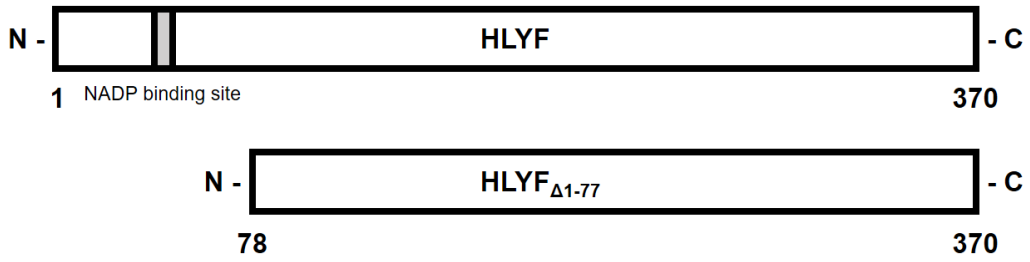

Figure 4.8 **A Schematic representation of HlyF protein and its truncation.** *E. coli* H16 expresses truncated version of hlyF gene, leading to protein synthesis with N-terminal deletion of 77 amino acids that results in a loss of an essential coenzyme (NAD-(P)) binding site. Due to the mutation, *E. coli* H16 released decreased amount of OMVs.

4.2.4 Overexpression of *hlyF* results in hypervesiculation in *E. coli* K12 DH10β

To further examine the relationship between expression of hemolysin F and production of OMV, complete *hlyF* gene was cloned into pUC19 in accordance with translational coupling strategy and recombinantly expressed in *E. coli* K12 DH10β. Subsequently, the resulting *E. coli* recombinant strain was analyzed for its vesiculation phenotype. OMVs isolated from *E. coli* harboring recombinant and empty plasmid were purified and quantified via Bradford, β-lactamase activity assay and transmission electron microscopy (TEM). The indirect analysis of vesicle formation determined by Bradford and β-lactamase activity assays demonstrated substantial increase in OMVs production, for recombinant of *E. coli* harboring pUC19::*hlyF* as compared to an empty vector control (Figure 4.9).

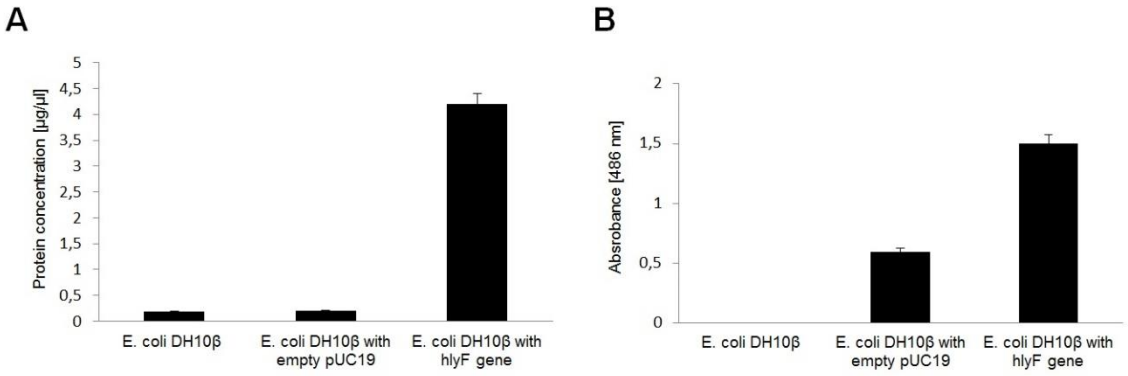

Figure 4.9 **The quantification of the OMV production in *E. coli* DH10β expressing *hlyF*.** OMVs were isolated from *E. coli* DH10β harbouring either no plasmid, empty pUC19 or pUC19::*hlyF*. Following the vesicles purification, the level of OMVs was estimated by Bradford assay **(A)** and β-Lactamase activity test **(B)**. Data are expressed as the mean value ± SEM of at least three independent experiments.

Additionally, the elevated production of OMV was further confirmed by transmission electron microscopy analysis, which revealed high numbers of OMVs in *hlyF* positive *E. coli* (Figure 4.10 and Figure 4.11).

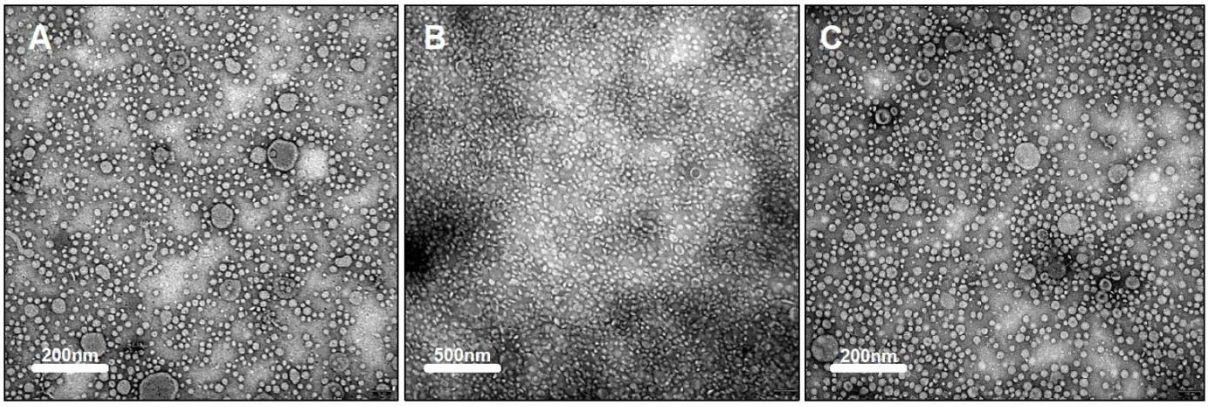

Figure 4.10 **Transmission electron micrographs of pelleted OMVs derived from *E. coli* DH10β expressing *hlyF*.** OMVs have been isolated from *E. coli* DH10β harboring either empty pUC19 plasmid or pUC19::*hlyF*. Following negative staining with 1% ammonium heptamolybdate (pH 7.0), OMVs were applied to 0.5% Formvar-coated 300-mesh copper grids and visualized by Zeiss EM900 transmission electron microscope. Photo A shows OMVs isolated from empty vector control. Photo B and C represent vesicles extracted from *E. coli* producing HlyF. Sample depicted in image C was diluted 1:100 in phosphate-buffered saline (PBS) for better visibility of OMVs.

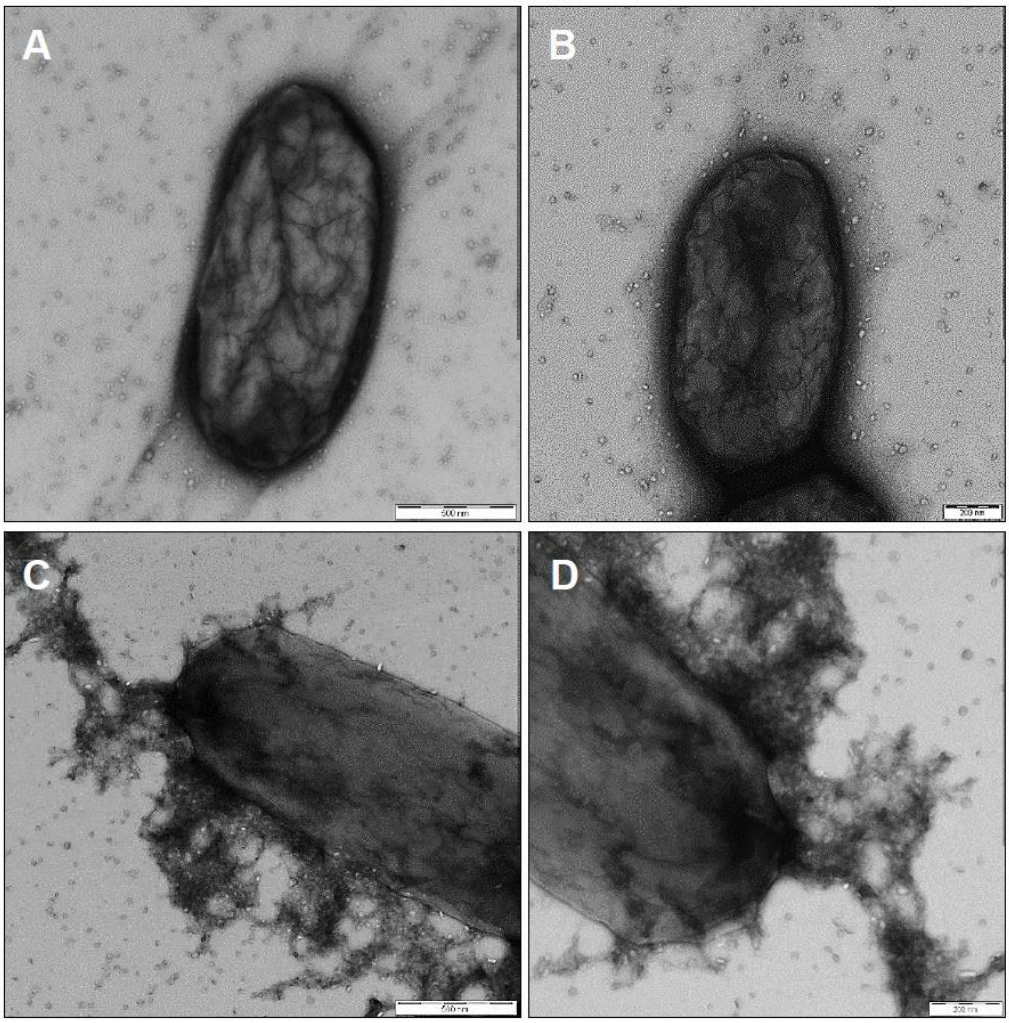

Figure 4.11 **Transmission electron micrographs of *E. coli* DH10β cells along with their OMVs.** Bacterial culture was fixed with 1% glutaraldehyde and applied intact to 0.5% Formvar-coated 300-mesh copper grids followed by negative staining and visualizing by Zeiss EM900 transmission electron microscope. Micrographs A and B represent *E. coli* harboring empty pUC19 plasmid, Micrographs C and D show *E. coli* expressing *hlyF* gene. A 1% ammonium heptamolybdate was used as a negative counterstain.

To gain different perspective on OMVs that are being released from bacterial cells, a field emission scanning electron microscopy (FE-SEM) analysis was performed. The FE-SEM indicated the significant increase of protruding OMVs from the cell surface of *E. coli* expressing recombinant *hlyF* gene as compared to *E. coli* harboring an empty plasmid. (Figure 4.12) Altogether, these outcomes showed that *hlyF* contributes to augmented OMVs formation in *E. coli* DH10β.

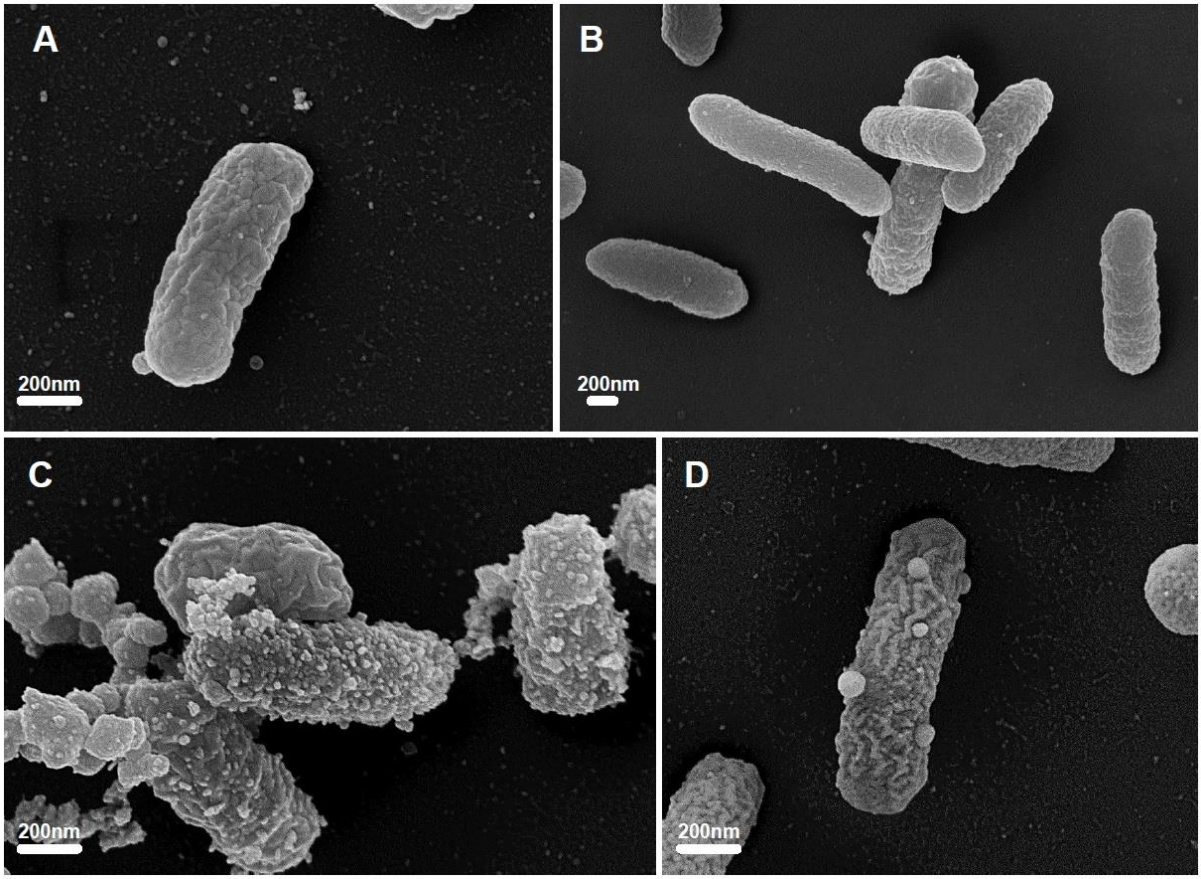

Figure 4.12 **The field-emission scanning electron micrographs of *E. coli* DH10β secreting vesicles.** Bacterial cells were fixed by incubation with 2.5% glutaraldehyde followed by post-fixation with 1% osmium tetroxide and dehydration in a graded series of acetone. After drying in a critical point dryer, the bacterial cells were mounted on specimen stubs, and gold/palladium-coated using a sputtering device. Images were acquired by Zeiss Merlin field-emission scanning electron microscope with an accelerating voltage of 20 kV. Micrographs A, B present *E. coli* harboring empty pUC19 plasmid. Micrographs C, D show *E. coli* expressing *hlyF* gene.

4.2.5 *hlyF*-induced OMVs trigger formation of autophagic vacuoles in eukaryotic cells

To examine the biological effects of *hlyF*-induced OMVs on eukaryotic cells, human epithelial carcinoma cell line (HeLa) had been transfected with a GFP-LC3 expressing plasmid and exposed to OMVs derived from *hlyF*-positive or negative *E. coli*. The expression of fusion gene followed by OMVs treatment revealed formation of autophagosomes, observed under fluorescence microscopy as green punctate structures in HeLa cells (Figure 4.13).

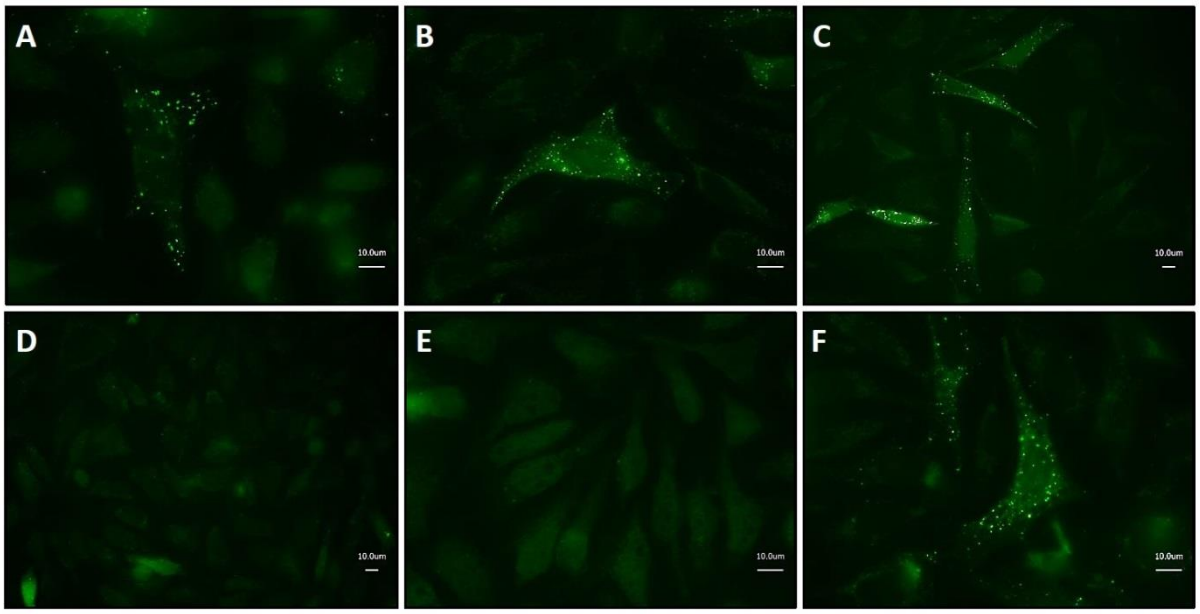

Figure 4.13 ***hlyF*-OMVs induced autophagy in HeLa cells.** HeLa cells expressing GFP-LC3 fusion protein were cultured on glass coverslips and treated with OMVs. The relocation of GFP-LC3 from a diffuse staining pattern in the cytoplasm and nucleus to a cytoplasmic punctuate structure was used to detect autophagy. Images (A-C) show autophagosome formation in response to *hlyF*-induced OMV. Images (D-E) present HeLa cells exposed to PBS, *hlyF* negative OMVs and Rapamycin, respectively. Rapamycin was used as positive control of LC3 conversion.

Autophagy induced by *hlyF*-OMVs was further investigated by transmission electron microscopy of ultrathin sections of HeLa cells. As shown in (Figure 4.14) upon the treatment with vesicles, an abundance of vacuoles were found in the cytoplasm of HeLa cells. Under high magnification, autophagic vacuoles were observed in *hlyF*-induced OMVs treated host cells. Rapamycin-treated cells were included as an autophagy control. These results suggest that *hlyF*-positive bacterial vesicles distinctively induce formation of autophagic vacuoles in HeLa cells.

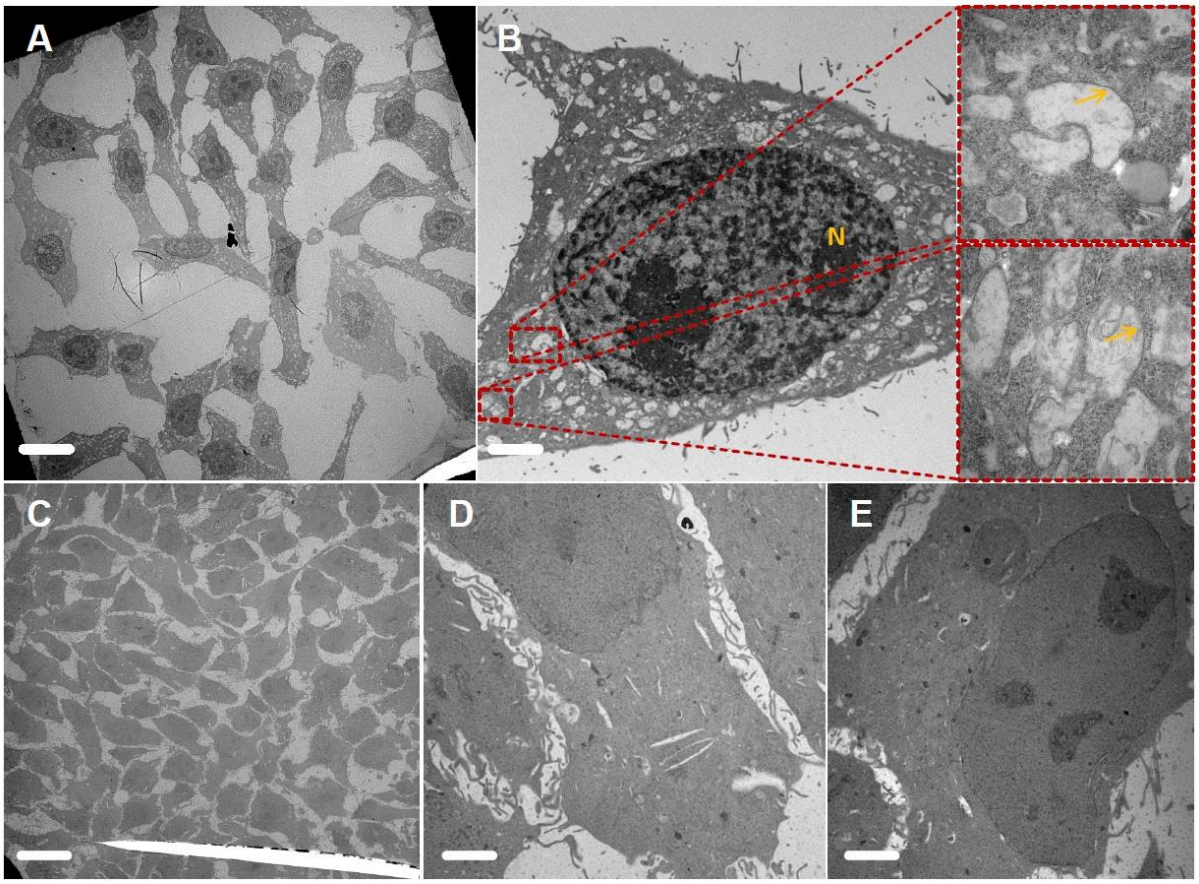

Figure 4.14 **TEM images of ultrathin sections of HeLa cells after OMV treatment.** HeLa cells showing the formation of autophagic vacuoles upon the treatment with *hlyF*-induced OMVs isolated from *E. coli* DH10β. The ultrathin sections (70-100 nm) of cells pretreated with vesicles were cut with ultra-microtome and applied to collodion-coated copper grids. Subsequently, the stained sections were analyzed using Leo 912 transmission electron microscope (Carl Zeiss, Germany) at an accelerating voltage of 80 kV equipped with a TRS Sharpeye slow scan dual speed CCD camera. Images (A and B) present HeLa cells exposed to Rapamycin and *hlyF*-induced OMVs, respectively. Images (C-E) show cells treated with PBS as a negative control. Rapamycin was used as positive control of LC3 conversion. (N = nuclear; arrows indicate the presence of autophagic vacuoles. Magnification was x500 for A, C, x3150, x31500 for B and x5000 for D, E.

4.3 Outbreak-causing, *Citrobacter freundii* carrying KPC-2 Carbapenemase gene and its vesicles-mediated genetic transformation potential

I analyzed a repertoire of carbapenemase-encoding *Enterobacteriaceae*, including multiple species of *Citrobacter* genus in the context of transferring of carbapenemase-encoding plasmids to other bacteria. I found several outbreak isolates of *C. freundii* harbouring plasmids that encodes KPC-2 resistance gene and were able to release vesicles into milieu. One particular isolate of *C. freundii* NRZ 08698 had a unique property of secreting the OMVs containing antibiotic resistance genes. This feature might play a pivotal role in success of this opportunistic pathogen and help bacteria to accommodate to the hostile environment. Therefore, I assessed the potential contribution of OMVs derived from the isolate of *C. freundii* to disseminate the carbapenem resistance genes into other members of the *Enterobacteriaceae* family.

4.3.1 *C. freundii* releases OMVs to surrounding environment

I first investigated whether *C. freundii* shed vesicles during *in vitro* growth. The OMVs were isolated from bacterial culture according to above-mentioned protocol (chapter 3.3.2). Thereafter, the FE-SEM and TEM microscopy were used to visualize the purified OMVs as well as vesicles that are being released from the surface of *C. freundii* cells. According to electron microscope images, *Citrobacter* isolate constantly spread vesicles into extracellular environment and they were clearly visible on the bacterial cells (Figure 4.15). There was no one place on the bacterial cell surface, which was involved in formation of OMVs, but the entire membrane of the bacterium was taking part in releasing of these molecular structures into the environment.

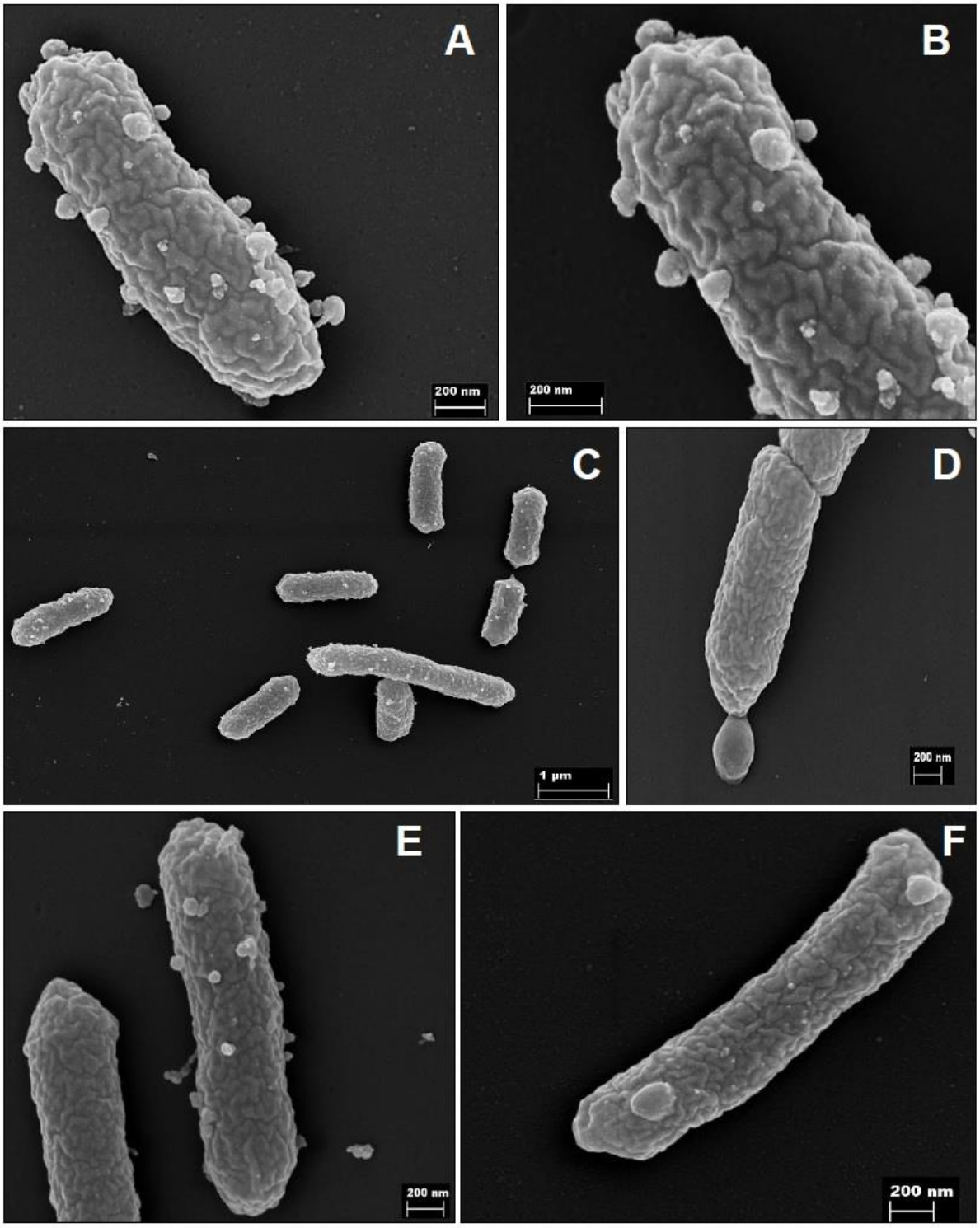

Figure 4.15 **The field-emission scanning electron micrographs of *C. freundii* NRZ 08698 cells secreting vesicles.** Intact bacterial culture was fixed with 1% glutaraldehyde followed by dehydration in a graded series of acetone. After drying in a critical point dryer, the samples were mounted on specimen stubs, and gold/palladium-coated using a sputtering device. Images were acquired by Zeiss Merlin field-emission scanning electron microscope with an accelerating voltage of 20 kV. Micrographs (A-F) represent *C. freundii* and its vesicles being released from the bacterial membranes. Bar, 200 nm.

OMV secreted from *C. freundii* were spherical, mono-, bi- layered, closed membranous structures, and no external material seemed to be associated with the vesicles (Figure 4.16).

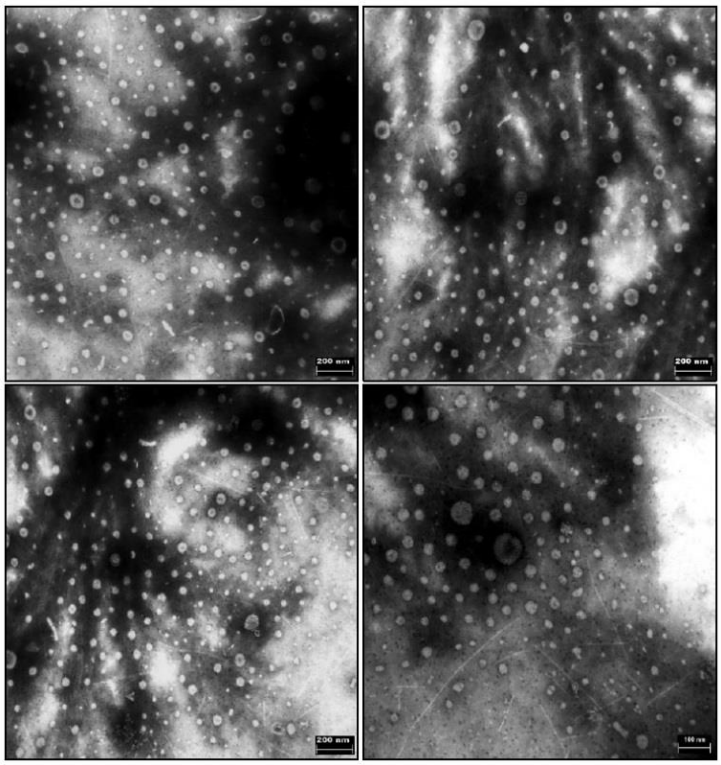

Figure 4.16 **Transmission electron micrographs of pelleted OMVs derived from *C. freundii*. NRZ 08698.** OMVs were extracted from isolate of *C. freundii* harboring KPC-2-encoding IncN plasmid. Following negative staining with 1% ammonium heptamolybdate, OMVs were applied to 0.5% Formvar-coated 300-mesh copper grids and visualized by Zeiss EM900 transmission electron microscope. Bar, 200 nm.

The size distribution of OMV was measured using imageJ software (Fiji). The diameter of *C. freundii* OMV (n = 500) was ranging from 15 to 103 nm, which is consistent with the size of OMV secreted by other Gram-negative bacteria (Figure 4.17). No bacteria, membrane whorls and cell debris were detected in analyzed vesicle samples, however fragments of flagella were visible among OMVs. Moreover, SDS-PAGE analysis of the vesicular proteins revealed that *C. freundii* OMVs have distinct protein band pattern compared to the WCL fraction (see chapter 4.4.2; Figure 4.26E), indicating that special protein sorting mechanisms are employed when OMVs are being released.

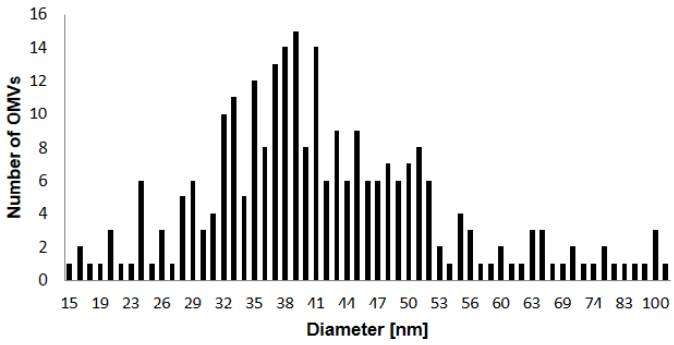

Figure 4.17 **The size distribution of outer membrane vesicles isolated from *C. freundii* NRZ 08698.** The OMVs were visualized by transmission electron microscopy and measured using ImageJ software. The diameter of *C. freundii* vesicles (n = 500) was ranging from 15 to 103 nm. The x axis presents the OMVs diameter in nanometers against their number.

4.3.2 Proteomic profiling of outer membrane vesicles from *C. freundii*

I conducted the proteomic analysis of purified *C. freundii*-derived OMVs to identify proteins that are present in vesicles, and consequently obtain insights into molecular mechanisms involved in OMV cargo sorting and biogenesis. Additionally, the study of vesicle proteome should provide clues for better understanding the pathophysiological roles of these macromolecular structures. Besides, MS analysis allowed us to confirm the purity of extracted blebs and exclude possible contamination from the phage particles, which have the comparable size to bacterial OMVs. A total of 706 vesicular proteins were identified in the OMV samples during three independent trials (see Table A-2, Appendix B). It is noteworthy that the three independent proteomic analyses exhibited high reproducibility. Of the total proteins from all trials, 85, 87 and 88%, respectively, were common to the first, second and third trial. By using the normalized spectral abundance factor (NSAF) approach (Zybailov et al. 2006), I determined the relative amounts of proteins within the OMV samples. All identified proteins were annotated by their subcellular localization based on the PSORTb algorithm. As shown in Figure 4.18A, 79 (50.4%), 45 (1.8%), 127 (12.1%), 451 (33.3%) and 5 (2,4%) proteins were classified as outer membrane, inner membrane, periplasmic, cytoplasmic and secreted, respectively. Compared with the theoretical proteome of *Citrobacter freundii* strain CFNIH1, 79 proteins out of theoretical 164 outer membrane and 451 out of 3367 cytoplasmic proteins were significantly enriched in the OMVs, whereas only 45 out of theoretical 926 inner membrane proteins were identified. These results indicate that the release of OMVs, which has been observed in all Gram-negative bacteria investigated to date may represent a novel avenue for protein secretion. Notable, many cytoplasmic proteins were detected in *Citrobacter* vesicles, most were metabolic

and ribosomal proteins, which is analogous to the observation of the several others researcher groups (Pérez-Cruz et al. 2015; Pérez-Cruz et al. 2013; Bai et al. 2014; Schwechheimer & Kuehn 2015). However, it is not surprising that OMVs are composed of cytoplasmic proteins. It is known that vesicles derived from Gram-negative bacteria can contain plasmid or chromosomal DNA (Jan 2017), suggesting there is a sorting mechanism, which is responsible for packaging intracellular compartments including cytoplasmic proteins into vesicles. Furthermore, the functions of identified proteins present in OMVs were categorized according to the Clusters of Orthologous Groups (COG) annotation with regard to the molecular function. Based on COG annotation, the vesicular proteins of *C. freundii* are involved in diverse processes, including cell wall/membrane/envelope biogenesis (13.2%), translation, ribosomal structure and biogenesis (12.6%), energy production and conversion (9.8%), carbohydrate transport and metabolism (9.6%), amino acid transport and metabolism (9.1%), posttranslational modification, protein turnover, chaperones (5.8%), and coenzyme transport and metabolism (4.7%), whereas the functions of 26 proteins (3.7%) are poorly characterized (Figure 4.18B).

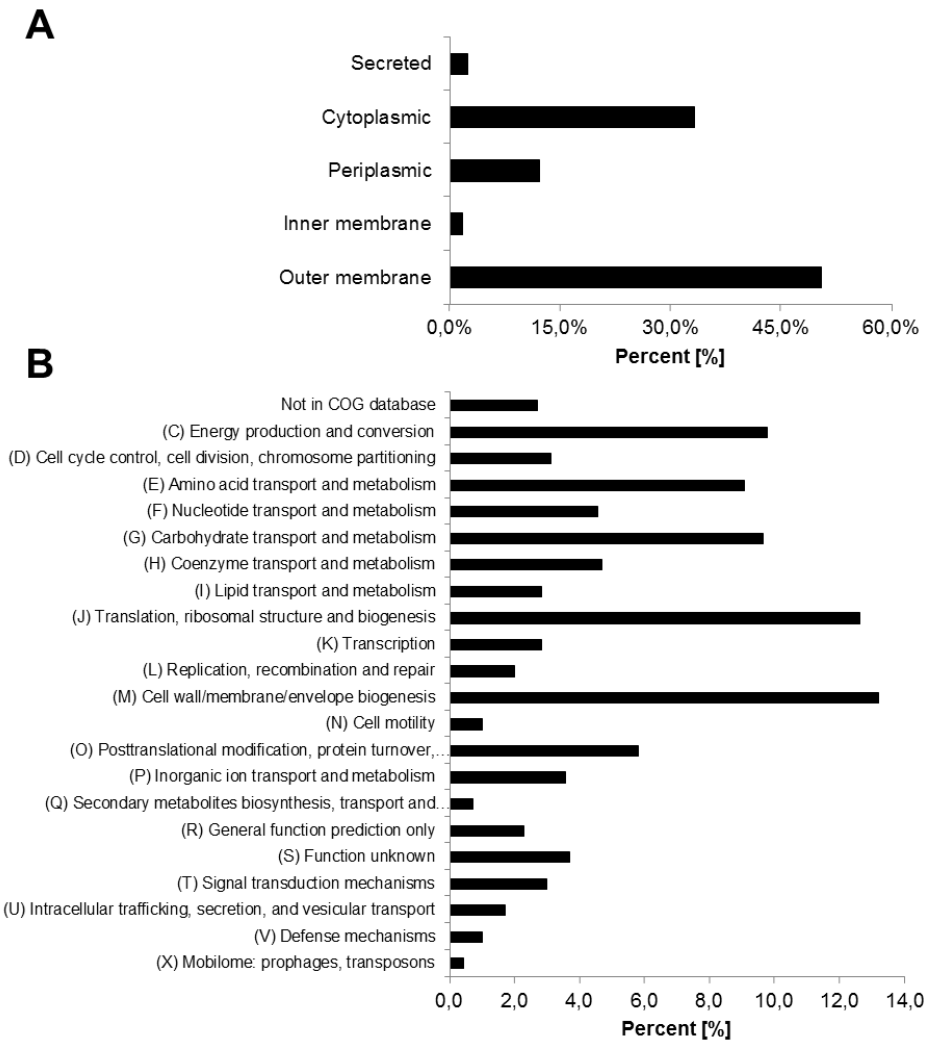

Figure 4.18 **Distribution of *C. freundii*-derived vesicular proteins based on their predicted subcellular locations and COG functional classes**. A total of 706 proteins were identified in outer membrane vesicles of *C. freundii* NRZ 08698 by MALDI-TOF-MS analysis. The vesicular proteins were grouped into families according to the predicted subcellular localization **(A)** and COG functional classes **(B)**. The subcellular localization was predicted based on the protein subcellular localization (SCL) prediction tool (Yu et al. 2010). The annotation of the Clusters of Orthologous Groups of proteins (COGs) was performed by COGsoft, a software for making Clusters of Orthologous Groups (Kristensen et al. 2010).

In addition, protein-protein interaction networks (PINs) for OMVs derived from *C. freundii* were constructed and analyzed in order to elucidate physical and functional interactions between vesicular proteins. Using experimentally verified data on the landscape of physical protein-protein interactions in *E. coli* (Rajagopala et al. 2014), I was able to map 337 of the 706 vesicular proteins into the PIN. The Figure 4.19 presents the constructed PIN of the vesicular proteins, comprising 337 nodes and 2976 interactions.

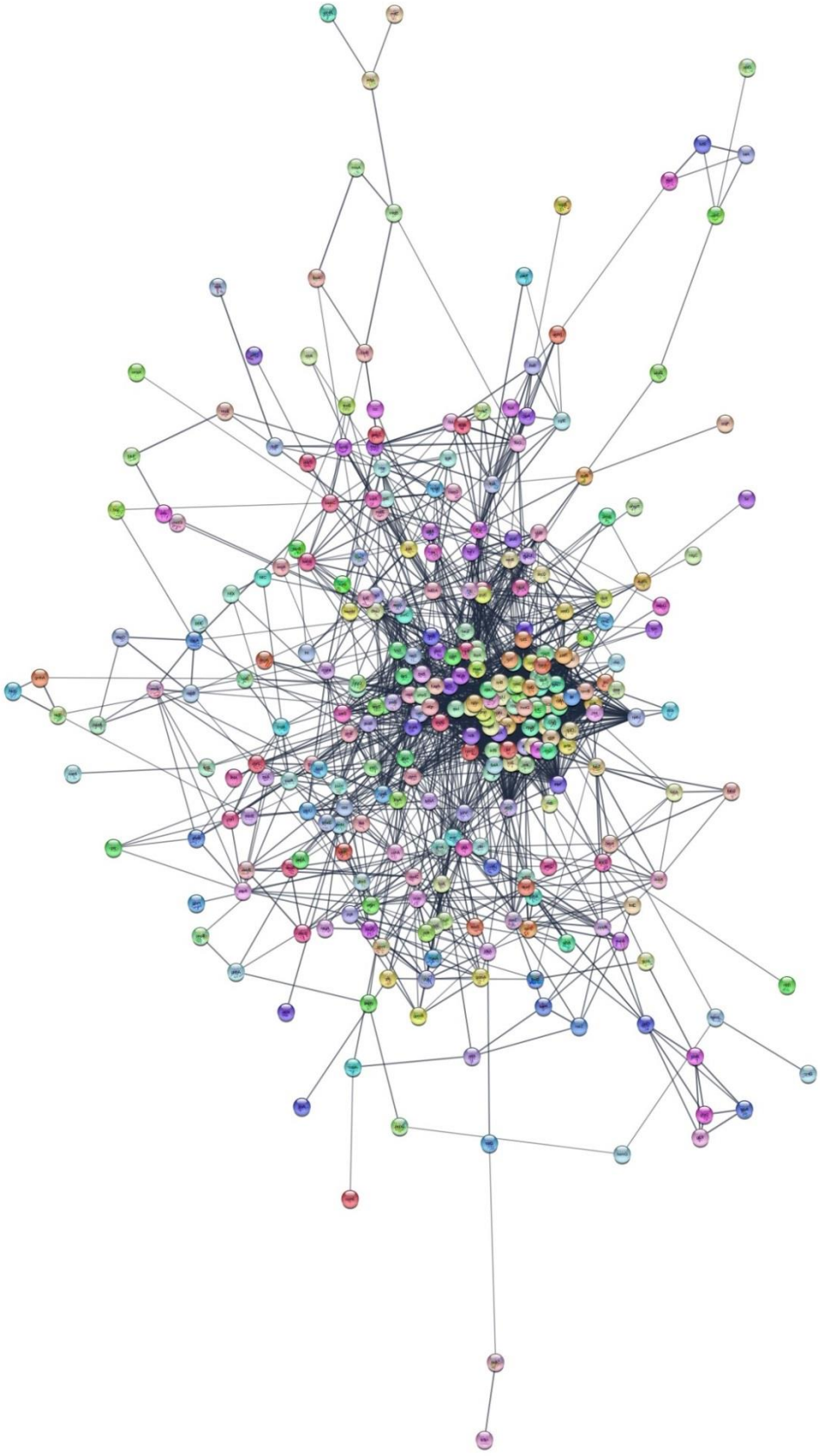

Figure 4.19 **Graphical representation of protein - protein interaction (PPI) network of outer membrane vesicle (OMV) isolated from *C. freundii* NRZ 08698.** Nodes represent proteins of

Citrobacter-derived OMV. Edges represent experimentally determined interactions. The PPI network has 337 nodes with 2976 edges. The PPI network was visualized by using Cytoscape software version 3.5.1 with self-interactions being removed prior to analysis.

Based on clustering algorithm MCODE (Bader & Hogue 2003) that detects densely connected regions in large protein-protein interaction networks and functional enrichment analyses, I identified subnetworks within PPI network of *Citrobacter*-derived OMV. Proteins with related functions were linked to each other, forming functional modules in the protein-protein networks (Figure 4.20). Within the PPI network of OMV, 12 subnetworks were detected. Cluster A represents proteins involved in metabolic processes, consisting of NADH oxidoreductases (NuoA, NuoB, NuoC), succinate dehydrogenase (SdhA, SdhB), nitrate reductase (NarH, NarZ) and other proteins associated with glycerol metabolism (GlpA, GlpD, GlpK, GlpT, GlpQ). Cluster B shows proteins linked to translation, including miscellaneous ribosomal proteins such as RpsQ, RpsP, RplA, RplC. Subnetwork C comprises proteins connected to membrane biogenesis (BamB, BamC, BamD, SurA), protein export (SecB, SecD, yajC), glycolysis (GpmA, Pgi, Eno) and unfolded protein binding (groL). Cluster D represents proteins involved in response to temperature stimulus (HtpG, HslU, HtpX, ClpB, DnaJ). Subnetwork E is composed of proteins associated with translation process, including methionyl-tRNA synthetase (MetG), cysteinyl-tRNA synthetase (CysS), isoleucyl-tRNA synthetase (IleS), tryptophanyl-tRNA synthetase (trps) or phenylalanine tRNA synthetase (PheT). Module F presents proteins linked to cell division, such as FtsX, FtsL, ZipA, MurE, DdlB and AmiC. Finally, clusters (G-L) include protein networks composed below of 6 nodes and include proteins connected to fatty acid biosynthetic process (FabA, FabG, FabZ), amino sugar metabolic process (GlmM, GlmS, NagA, NagB) and protein transport by the Tat complex (TatA and TatB).

In conclusion, by interrogating proteomic data obtained from MS analysis and by using systems approaches, I have built a protein interaction network of *Citrobacter* OMVs. Based on PIN, I defined how these macromolecular, extracellular protein structures are organized, revealing that vesicular proteins are closely interconnected via different interactions and group into functional modules likely involved in their functions and biogenesis.

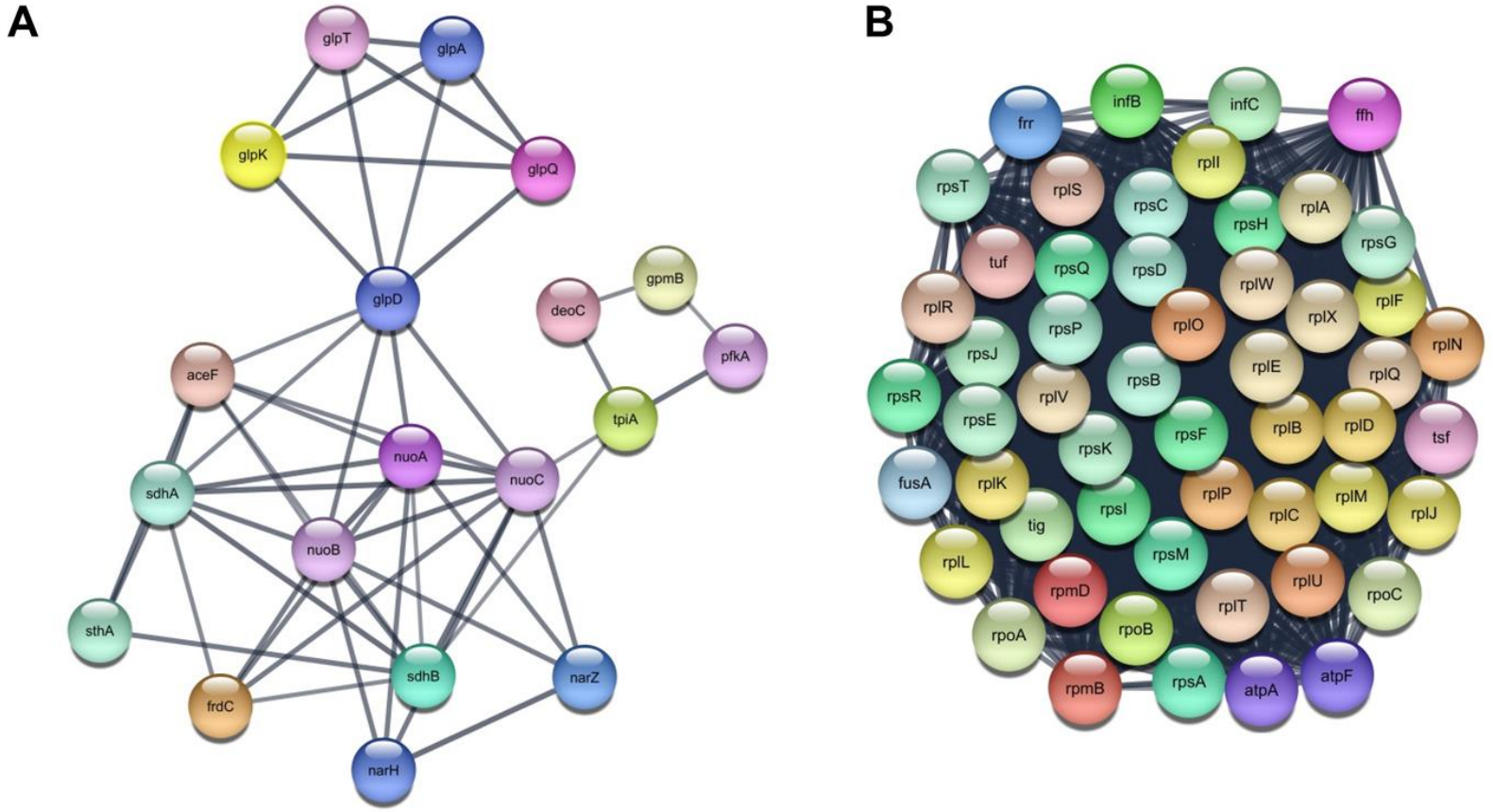
A
glpT
glpA
glpK
glpQ
glpD
gpmB
deoC
pfkA
aceF
tpiA
nuoA
nuoC
sdhA
nuoB
sthA
sdhB
narZ
frdC
narH
B
infB
infC
ffh
frr
rplI
rpsT
rplS
rpsC
rplA
rpsH
rpsG
tuf
rpsQ
rpsD
rplW
rplF
rplR
rpsP
rplO
rplX
rplN
rpsJ
rplE
rplQ
rpsB
rpsR
rplV
rpsE
rplB
rplD
tsf
rpsK
rpsF
fusA
rplK
rplP
rplM
rplJ
rpsI
rplC
tig
rpsM
rplL
rplU
rpoC
rpmD
rplT
rpoA
rpoB
rpsA
atpA
atpF
rpmB

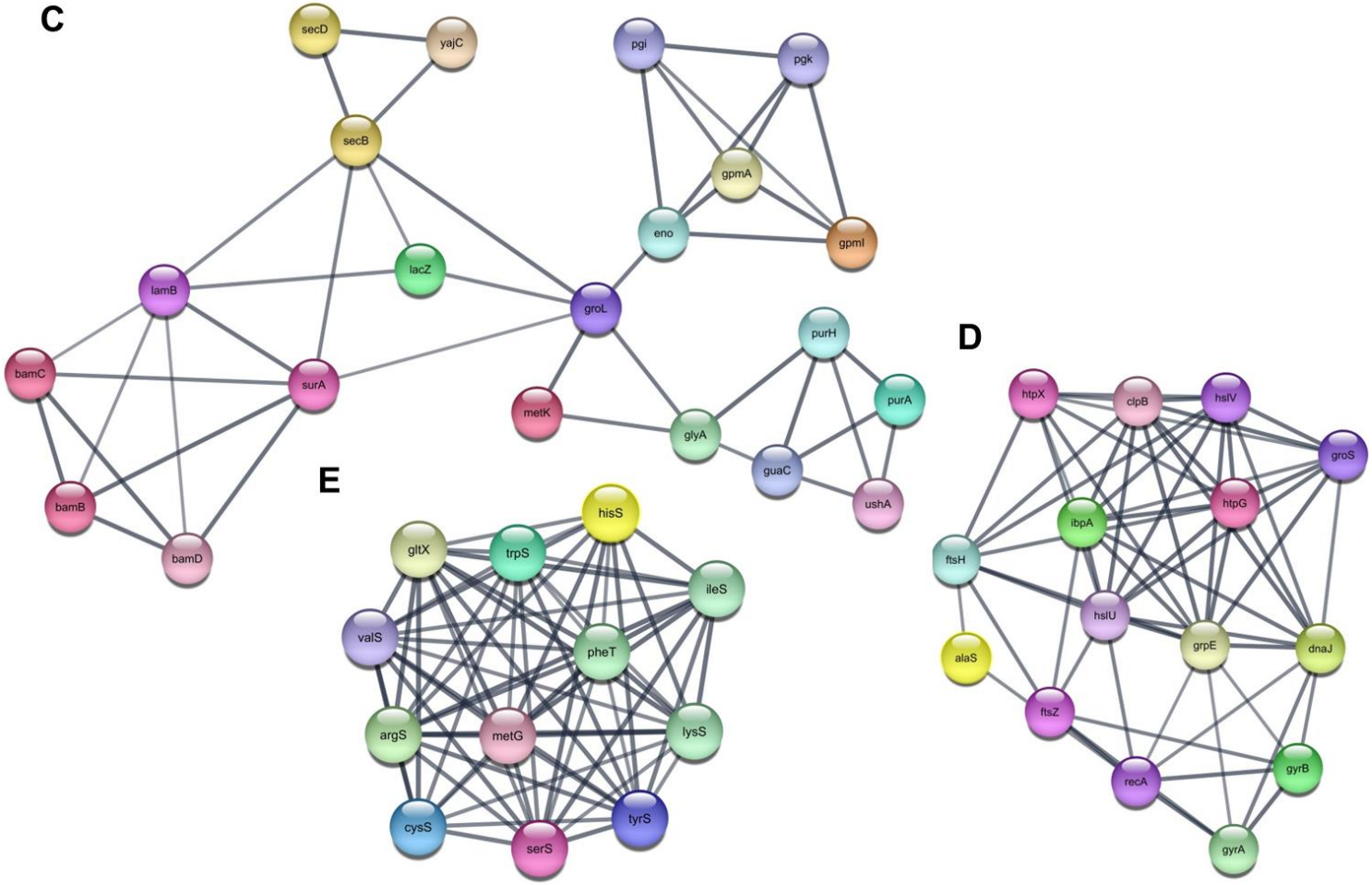
C
secD
yajC
secB
lacZ
lamB
bamC
surA
bamB
bamD
groL
metK
pgi
pgk
gpmA
eno
gpmI
purH
purA
glyA
guaC
ushA
D
htpX
clpB
hslV
groS
htpG
ibpA
ftsH
hslU
grpE
dnaJ
alaS
ftsZ
recA
gyrB
gyrA
E
hisS
gltX
trpS
ileS
valS
pheT
argS
metG
lysS
cysS
serS
tyrS

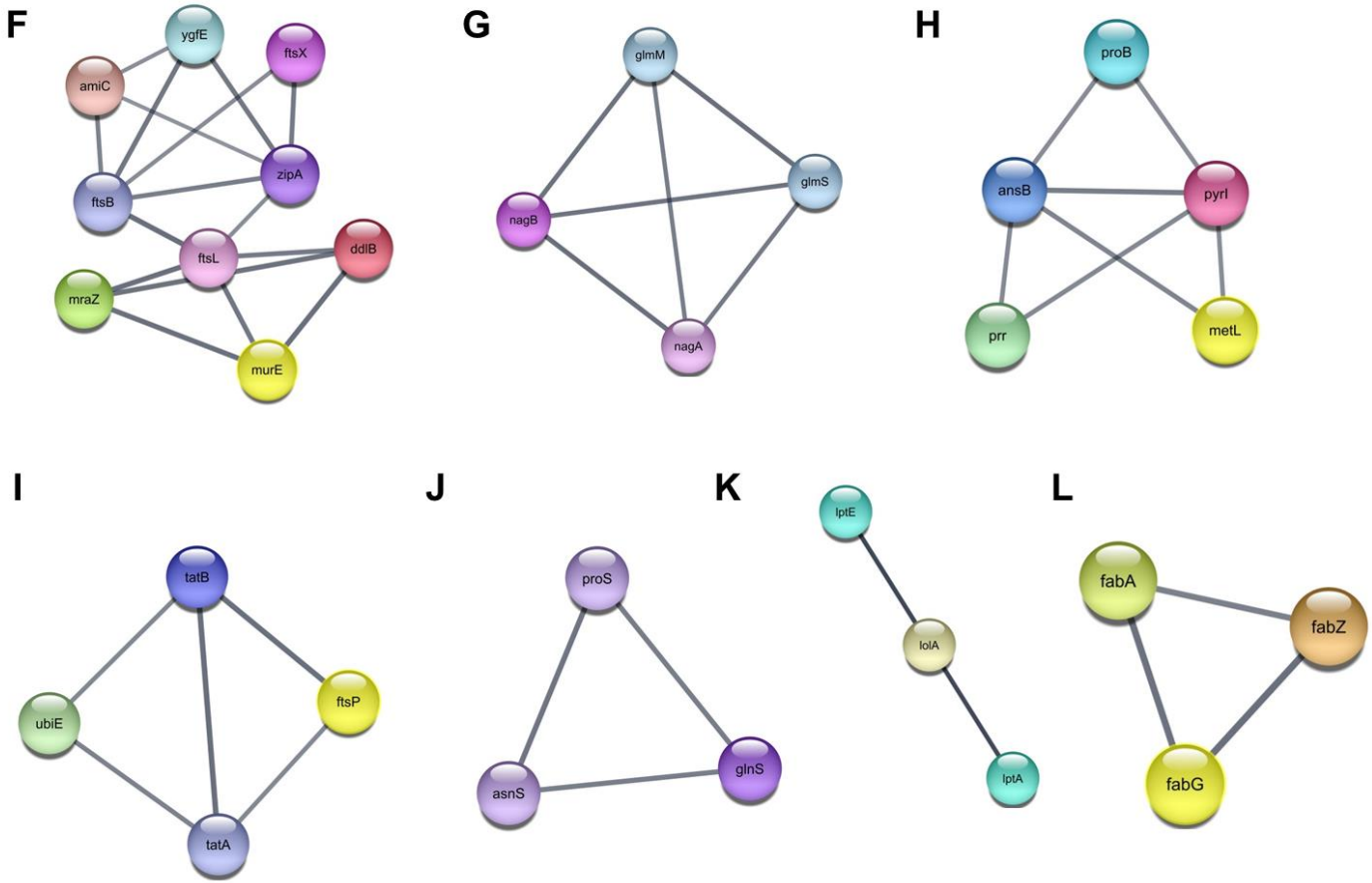

Figure 4.20 **Subnetworks detected in the protein-protein interaction (PPI) network of *Citrobacter*-derived outer membrane vesicles (OMVs).** A large number of proteins are involved in building of OMVs. To extract meaningful information from such a highly interconnected network, clustering of the proteins according to their functional classes may be of use. The highly dense nodes (proteins) and their interconnected nodes were identified and extracted from the PPI network of OMVs to construct new small sub-PPI networks (A to L). Clustering of proteins was done by the MCODE algorithm (Bader & Hogue 2003). The PPI networks were visualized by using Cytoscape software version 3.5.1 with self-interactions being removed prior to analysis.

4.3.3 OMVs derived from *C. freundii* contain blaKPC-2 gene.

To date, several research groups have reported the presence of chromosomal and plasmid DNA inside the OMVs secreted from various isolates of *Acinetobacter*, *Escherichia*, *Pseudomonas* and *Neisseria* (see chapter 1.4.2). The encapsulation of DNA within vesicles would suggest that pathogens can transport genetic material to other bacterial cells in a long-distance manner. Therefore, in order to determine whether plasmid DNA coding for carbapenem resistance gene blaKPC-2 is associated with OMVs derived from KPC-2-positive *C. freundii* NRZ08698, vesicle fraction was purified and the presence of blaKPC-2 gene was analysed by PCR. The carbapenemase gene was detected using primers targeting blaKPC-2, as indicated by a band at 570bp (Figure 4.21). The positive PCR amplification result indicates that plasmid DNA was internally associated with OMVs as the PCR product was produced after DNase I treatment of intact OMVs. In contrast, the blaKPC-2 gene was not detected in negative sample prepared from *E. coli* DH10β cells, which did not harbour any plasmid DNA. This outcome suggests that plasmid DNA or its part was packaged into *C. freundii* OMVs and then was released out of the bacterial cell into milieu.

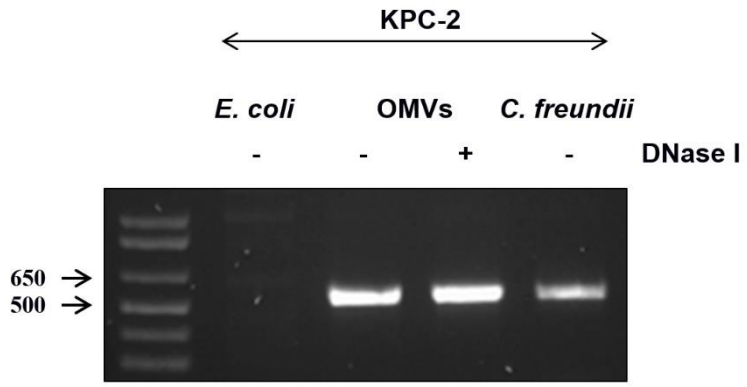

Figure 4.21 **PCR detection of blaKPC-2 gene in OMV isolated form *C. freundii* NRZ 08698.** Agarose gel showing detection of plasmid DNA by PCR reaction specific for blaKPC-2. Plasmid DNA for PCR amplification has been isolated from intact DNase I pretreated OMVs.

4.3.4 OMVs isolated from *C. freundii* facilitate transfer of plasmid DNA to neighboring bacteria

The packaging of DNA into OMVs might be an additional mechanism by which *C. freundii* disseminates genetic material, including different resistance genes to neighboring bacteria. The ability of vesicles derived from *C. freundii* for transferring a plasmid DNA to other bacterial cells was investigated by performing OMVs-mediated transformation. Cefotaxime-susceptible,

non-competent *E. coli* J53 was mixed with outer membrane vesicles, which have been pretreated with DNase I, and the transfer of the KPC-2-encoding plasmid from OMVs to bacterial cells was quantified after 24 h of incubation (Table 4.1 and Table 4.2). The results of these experiments indicate that vesicles-transformed *E. coli* J53 acquired cefotaxime resistance at an average rate of 41 OMVs-transformants (transformed bacteria by exposure to OMVs) per 10µg of OMVs. In contrast, the gene transfer events obtained with OMVs, which have not been pretreated with DNase I were significantly higher (126 transformants), suggesting either DNase I prohibits transfer of free DNA or enzyme treatment can affect the integrity of the bacterial blebs, and consequently influence vesicle-mediated transfer. In parallel, no OMVs-transformants were found when *E. coli* J53 was incubated with 1,000 ng of free plasmid DNA isolated from isolate of *C. freundii* NRZ 08698 or when the recipient strain was incubated in the absence of vesicles.

Table 4.1 OMVs-mediated transformation obtained after 24 h of incubation with OMVs derived from *C. freundii* NRZ 08698 in LB plates supplemented with 1 mg/L of cefotaxime (CTX) and 200 mg/L of sodium azide.

Treatment	**No. of transformants***
E. coli J53 + *C. freundii's* OMVs	126
E. coli J53 + *C. freundii's* OMVs pretreated with DNase I	41
E. coli J53 + Exogenous DNA	0
LB + *C. freundii's* OMVs	0

*The OMV-mediated transformation experiments were carried out in three time-independent assays. Data are expressed as the mean ± SEM from three experiments.

Table 4.2 Efficiency of C. freundii's OMVs transformation.

Number of Recipients [cfu]	**Number of OMVs transformants [cfu]**	**Efficiency of OMVs-mediated transformation***
$4{,}0 \times 10^{7}$	41	1×10^{-6}

* The gene transfer efficiency is calculated as the number of OMV-transformants per the number of recipient cells.

In order to confirm whether OMVs-transformed recipient J53 selected on LB plate supplemented with cefotaxime contained plasmid DNA, PCR targeting blaKPC-2 gene was carried out. Figure 4.22 presents the amplification of KPC-2 gene detected in OMVs-transformed *E. coli* J53. These results support the previous reports that Gram-negative bacteria can harness their OMVs as a vehicle for transferring the plasmid DNA into other bacterial cells.

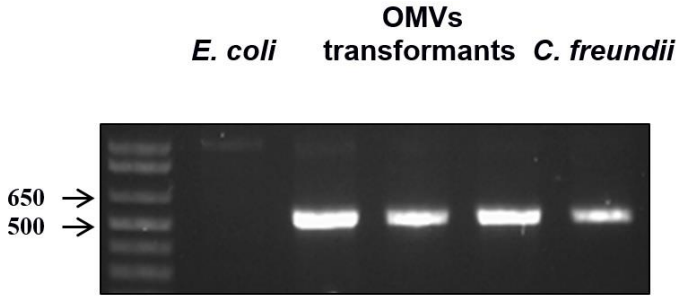

Figure 4.22 ***E. coli* J53 transformed with OMVs from *C. freundii* NRZ 08698 harbors KPC-2 gene**. Agarose gel presents detection of plasmid DNA by PCR reaction specific for blaKPC-2. Plasmid DNA for PCR amplification was isolated from *E. coli* J53 that has been transformed with OMVs derived from isolate of *C. freundii***.**

4.3.5 S1-PFGE and sequencing analysis of plasmid DNA transferred by *C. freundii* OMVs

To visualize and determine the size of plasmids in OMVs-transformants, S1 nuclease digestion followed by pulsed-field gel electrophoresis was performed. As shown in Figure 4.23, the presence of plasmid DNA that varied in length from ~60 kb to ~90 kb was detected in case of vesicles-transformed *E. coli* J53. This data confirms the transfer of a complete plasmid between OMVs secreted from *C. freundii* and recipient J53 cells. According to my best knowledge, it has been shown for the first time that *C. freundii* OMVs can serve as a vehicle to transfer such a large-sized plasmid (~90 kb) encoding carbapenem resistance gene blaKPC-2.

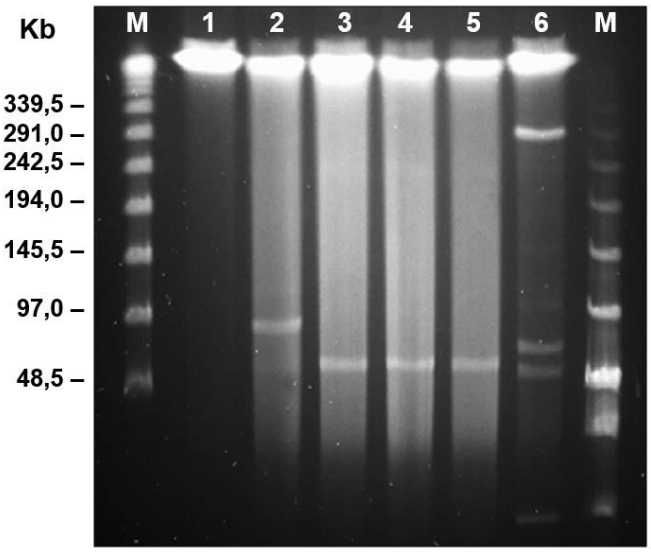

Figure 4.23 **Detection and size determination of plasmids transferred by *C. freundii* OMVs.** Plasmids were digested by S1 nuclease and visualized on a pulsed-field gel. The sources of plasmid DNA were *E. coli* J53 (lane 1), OMVs-transformed *E. coli* J53 (lanes 2, 3, 4 and 5) and *C. freundii* NRZ

08698 (lane 6). The markers which were used are Lambda marker (the first lane) and low range marker (the last lane).

In addition, the plasmids from three OMVs-transformed *E. coli* J53 were extracted and subsequently sequenced to determine their origin using the MiSeq benchtop sequencer (Illumina, USA). The genetic similarity of the sequenced plasmids is depicted in Figure 4.24. As indicated in the map, the sequencing analysis confirmed that all OMVs-transformed *E. coli* J53 harboured IncN plasmids that descend from *C. freundii* NRZ 08698. The ancestor IncN plasmid (pCF08698_KPC2) has 78.021 bp and is harboured by donor *C. freundii* cells. Plasmids found in recipient J53 differ in size due to recombination events that occurred in regions encoding antibiotic resistance genes leading to insertion and deletion of different DNA fragments. In case of two smaller plasmids (68 kb), a deletion of approximately 10 kb fragment has taken place due to the presence of the insertion sequence *IS26* flanking region B. The larger plasmid identified in *E. coli* J53 has a duplicated region C (28 kb) compare to original pCF08698_KPC2, therefore its size exceeds 90 kb. However, the mechanism underlying duplication of region C remains elusive. Taken together, this analysis confirmed that all plasmids identified in *E. coli* J53 are from *C. freundii* origin and the release of OMVs can contribute to a long-distance delivery of plasmids encoding KPC-2 resistance genes.

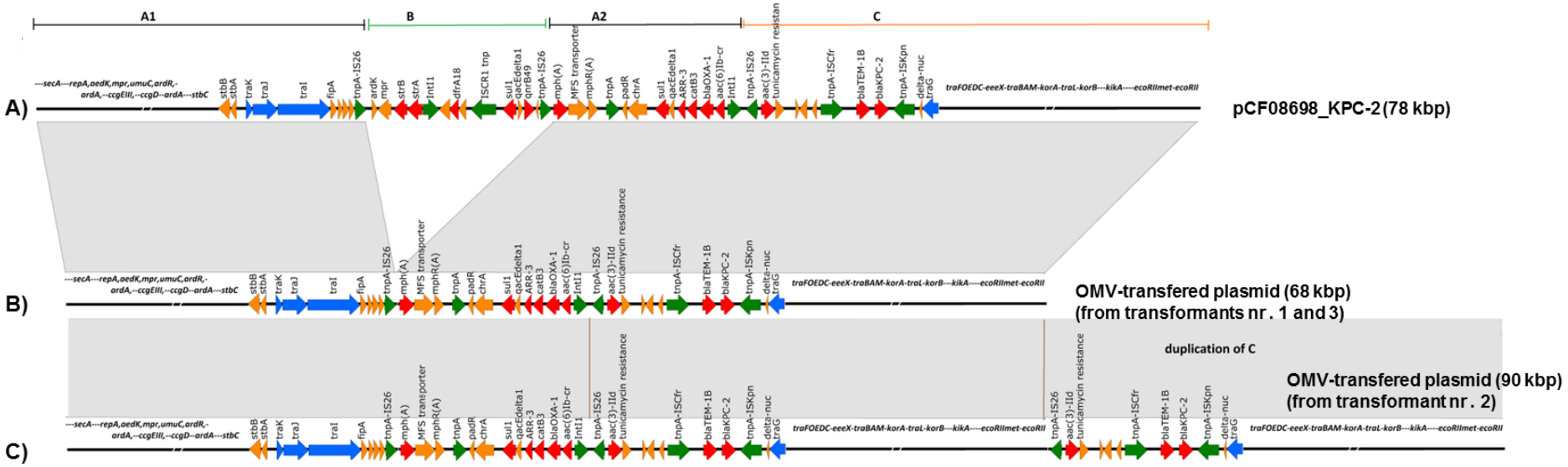

Figure 4.24 **Comparison of plasmids present in *E. coli* J53 transformed with *C. freundii* OMVs. (A)** Reference pCF0869_KPC2 plasmid harbored by *C. freundii* NRZ08698. **(B)** KPC-2 positive plasmids found in OMVs-transformed *E. coli* J53, including deletion of region B. **(C)** KPC-2-positive plasmid found in OMVs transformed *E. coli* J53 including duplicated of region C. Plasmid 1 and 3 have identical sequences. Insertion and deletion region are marked with orange C and green B line, respectively. Gray ribbons between panels mark regions of 100% sequence similarity. Transposase genes are colored green, antibiotic resistance genes are red, tra genes are dark blue, other genes are orange and black.

4.4 Formation of OMV in other tested Gram-negative bacteria

4.4.1 Gram-negative bacteria continuously release OMVs into milieu

Previous reports indicated that OMVs are secreted ubiquitously from all Gram-negative and some Gram-positive bacteria investigated to date (Deatheragea & Cooksona 2012; Gurung et al. 2011). Accordingly, I wanted to confirm by using the optimized OMV isolation protocol (see chapter 4.1.1) that all Gram-negative pathogens examined in this thesis were able to release vesicles during *in vitro* growth. Vesicles were harvested from cell-free supernatant of overnight culture as described in chapter 3.3.2. The purified OMV were re-suspended in phosphate-buffered saline and then examined using transmission electron microscopy (TEM). As shown in Figure 4.25, vesicles were spherical-shaped, mono- and bi- layered structures, uniform in size. When I examined the diameters of OMVs (n = 500, for each isolate), I found that their diameter was ranging from 15 to 120 nm, and most of the vesicles (70%) had a diameter of 20 to 50 nm. This range is similar to previously described for OMVs, which have been isolated from other Gram-negative bacteria (Jang et al. 2014; Yáñez-Mó et al. 2015; Pérez-Cruz et al. 2013). No bacteria contamination was observed in OMV samples.

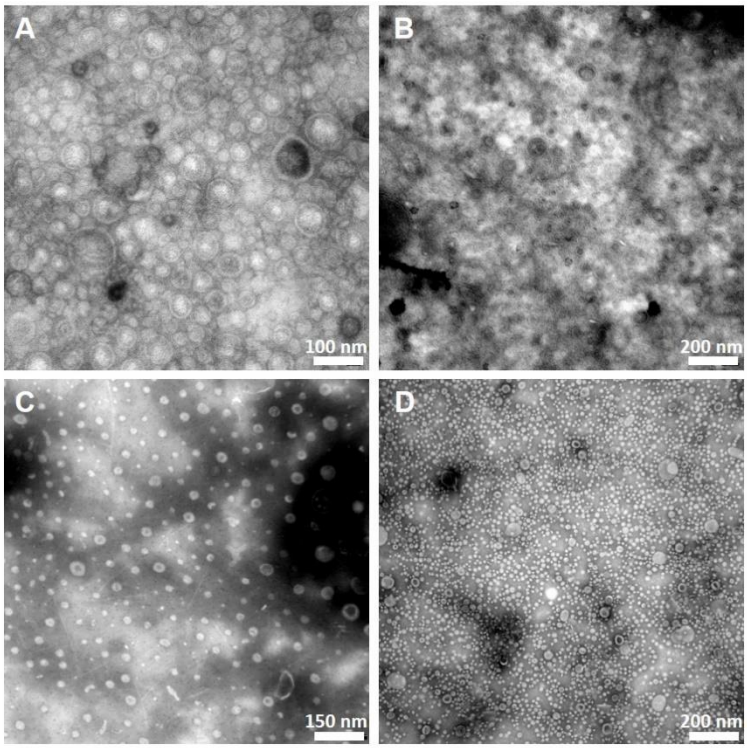

Figure 4.25 **Transmission electron micrographs of negatively stained bacterial outer membrane vesicles**. OMVs were isolated by different filtration and centrifugation steps from *Acinetobacter* sp., **(A)**; *Serratia* sp., **(B)**; *Citrobacter* sp., **(C)** and *Escherichia* sp. **(D)** followed by staining with 1% ammonium

heptamolybdate (pH 7.0) and OMVs were applied directly to 0.5% Formvar-coated 300-mesh copper grids. Vesicles samples were observed with a Zeiss EM900 transmission electron microscope (Carl Zeiss, Germany). Electron micrographs were taken at an accelerating voltage of 80 kV.

4.4.2 Vesicles exhibit a different protein profile compared to whole cell lysate fraction

It has been demonstrated that OMV derived from *E. coli* have a different protein distribution pattern compared to whole cell lysate fraction (WCL) of bacteria they originate from (Lee et al. 2007). I investigated whether OMV cargo packaging occurs in bacteria which have been analysed in this thesis. To study protein sorting process, both WCL and OMV proteins were isolated and separated by SDS-PAGE followed by Coomassie Blue staining (Figure 4.26). The OMV fraction demonstrated differences in protein profile compared to the WCL of the studied bacteria. The proteins of 24 to 45 kDa were enriched, whereas others were excluded. The different protein pattern suggests that specific protein sorting mechanisms exist when OMVs are released.

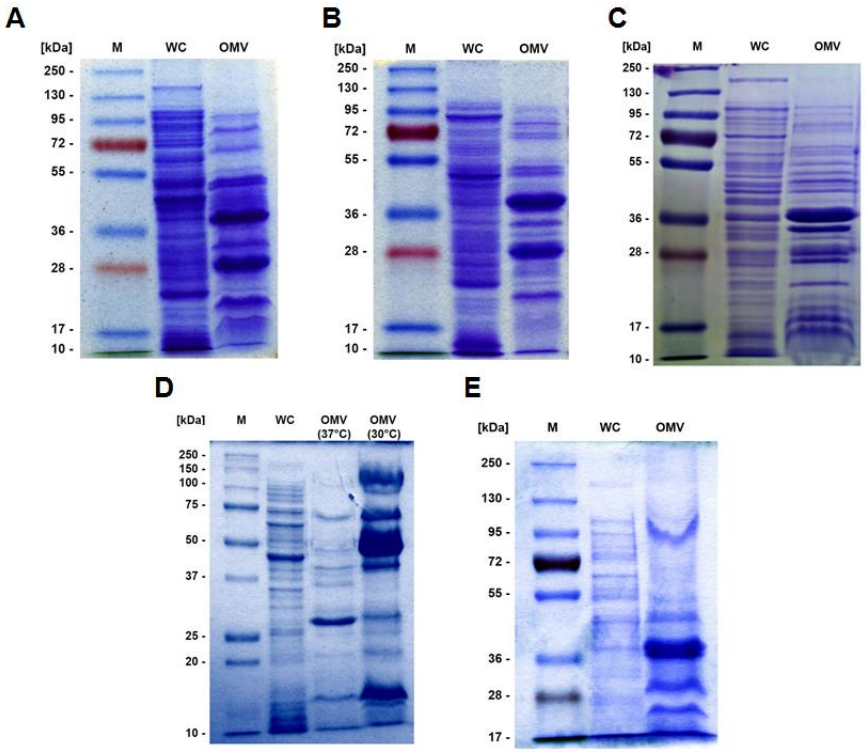

Figure 4.26 **A representative of Coomassie Brilliant Blue-stained SDS-PAGE of whole-cell lysates (WC) and outer membrane vesicle (OMV) fractions.** The protein content of WC and OMV preparations was isolated from *A. baumannii* 13 (A), *A. baumannii* 65 (B), *E. coli* DH10β (C), *S. marcescens* 2099 (D), *C. freundii* 08698 (E). A portion of each fraction was analysed by SDS-PAGE in combination with 10% polyacrylamide gels using the Prestained Protein Marker Broad Range

(Invitrogen, USA) as a molecular mass standard. Protein bands were visualized by a staining with Coomassie Brilliant Blue G250. Molecular weight standards are indicated on the left (kDa).

4.4.3 OMVs induce protective immune responses in invertebrate *Galleria mellonella* model

In this study, I evaluated the protective efficacy of OMVs isolated from *Enterobacter* sp. and *Serratia* sp. isolates against bacteria-induced lethality in *G. mellonella* infection model. It has been previously reported that OMV derived from Gram-negative bacteria are composed of abundant immunogenic proteins, such as outer membrane proteins (OMPs), protective capsular polysaccharide (CPS) and lipopolysaccharide (LPS) antigens. Therefore, vesicles can presumably induce protective immune response in vertebrates and invertebrates. To determine the contribution of OMVs to the activation of the innate immune response in *G. mellonella*, I primed larvae with 100 ng of OMV derived from either *Enterobacter* 247 and *S. marcescens* 2099 24 h prior bacterial infection. *G. mellonella* were challenged by injecting a dose of 10^6 or 10^1 cfu/larva of *Enterobacter* 247 or *S. marcescens* 2099 isolates, respectively. OMV-mediated activation of immune system provided potent protection against subsequent infection by a lethal dose of bacteria (Figure 4.27). These results indicate that *G. mellonella* invertebrate model possess inducible immune defense molecules (i.e. antimicrobial peptides, AMPs) that provide long-lasting antimicrobial responses to bacterial challenge.

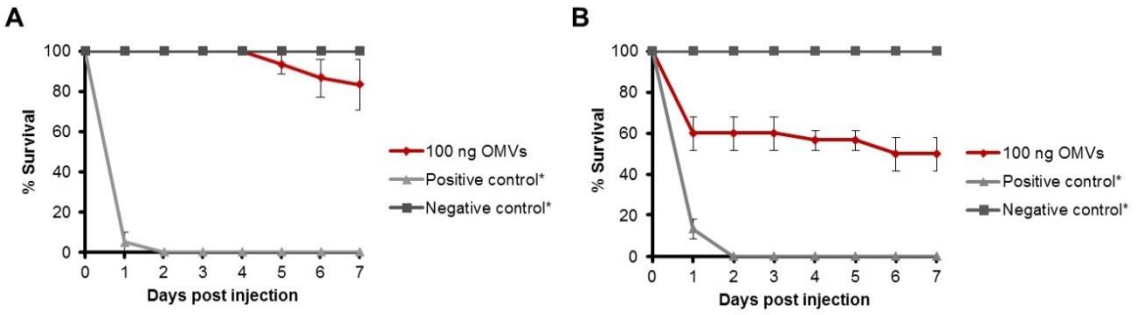

Figure 4.27 **The effect of priming *Galleria mellonella* larvae with OMVs on immune protection against bacterial challenge.** Activation of the immune system by injecting 100 ng of OMV derived from *Enterobacter* 247 (A) or *S. marcescens* 2099 (B) 24 h prior bacterial challenge. Priming of *G. mellonella* resulted in a significant increase of survival of larvae compare to untreated larvae. Negative control represents larvae injected with 10 µl of PBS. Positive control is larvae challenged with bacteria, without prior OMV injection. Data are expressed as the mean ± SEM for 10 larvae per treatment from three independent experiments.

To examine the basis for increased survival rates of *G. mellonella* primed with OMVs, individual wax worms were homogenized in LB medium containing 1% Triton X-100 and then plated for bacterial enumeration. As expected, the larvae that have been pretreated with OMVs prior bacterial challenge were free of bacteria at 7 days post-infection, indicating that the immune defenses of *G. mellonella* were highly effective in killing the pathogens (Figure 4.28). No activation of innate immunity was observed when I used PBS instead of OMV as a priming agent.

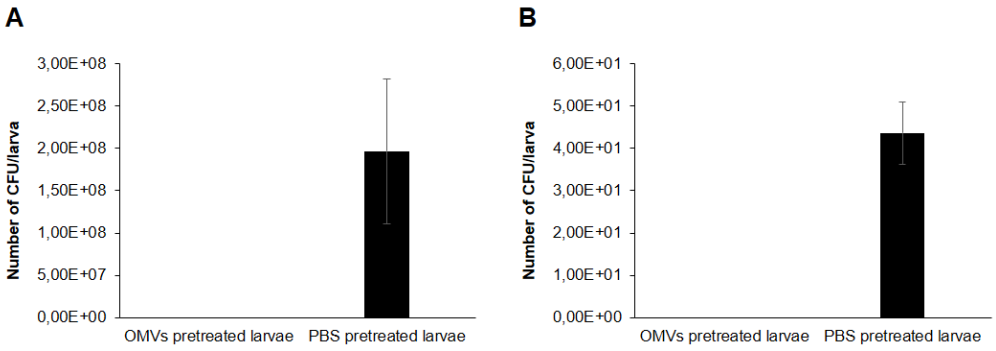

Figure 4.28 **Determination of bacterial load from infected larvae.** *G. mellonella* larvae infected with *Enterobacter* 247 at 10^6 cfu/larva **(A)** and *S. marcescens* at 10^1 cfu/larva **(B)** were homogenized in LB medium supplemented with 1% Triton X-100, followed by plating onto LB agar plates. Bacterial colonies were counted after 24 h of incubation at 37°C. No bacteria detected in OMVs pretreated larvae, suggesting that the constitutive immune defenses of *G. mellonella* were highly effective in killing injected pathogens. Data are expressed as the mean ± SEM for 3 larvae per counting from three independent experiments

.

Discussion - Section I

The cell wall is a rigid, yet dynamic structure that is essential for viability in all Gram-negative and Gram-positive bacteria. It does not only constitute a barrier between the extracellular and intracellular milieu, but also plays a fundamental role in many physiological processes, such as bacterial growth, communication between cells and their environment as well as survival and pathogenesis (Bohuszewicz et al. 2016; de Pedro & Cava 2015). Changes in the cell wall are one of the ways by which bacteria can adapt to constantly changing milieu. In this section of the thesis, I investigated the influence of the remodeling of bacterial cell membranes on antibiotic resistance and OMV formation. I chose different species of *Acinetobacter*, *Citrobacter*, *Enterobacter*, *Escherichia* and *Serratia*, which represent common opportunistic pathogens that are clinically significant for immunocompromised individuals. All tested bacteria were able to secrete vesicles during *in vitro* growth and some of the blebs could serve as vectors for dissemination of the enzymatically active enzymes (e.g., β-lactamases) and antibiotic resistance genes (e.g., KPC-2) in a long-distance manner. Furthermore, I discovered that a hemolysin F (*hlyF*) gene, which is associated with ColV plasmids harbored by invasive strains of *E. coli*, contributes to increased vesicle production. I demonstrated that *hlyF* is the first virulence factor, which may act as a natural biological switch that regulates vesiculation rate in bacteria. In the following sections of this chapter, the overview of obtained outputs is given to summarize and discuss the data from the first part of this thesis.

Vesiculation in Gram-negative bacteria

The cell wall of Gram-negative bacteria has dynamic features that facilitate adaptation to unique surroundings. The modification of the bacterial membranes are involved in acquiring nutrients, defending against other microbes, or evading the host immune system (Bohuszewicz et al. 2016). Formation of outer membrane vesicles is one of the membrane remodeling events that are constantly ongoing at the surface of the bacterial cells.

One aim of this thesis was to investigate the secretion of outer membrane vesicles derived from different clinically important Gram-negative pathogens. The OMVs were examined with respect to their ability to transfer various bacterial intracellular compartments e.g., active β-lactamase or metabolites and to induce protective immune responses in wax moth larva, *Galleria mellonella*. I validated the production and release of OMVs in all investigated bacterial species. These observations are consistent with others in the literature (Yáñez-Mó et

al. 2015; Deatheragea & Cooksona 2012) and confirmed that the secretion of vesicles into the extracellular milieu is an evolutionally conserved, universal process that occurs not only in complex multicellular organisms but also in simple bacteria. Examination of purified OMVs by TEM revealed spherical, mono- and bilayer structures with size ranging from 15 to 200 nm in diameter. As reported in previous studies (Lee et al. 2007; Frias et al. 2010; Sharpe et al. 2011; Kulkarni & Jagannadham 2014), my analysis of the vesicular proteins by SDS-PAGE demonstrated that OMVs fraction exhibits distinct protein profile compare to whole cell lysate fraction, suggesting that specific protein sorting mechanisms are in effect when OMVs are secreted.

Moreover, a MALDI-TOF-MS-based proteomic study was conducted to identify proteins, which were present in the isolated vesicles. Proteomic analyses have shown that OMVs are composed of not only outer membrane and periplasmic proteins, but also inner membrane and cytoplasmic proteins. The most abundant were outer membrane and cytoplasmic proteins. However, when compared with a total bacterial proteome, outer membrane proteins were significantly enriched in the OMVs, whereas cytoplasmic proteins were deprived. While outer membrane and periplasmic proteins are considered as a natural component of bacterial vesicles, the presence of cytoplasmic and inner membrane proteins still lacks a clear explanation. Nevertheless, detection of cytoplasmic components, such as ribosomal proteins, chaperones, and elongation factors in OMVs should not be surprising. The fact that OMVs contain DNA and RNA molecules, and that translation of outer membrane proteins may take place simultaneously with their integration into the vesicles, indicates that ribosomal and transcriptional proteins might be exported into bacterial blebs. The presence of intracellular proteins in OMVs has also been confirmed by many other research groups (Toyofuku et al. 2012; Pérez-Cruz et al. 2015; Kwon et al. 2009; Choi et al. 2011). The incorporation of cytoplasmic and inner membrane proteins into bacterial vesicles can be only explained by the presence of double-bilayer membranes in OMVs, which was previously supported by Kadurugamuwa et al. and Pérez-Cruz et al. (Pérez-Cruz et al. 2013; Kadurugamuwa & Beveridge 1995). The formation of vesicles that contain both inner and outer membranes could also result in trapping cytoplasmic constituents such as plasmids, fragments of chromosomal DNA and different ribosomal proteins. Due to the fact that OMVs are composed of not only outer membrane and periplasmic proteins but also cytoplasmic compartments, the nomenclature for the outer membrane vesicles should be changed to vesicles only as these macromolecular structures represent more than only blebs of bacterial membrane.

Additionally, in this thesis, the potential of OMVs as immunogens was examined. Since vesicles contain abundant outer membrane proteins and lipoproteins, they can be regarded as representing bacterial surfaces and an acellular source of bacterial antigens (Irving et al. 2014; Alaniz et al. 2007; Ellis & Kuehn 2010). Therefore, I assessed the protective immune response of OMVs using larva *G. mellonella* as a non-vertebrate model organism. Priming moth larvae with OMVs significantly conferred immune protection against bacterial-induced lethality. The increase in survival rates of *G. mellonella* that have been pretreated with OMVs was 80% compared to PBS injected larvae as negative controls. These results suggest that bacterial membrane vesicles are potent immunogenic structures, which are effective inducers of protective immunity. My outcomes add to the growing body of literature indicating that OMVs are important in stimulation of immune responses and bacterial infection events, consistent with what was previously reported (Kaparakis-Liaskos & Ferrero 2015; Kulkarni & Jagannadham 2014).

Furthermore, I have shown the protective role of bacterial outer membrane vesicles against antibiotics. The nitrocefin based spectrophotometric assay determined active β-lactamases in OMVs isolated from β-lactam resistant isolates of *E. coli* and *Enterobacter* sp. Their vesicles were able to protect ampicillin-susceptible bacteria, against ampicillin-induced killing. The detection of active β-lactamases in OMVs can be considered as a novel mechanism by which bacteria not only enhance survival of their own species but also promote existence of co-inhabiting pathogens which might be antibiotic-susceptible. It was previously described that *S. pneumoniae* cells growing in the presence of β-lactamase-positive *M. catarrhalis* were protected against killing when they were treated with amoxicillin antibiotic (Budhani & Struthers 1998). Schaar V. et al. (Schaar et al. 2011) noted that preincubation of amoxicillin with purified *M. catarrhalis* OMVs fully rescued amoxicillin-susceptible *M. catarrhalis*, *S. pneumoniae*, and *H. influenzae* from β-lactam-induced killing. These results, along with the outcomes from this thesis indicate that OMVs can serve as an additional mechanism by which bacteria can evade antibiotic-induced killing by hydrolyzing antimicrobial agents.

Additionally, I investigated whether bacteria can secrete OMVs into the extracellular environment in order to exchange metabolites between bacterial communities. The preincubation of OMVs derived from leu auxotroph of *E. coli* harboring a EGFP-pJBA27 plasmid with Δpro, Δmet *E. coli* J53 strain resulted in exchange of nutrients and proteins. Transfer of the enhanced green fluorescent protein (EGFP) mediated by OMVs was evaluated by quantifying the population-level proportion of J53 cells that fluoresced in green colour via

fluorescence microscopy. However, the fluorescence of recipient bacteria was transient, suggesting that vesicles only contributed to the transfer of already expressed green fluorescence protein, yet OMVs provided no evidence for a transfer of plasmid DNA under the given conditions. Pande S. et al. (Pande et al. 2015) demonstrated the transfer of metabolites in nanotube-dependent manner but in their experiment, the functional role of OMV in exchange of proteins remained elusive. Although, all Gram-negative bacteria investigated to date are known to produce membrane vesicles and our knowledge of OMV functions and biogenesis has increased substantially in recent years, so far, the mechanistic proof of principle for their roles remains unclear. The formation and shedding of OMVs are rapid processes and extremely difficult to capture, therefore only employment of cutting-edge microscopy approaches for cellular and molecular visualization will enable us to unambiguously determine their functions in bacterial communities.

Regulation of vesicle production by *hlyF* gene

The multidrug (MDR) resistant isolates of *E. coli* constitute an emerging threat to healthcare institutions and their patients worldwide, and are therefore being extensively investigated (Kempke et al. 2016; Johnson et al. 2010). The collection of MDR *E. coli* originated from human and animal clinical cases were examined in the context of their virulence properties. Whole genome sequencing and comparative genomics-based approaches revealed the presence of ColV plasmids among a few analyzed isolates. The ColV plasmid has been shown to be implicated in the virulence of Avian Pathogenic *E. coli* (APEC) and of Neonatal Meningitis *E. coli* (NMEC) (Mellata 2013). These plasmids harbor many virulence genes, including *hlyF*, a putative hemolysin; tsh, a temperature-sensitive hemagglutinin; iss, the serum survival gene contributing to complement resistance; ompT, an outer membrane protease; the ColV operon, encoding ColV bacteriocin and several iron-related genes (Schouler et al. 2012; Johnson et al. 2006). Several studies demonstrated that *hlyF* is an important virulence factor for pathogenicity, although no protein domain responsible for a hemolytic activity of *hlyF* was identified (Mellata et al. 2009; Johnson et al. 2006; Morales et al. 2004). In this work, an *in silico* analysis demonstrated that the *hlyF* gene encodes for protein belonging to NADB-Rossman family, thereby most probably functioning as fatty acyl coenzyme A (CoA) reductase or nucleoside-diphosphate-sugar epimerase. Therefore, this virulence factor may be involved in the modification of the Gram-negative cell envelope. It was previously observed that remodeling of cell wall can affect formation of OMVs that originate from the cell wall by a process of

bulging out and pinching off a portion of the membranes (McBroom et al. 2006; Kulkarni & Jagannadham 2014; Roier et al. 2016). Taken collectively, these facts indicate the probable connection between *hlyF* gene and vesiculation process.

In this thesis, I examined the involvement of *hlyF* gene in production of outer membrane vesicles. The vesiculation rate of two *E. coli* ST131 isolates expressing normal and truncated version of *hlyF* genes were compared. The truncation of *hlyF* resulted in decreased OMVs formation compare to *E. coli* harboring a complete gene, suggesting that this virulence factor could be associated with the OMV biogenesis. The blast analysis of amino acids sequences revealed the deletion of 77 amino acids from N-terminal side of the truncated hemolysin F gene, leading to loss of NADP-binding motif 'TGXXGXXG' and therefore result in expression of a non-functional protein. To exclude the contribution of other genes located on ColV plasmid to vesicles formation and confirm that only *hlyF* is involved in modulation of OMVs production, I cloned the complete hemolysin F gene into pUC19 vector, followed by transformation of constructed plasmid into *E. coli* K12 DH10β. The resulting recombinant strain exhibited significantly increased vesiculation rates compared to control *E. coli* harboring an empty pUC19 plasmid as was shown by TEM, β-lactamase activity and Bradford assays. These outcomes clearly demonstrated that the expression of *hlyF* triggers increased production of outer membrane vesicle, whereas the mutation of this gene leads to hypovesiculation phenotype. Therefore, this is the first identified virulence factor which may serve as a natural biological switch that controls OMV formation in *E. coli*.

Additionally, I showed that the OMVs derived from *E. coli* expressing *hlyF* gene have a potential to induce autophagy in eukaryotic epithelial cells. It was reported previously that bacterial OMVs trigger autophagosome formation associated with inflammatory interleukin 8 responses in epithelial cells via NOD1 and RIP2 signaling pathway (Irving et al. 2014). Hence, due to the fact that OMV are involved in a number of biological functions, the induction of vesicle production mediated by *hlyF* may contribute to a wide range of processes in bacterial communities. It is important to pass a remark that I encountered isolates exhibiting hypervesiculation phenotype but did not harbor the *hlyF* gene. It has been previously noted that various proteins which are involved in LPS modification, cell wall integrity and peptidoglycan synthesis may affect the process of vesicle formation (Cascales et al. 2000; McBroom et al. 2006; Elhenawy et al. 2016), indicating that there is not one mechanism underlying vesiculation but rather multiple events can lead to the production of vesicles in bacteria. Taken together, this data indicates that the presence of *hlyF* gene in *E. coli* not only triggers increased OMVs

formation but also induces autophagosome formation in HeLa cells exposed to *hlyF*-induced vesicles. However, bioinformatics analysis does not give an exact hint towards the molecular basis underlying this process and further work is required to precisely understand this mechanism. My study is parallel and supportive to recently published. investigation (Murase et al. 2016), which provided the first evidence for the contribution of *hlyF* to vesicle production. Murase et al. observed that the culture supernatant of *E. coli* expressing *hlyF* induced autophagosome formation in eukaryotic cells, and this phenomenon concurred with the increased formation of vesicle, which led them to speculate the role of *hlyF* protein.

My discovery that bacteria utilize hemolysin F gene to regulate production of OMVs has significant implications for microbial ecology and physiology. By expression of *hlyF,* bacteria can modulate the formation of OMV, and therefore meaningfully extends their ability to interact with surrounding milieu in long-distance manner without the need for direct contact.

Dissemination of antibiotic resistance genes via bacterial vesicles

The capability of bacteria to extend their influence in a long-distance manner is crucial to their activity and survival, and can be achieved by formation of nanotubes or release of small macromolecular structures, such as outer membrane vesicles (Dubey et al. 2016; Shetty et al. 2011; Kulkarni & Jagannadham 2014). OMVs are highly versatile and mediate a variety of processes, including delivery of small molecules for signaling and various proteins that effect virulence (Kadurugamuwa & Beveridge 1995; Ellis & Kuehn 2010). Additionally, several groups observed that OMVs are composed of double-stranded DNA, and therefore might be involved in transferring of genetic material to milieu (Yaron et al. 2000; Rumbo et al. 2011; Renelli et al. 2004; Kadurugamuwa & Beveridge 1995; Dorward et al. 1989). Since multidrug resistant *Enterobacteriaceae*, in particular those producing carbapenemases are a worrying problem in hospital settings in Europe and beyond, I wanted to know whether the vesicles secreted by these microorganisms could serve as vectors for the spread of antibiotic resistance genes. Genetic material can be transferred between bacteria by several mechanisms including transformation, conjugation or transduction (Thomas & Nielsen 2005). Transformation is the process that occurs when a bacterial cell takes up foreign DNA from its surroundings. The bacteria which are able to ingest naked DNA are called recipients and after transformation, microorganisms that have taken up foreign DNA are termed transformants. During the transformation process, donor cells need to be lysed to release the free DNA molecules in order for it to be taken up by the recipient. In this thesis, I revealed that *C. freundii* isolates secrete

vesicles containing the bla_{KPC-2} carbapenemase gene without a loss of viability, hence representing a novel avenue of spreading plasmids with antibiotic resistance genes that are clinically important. Moreover, I provided evidence of DNA transfer, which has been mediated by OMVs derived from of *C. freundii* cells.

Initially, the release of vesicles by isolates of *C. freundii* was confirmed by electron microscopy. According to SEM analysis, the OMVs were visible uniformly on the entire surface of a bacterial cell, suggesting that whole Gram-negative envelope is involved in vesiculation process. The OMVs size measurements revealed that *C. freundii* secrete vesicles of different sizes during growth. However, the biological consequence of this observation needs to be determined. The various range of OMV size indicates that vesicle production is a physiologically regulated and reproducible event. Vesicle diameter diversity may depend on different growth phases of bacterial blebs.

Moreover, the vesicles were also further characterized for their protein composition by comprehensive mass spectrometry analysis. According to the normalized spectral abundance factor (NSAF), the most abundant were membrane proteins, but cytoplasmic compounds were also detected. It is known that OMVs contain inner and outer membrane, and consequently trap underlying cytoplasmic compartments, such as plasmids, cytosolic proteins or even fragmented chromosome (Kadurugamuwa & Beveridge 1995). To obtain insights into the interrelationships between proteins identified by MS analysis, I constructed and analyzed a protein - protein interaction (PPI) networks for OMVs derived from *C. freundii* isolate. PPIs revealed that vesicular proteins were closely interconnected via physical interactions and cluster into functional modules. According to constructed PPI networks, I was able to identify functional modules that appear to be involved in bacterial cell wall and membrane biogenesis, amino acid transport and metabolism, translation, ribosomal structure and biogenesis and cell division. Since recent studies have drawn attention to the importance of OMVs in bacterial pathogenesis, a better understanding of interrelationships between vesicular proteins will be useful in finding a novel, promising antimicrobial targets (Schwechheimer & Kuehn 2015; Lim & Yoon 2015). One such potential virulence target has been detected in *C. freundii* OMVs (Figure 4.20, subnetwork C) and is called survival protein A (SurA). This protein has been shown to be pivotal for outer membrane biogenesis in several species of bacteria and its loss leads to hypersensitivity to hydrophobic antibiotics and a reduction in outer membrane protein production (Southern et al. 2016). Investigating the function of SurA in OMVs might contribute to development of novel therapeutic strategies for the inhibition of the vesicle biogenesis and

consequently attenuate bacterial virulence potential. Another interesting antimicrobial target, which has been also identified in *Citrobacter*'s OMV, is filamentous temperature-sensitive protein Z (FtsZ). It is an essential cell-division protein involved in formation a highly dynamic cytokinetic ring at the septum site. As inactivation of FtsZ or an alteration in its assembly leads to the inhibition of Z-ring, septum formation and likely OMV formation, the FtsZ constitutes a very promising factor for novel antimicrobial drug development (Kumar et al. 2011).

Members of the *Enterobacteriaceae* are known to disseminate genes horizontally, mainly via conjugation. However, my results reinforce another possible pathway of horizontal gene transfer (HGT). I showed that KPC-2-producing *C. freundii* secretes vesicles containing KPC-2 gene. Further, I demonstrated that non-competent *E. coli* J53 exposed to KPC-2-containing OMVs results in an intergenus gene transfer mediated by a DNA transport mechanism that did not rely on the bacterial cells. The frequency of vesicle-mediated gene transfer between *C. freundii* OMVs and recipient *E. coli* J53 cells was low and yielded 41 vesiculants per 10 μg of OMVs, which was four orders of magnitudes lower comparable to conjugation efficacy. Additionally, the presence of plasmid DNA in OMVs-transformants was confirmed by positive amplification of bla_{KPC-2} gene. To further verify the origin of DNA inside OMVs-transformed *E. coli* J53, the plasmid was isolated and sequenced. The sequencing analysis confirmed that the DNA found in *E. coli* J53 that has been preincubated with OMVs originated from *C. freundii* cells. My results correspond to previous reports indicating that OMVs can act as an additional mechanism for transferring genetic material to other bacteria (Fulsundar et al. 2014; Yaron et al. 2000; Klieve et al. 2005; Rumbo et al. 2011; Dorward et al. 1989). However, not all OMV containing DNA have been found to allow vesicle-mediated horizontal gene transfer (Renelli et al. 2004). The molecular mechanism leading to encapsulation of DNA into vesicles and subsequently delivery of genes into the host cell surface is not completely known yet. The observations of previous research groups suggest that OMVs utilize various endocytic routes to enter the cells, but the exact action mode need to be determined (Kaparakis-Liaskos & Ferrero 2015; Kulp & Kuehn 2010).

Taken together, my outcomes provide evidence that *C. freundii* produces OMVs of distinct-size populations that offer a nuclease-resistant mechanism of gene transfer within unrelated bacteria. Further investigations should be conducted to determine the biological relevance of this transfer as well as the surface and adherence properties of OMVs. Nonetheless, the prospect that OMVs provide a unique, long-distance manner for the secretion of cytoplasmic constituents, including plasmid DNA sheds completely new light on the interaction between

bacterial communities and their environment. Collectively, my discovery that outbreak isolates utilize, along with conjugation, vesicles to transfer antibiotic resistance genes, and thus convert susceptible isolates to resistant, has significant implications for the current understanding the interplay between microbial populations. The possibility that by the release of OMVs pathogens can significantly extend their spread beyond the limitations of traditional conjugation machinery indicates that bacteria may act as multicellular, indirectly connected elements without the need for immediate cell-cell contact.

Section II

4.5 Examination of mechanism of colistin resistance conferred by the mobile, plasmid-mediated colistin resistance gene 1 (*mcr-1*).

Colistin is a last-resort antibiotic against infections caused by multidrug-resistant (MDR) Gram-negative bacteria. However, colistin treatment has resulted in the selection of MDR bacterial isolates with chromosomal mutations leading to polymyxin resistance and, more recently, the appearance of a plasmid-encoded colistin resistance mechanism (*mcr-1*) (Liu et al. 2015). The *mcr-1* gene encodes a member of the family of phosphoethanolamine (pEtN) transferases that catalyze the transfer of pEtN group onto the glucosamine-disaccharide of lipid A in the outer leaflet of the bacterial outer membrane (Y. Y. Liu et al. 2017). This increases the net negative charge of the lipid A head group and, consequently, affinity between cationic antimicrobial peptides (CAMPs), such as colistin and bacterial membrane. The *mcr-1* gene is encoded on nonrelated types of plasmid replicons such as IncI2, IncX4, IncHI2 and IncP and was rarely detected to be located on the chromosome (Zurfluh, Kieffer, et al. 2016; Zurfluh, Tasara, et al. 2016). It is a part of a highly conserved operon that includes an additional open reading frame encoding a putative membrane-bound phosphatase belonging to PAP2 protein superfamily according to conserved domain blast analysis. Although *mcr-1* gene has been discovered in the late 2015, so far, the detailed mechanism for MCR-1 colistin resistance in not fully understood, mainly due to the lack of the biochemical analysis and the crystal structure of complete MCR-1 enzyme.

4.5.1 The structure of MCR-1

The structure of MCR-1 closely resembles two members of the pEtN transferases derived from *Neisseria meningitides*, LptA and *Campylobacter jejuni*, EptC, which belongs to the alkaline phosphatase protein super-family. The MCR-1 contains two discretely folded domains: one N-terminal transmembrane (TM) domain and one C-terminal presumably periplasmic-facing catalytic domain (Ma et al. 2016). Transmembrane helices prediction method (TMHMM) (Sonnhammer et al. 1998) predicted that the TM domain is composed of five transmembrane helices (TMH1-TMH5; Figure 4.29A) located approximately parallel to one another and crossing the inner membrane. The computer modeling of the complete MCR-1 protein structure performed by a web portal for protein structure and function prediction (RaptorX) (Källberg et

al. 2012) indicated that the catalytic domain of MCR-1 has a hemispherical shape and includes seven β-strands flanked by α-helical structures (Figure 4.29B). Its α/β/α fold is characteristic for the alkaline phosphatase protein superfamily, therefore MCR-1 enzyme may act similarly to other pEtN transferases (Stojanoski et al. 2016). Genetic studies revealed that both the TM region and a catalytic domain are essential for MCR-1 activity (Gao et al. 2016). However, to date only the C-terminal, soluble domain has been crystallized and the catalytic mechanism of MCR-1 still needs to be elucidated (Hinchliffe et al. 2017).

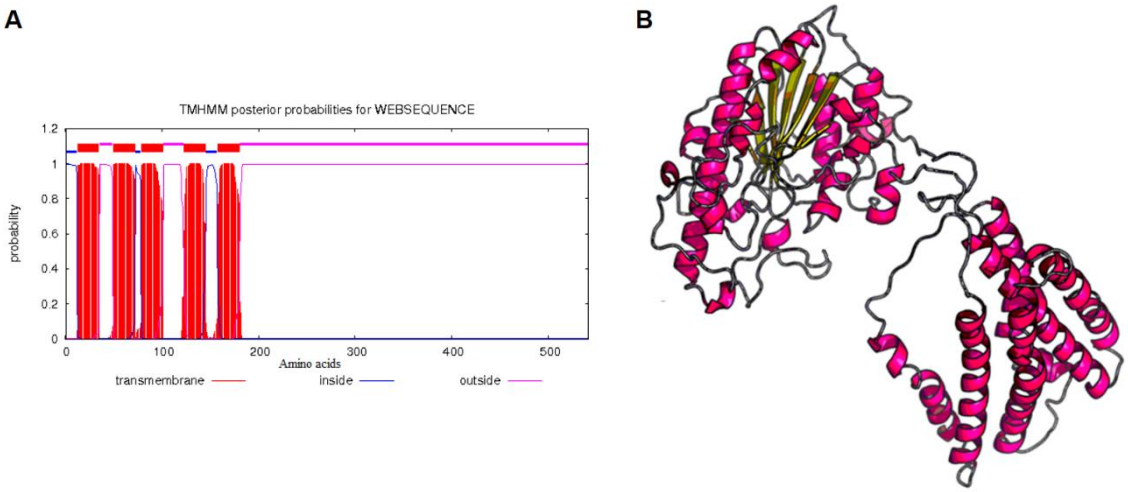

Figure 4.29 ***In silico* characterization of full-length MCR-1 protein. (A)** The transmembrane helices prediction method (TMHMM) predicted 5 transmembrane α-helices at the N-terminus of MCR-1 amino acids sequence (Sonnhammer et al. 1998). **(B)** Predicted 3D structure of MCR-1 protein based on RaptorX protein structure prediction tool (Källberg et al. 2012). MCR-1 contains two regions annotated as a transmembrane domain (TM) at N-terminus and a catalytic domain at C-terminus. The crystal structures of MCR-1 catalytic domain (PDB code: 5K4P) and eukaryotic phosphate transporter (PDB code: 4J05) were used as templates for 3D structure prediction.

4.5.2 Functional analysis of MCR-1 mediated colistin resistance

As yet, the contribution of the MCR-1 enzyme to polymyxin resistance has been examined by cloning the *mcr-1* gene into expression vectors followed by determination of MICs towards colistin and analysis of structural changes in lipid A. However, this gene is encoded on different plasmids and is a part of an operon including an open reading frame (ORF) predicted to encode a membrane-bound phosphatase. So far, the association of the putative phosphatase and other plasmid-encoded factors with the expression of the *mcr-1* gene and subsequently with colistin resistance is not known. Therefore, I aimed to address this concern by performing a mutagenesis of *mcr-1*-encoding IncX4-type plasmid. Initially, to investigate the level of protection mediated

by MCR-1 and assess the involvement of other plasmid-borne genes in colistin resistance, the *mcr-1* was removed from a wild type (WT) IncX4 plasmid of *E. coli* 002 (p002) to create the isogenic variant p002::Δ*mcr-1* (Figure A-0.1, Appendix C). Following the transformation of the mutated IncX4 plasmid into *E. coli* K12 DH10β, the broth microdilution method (BMD) was performed to determine colistin MICs for the resulting transformants (Table 4.3). The MIC value for *E. coli* DH10β, containing the WT p002 was 4 mg/L. The *E. coli* DH10β harboring p002::Δ*mcr-1* became susceptible to colistin at 2mg/L. These results proved the essential role of *mcr-1* gene in conferring resistance to colistin.

Table 4.3 Colistin susceptibility testing for *E. coli* DH10β. The MICs were determined by broth microdilution (BMD) in cation-adjusted Mueller-Hinton broth (CA-MHB).

***E. coli* DH10β**	**MIC* of colistin [mg/L]**
p002	4
p002::Δ*mcr-1*	2

*The MIC is defined as the lowest concentration of the colistin that inhibits visible growth of the tested isolate as observed with the unaided eye.

To further confirm that the *mcr-1* gene encoded on IncX4 plasmid is functional and leads to modification of bacterial outer membrane and consequently to colistin resistance, a lipid A fractions from transformants of *E. coli* DH10β carrying either WT or mutated IncX4 (p002::Δ*mcr-1*) were isolated and analyzed by MALDI-TOF-MS. The MS results revealed that unlike the negative-control DH10β with p002::Δ*mcr-1* or without any plasmid, the pEtN-modified lipid A occurs consistently in the strain carrying *mcr-1* gene (Figure 4.30). The addition of pEtN group to lipid A domain of LPS was confirmed in *E. coli* harboring p002 by detection of the mass shift (Δ*m/z* 123) in the spectrum of lipid A structure, which corresponds to a molecular weight (MW) of pEtN in negative ion mode (Figure 4.30B). No changes in mass spectra of lipid A were noted for *E. coli* carrying no or a mutated plasmid (Figure 4.30A, C). The mass differences of *m/z* ~ 28 (*m/z* 1768 and 1823) and ~ 43 (*m/z* 1839) correspond to heterogeneity of the length in fatty acid chain. The peak at *m/z* 1716 was assigned to the structure of lipid A with a monophosphate group. These outcomes indicate that neither the phosphatase gene nor any components of the IncX4 plasmid could confer resistance to colistin in the absence of the *mcr-1* gene.

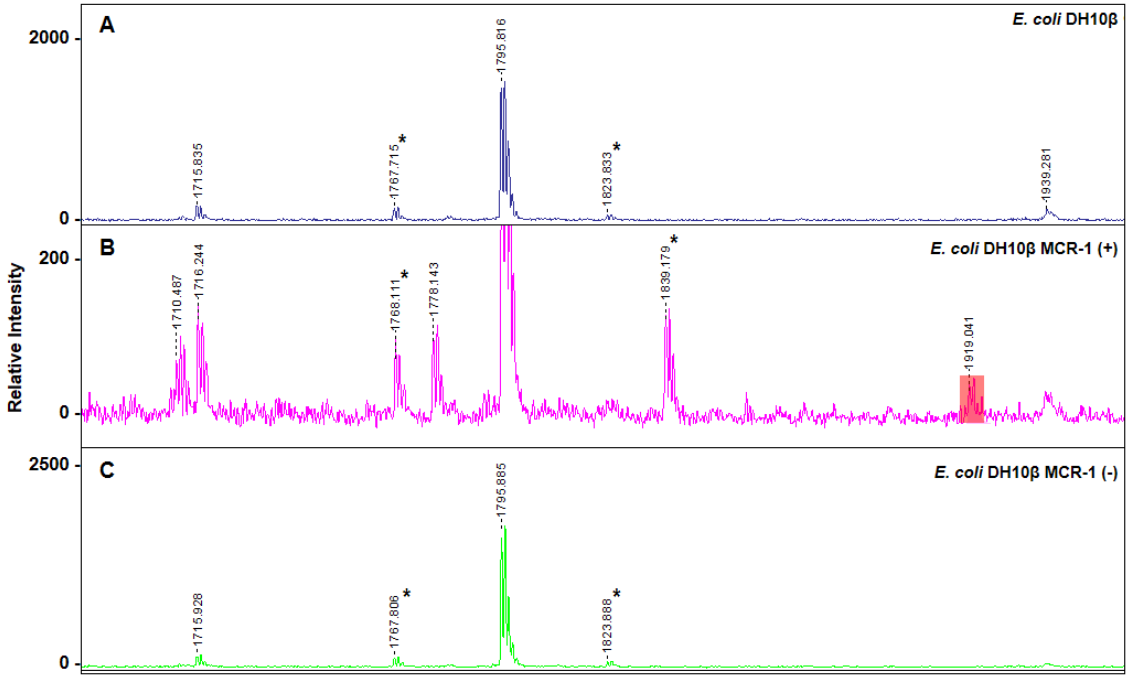

Figure 4.30 **MALDI-TOF-MS analysis of lipid A fractions isolated form *E. coli*.** The Lipid A was extracted from *E. coli* DH10β (A) and *E. coli* DH10β harboring either WT p002 (B) or *mcr-1* deletion mutant (p002::Δ*mcr-1*) (C). The pEtN-modified species are represented in red (*m/z* 1919). Asterisk (*) represents lipid A structure that varies in acyl chain length.

4.5.3 Purification and activity of MCR-1 enzyme

To further gain detailed insights into biochemical properties of full-length MCR-1, the *mcr-1* was engineered as a C-terminal hexahistidine gene fusion by cloning into pET-28a expression vector under an inducible T7 promoter. Subsequently, the protein was overexpressed by IPTG induction for 3 hours at 37°C, and then the membrane-bound MCR-1 was extracted from the collected membrane fraction in the presence of the 1% detergent dodecyl-β-D-maltoside (DDM). The protein-DDM micelles were loaded onto an immobilized metal-affinity chromatography (IMAC) Ni-NTA column and the MCR-1 bound protein was eluted with an increasing concentration of imidazole in elution buffer containing DDM, yielding approximately 2.6 mg/L. The homogeneity of the purified enzyme, as evaluated by SDS–PAGE, was 98% (Figure 4.31). MCR-1 polypeptide was visible as a single protein band of about 55 kDa, similar to the expected molecular mass of MCR-1. MS analysis further confirmed the identity of the recombinant MCR-1 transmembrane protein (Figure 4.33A).

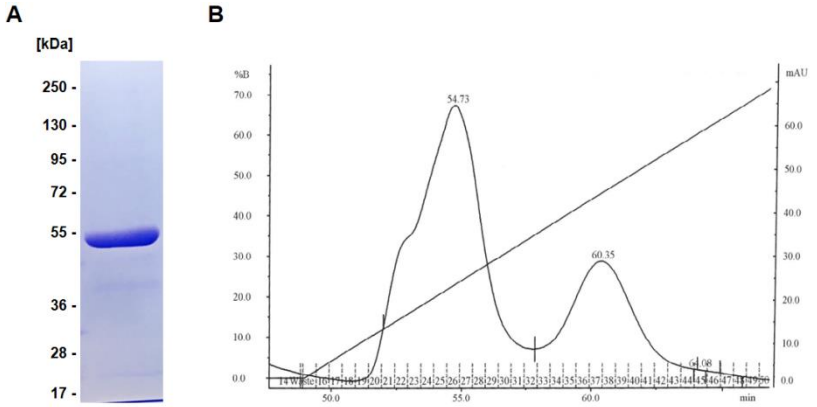

Figure 4.31 **Purification of full-length MCR-1. (A)** Coomassie blue stained 10% SDS-PAGE of purified MCR-1. Mass spectrometry analysis verified the identity of the recombinant MCR-1 protein (Figure 4.33A). **(B)** Elution profile of MCR-1 on HisTrap HP column, equilibrated with binding buffer (BB) (pH 7.4). Elution of proteins with linear gradient of imidazol (0 – 500mM) in BB, column volume: 5ml, flow rate: 2.5 mL/min, time of elution: 80 min.

Additionally, a deletion mutant of the gene (*mcr-1*$_{\Delta 1\text{-}214}$) was engineered and cloned into pET-28a vector in order to have a negative control for MCR-1 activity assay. The MCR-1$_{\Delta 1\text{-}214}$ protein was overexpressed and purified under native conditions with yield of up to 27 mg/L as previously described (Stojanoski et al. 2016) (Figure 4.32, Figure 4.33B).

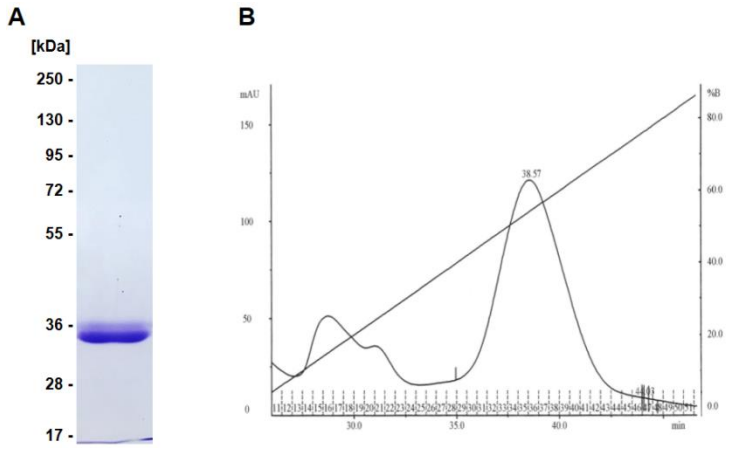

Figure 4.32 **Purification of catalytic domain of MCR-1 (MCR-1$_{\Delta 1\text{-}214}$). (A)** Coomassie blue stained 10% SDS-PAGE of purified MCR-1$_{\Delta 1\text{-}214}$. Mass spectrometry analysis verified the identity of the recombinant MCR-1 protein (Figure 4.3B). **(B)** Elution profile of MCR-1$_{\Delta 1\text{-}214}$ on HisTrap HP column, equilibrated with binding buffer (BB) (pH 7.4). Elution of proteins with linear gradient of imidazol (0 – 500mM) in BB, column volume: 5ml, flow rate: 2.5 mL/min, time of elution: 50 min.

Figure 4.33 **MS analysis of purified MCR-1. (A)** The full-length MCR-1. **(B)** The catalytic domain of MCR-1 (MCR-1$_{\Delta 1\text{-}214}$). The proteins were identified based on matches to their sequences resulting from comparing of observed peptide MS/MS spectra to theoretical spectra.

To assess the activity of the purified MCR-1 and soluble domain (MCR$_{\Delta 1\text{-}214}$) used as a negative control, a fluorescence-based TLC enzyme assay was performed using a lipid substrate tagged with a fluorescent label (Acyl-NBD-PE). As shown in Figure 4.34A, the MCR-1 was able to successfully remove pEtN group from the lipid substrate, confirming that the purified enzyme adopted a proper conformational state in DDM detergent micelles and was enzymatically active. The product formed by reaction with the full-length MCR-1 was confirmed by MS to be 1-acyl-2-{12-[(7-nitro-2-1,3-benzoxadiazol-4-yl)amino]dodecanoyl}-sn-glycerol (Figure 4.34 B). In contrast, a MCR$_{\Delta 1\text{-}214}$ construct was unable to catalyze pEtN hydrolysis, confirming that the transmembrane domain of MCR-1 is required for its activity on a lipid substrate.

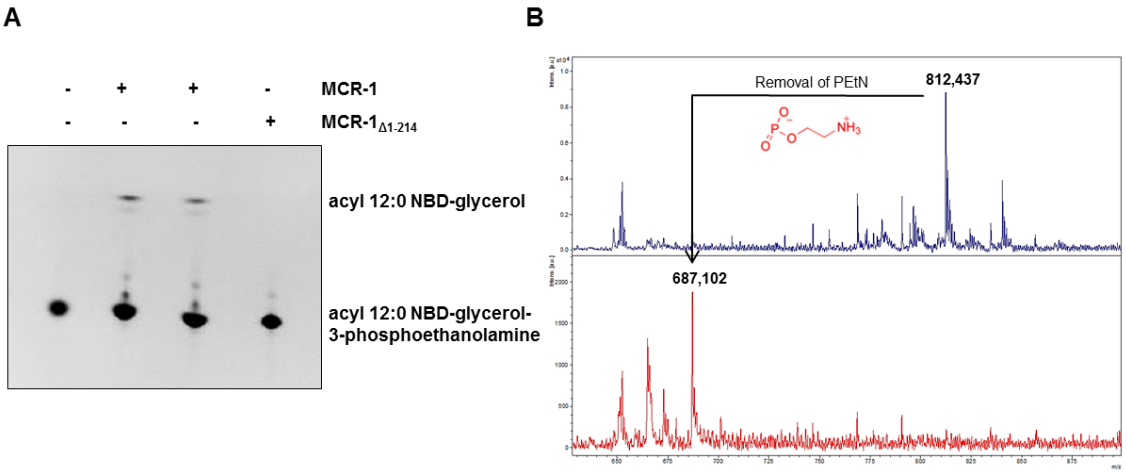

Figure 4.34 **Activity of purified MCR-1 enzyme. (A).** The fluorescence-based TLC enzyme assay of recombinant MCR-1 purified in n-Dodecyl β-D-maltoside (DDM) detergent micelles. **(B)** MS analysis of the product formed by reaction of acyl-NBD-PE with the MCR-1 enzyme. The substrate is labeled as an acyl 12:0 NBD-glycerol-3-phosphoethanolamine and the product is labeled as an acyl 12:0 NBD-glycerol.

4.5.4 Calcium-dependence of *mcr-1*-mediated resistance to colistin

Although the expression of *mcr-1* gene leads to the modification of the outer leaflet of the outer membrane and results in increased resistance to colistin, many MCR-1 producers show a MIC of 2 mg/L for colistin, and therefore are categorized as sensitive according to EUCAST guidance (Chew et al. 2017). This suggests that the *mcr-1* gene is able to confer resistance to colistin but clearly only under defined conditions. These observations have encouraged a joint CLSI-EUCAST subcommittee to announce warnings related to the overall poor credibility of colistin susceptibility testing (Eucast 2016). Therefore, all methods to simplify and improve determination of MIC towards polymyxins, i.e. colistin are highly wanted. By analyzing the minimum inhibitory concentration of colistin for *mcr-1*-producing *Enterobacteriaceae* isolates, we observed that MCR-1 producers exhibited increased resistance to colistin when they were grown in the presence of heat-inactivated serum (Table 4.4).

Table 4.4 The colistin MIC susceptibility for subset of *mcr-1*-producing *E. coli* isolates. The MICs were determined by microdilution method in the reference cation-adjusted Mueller Hinton broth (CA-MHB) containing 20% of heat-inactivated normal human serum (iNHS).

Isolate (Inc group)	**Broth microdilution MIC* [mg/L]**	
	CA-MHB	CA-MHB supplemented with 20% NHS
E. coli _001 (IncHI2)	4	6
E. coli _002 (IncX4)	4	6
E. coli _006 (IncX4)	4	6
E. coli _018 (chromosomal)	4	6
E. coli _055 (ND)	4	6
E. coli DO14** (NA)	0.5	0.5
E. coli DO21** (NA)	0.5	0.5
*E. coli*_017** (NA)	0.5	0.5

*The MIC is defined as the lowest concentration of the colistin that inhibits visible growth of the tested isolate as observed with the unaided eye. ** *mcr-1*-negative isolate; ND – not determined; NA – not applicable.

Since serum comprises high levels of calcium ions, I evaluated whether addition of Ca^{2+} to broth could be used as an enhancing agent for the detection of *mcr-1*-encoding *Enterobacteriaceae*. I noted that elevated concentrations of Ca^{2+} in the media are optimal for the reliable detection of *mcr-1*-positive isolates. Therefore, I formulated the calcium-enhanced medium (CE-MHB) containing 200 mg/L Ca^{2+} and compared it to the reference broth (CA-MHB) by using microdilution and Etest methods. Initially, a subset of *mcr-1*-positive isolates was examined by microdilution and Etest methods. A pronounced difference in MIC values between CA-MHB and the CE-MHB was observed. The MIC for colistin ranged from between

4 mg/L and 8 mg/L in CA-MHB, and increased to between 16 and 32 mg/L in CE-MHB (Table 4.5).

Table 4.5 Colistin susceptibility results for a subset of *mcr-1*-positive *E. coli* isolates. The MICs were determined in cation-adjusted Mueller-Hinton broth (CA-MHB) and calcium-enhanced Mueller-Hinton broth (CE-MHB) by broth microdilution and Etest.

Isolate (Inc type)	Broth microdilution MIC* [mg/L]		Etest MIC* [mg/L]	
	CA-MHB	CE-MHB	CA-MHB	CE-MHB
*E. coli*_017** (NA)	0.5	0.5	1.5	1.5
*E. coli*_020 (IncHI2)	4	16	3	12
*E. coli*_041 (IncX4)	4	16	4	16
*E. coli*_044 (IncHI2)	8	32	4	24
*E. coli*_053 (ND)	8	32	4	24
*E. coli*_055 (ND)	4	32	4	24
*E. coli*_059 (IncX4)	4	32	4	24

*The MIC is defined as the lowest concentration of the colistin that inhibits visible growth of the tested isolate as observed with the unaided eye. ** *mcr-1*-negative isolate; NA – not applicable; ND – not determined.

I also detected a significant increase in MIC values for colistin with CE-MHB, compared to the reference CA-MHB when using Etest (Figure 4.35). Therefore, CE-MHB clearly determines *mcr-1*-positive bacteria regardless of the assay format (liquid, solid) used. It is noteworthy that isolates lacking *mcr-1* gene and being susceptible to colistin did not exhibit an increased MIC towards colistin in CE-MHB. Moreover, the concentration of Ca^{2+} used has no adverse effects on bacterial growth (results not shown).

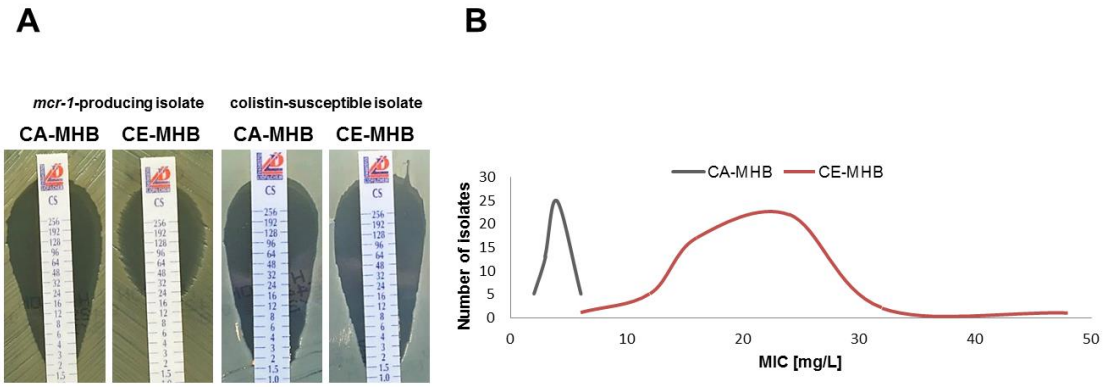

Figure 4.35 **The effect of increased calcium concentration on the minimum inhibitory concentration (MIC) of colistin for MCR-1 producers. (A)** The colistin MIC values of colistin-susceptible and a representative *mcr-1*-positive isolate. **(B)** Colistin susceptibility testing of 49 isolates expressing *mcr-1* gene. A significant upward shift in colistin MIC values was observed in CE-MHB, as compared to the reference CA-MHB. The MICs were determined in cation-adjusted Mueller Hinton broth (CA-MHB) and calcium-enhanced Mueller Hinton broth (CE-MHB) by Etest.

To directly confirm the contribution of the *mcr-1* gene to calcium-induced resistance to colistin, the gene was removed from the IncX4-plasmid p002 in order to create the isogenic variant p002::Δ*mcr-1* (Figure A-0.1, Appendix C). The MICs towards colistin of *E. coli* DH10β, containing either the wild type p002 or p002::Δ*mcr-1* was determined in CA-MHB to be 4 mg/L and 2 mg/L, respectively. However, the MIC values of the strain harboring p002 increased to 32 mg/L when grown in CE-MHB broth. The isogenic *E. coli* DH10β strain harboring p002::Δ*mcr-1* remained susceptible to colistin at 2mg/L, demonstrating an essential role of *mcr-1* gene in calcium-induced colistin resistance (Figure 4.36).

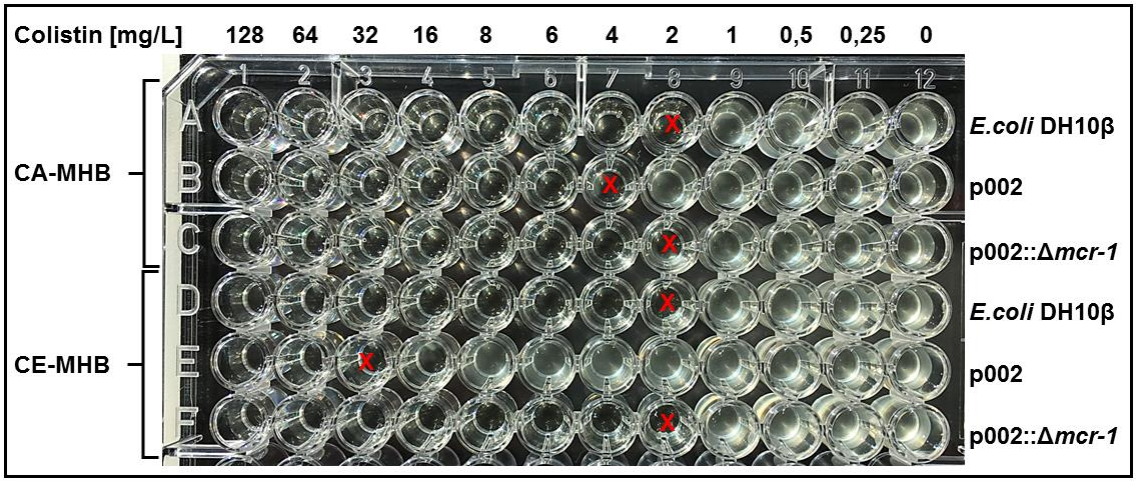

Figure 4.36 **The image of microtiter plate presenting the results of MIC determination to colistin.** Colistin susceptibility testing for *E. coli* DH10β harboring p002 or p002::Δ*mcr-1* determined by broth microdilution in cation-adjusted Mueller-Hinton broth (CA-MHB) and calcium-enhanced Mueller-Hinton broth (CE-MHB). The MIC is defined as the lowest concentration of the colistin that inhibits visible growth of the tested isolate as observed with the unaided eye and was marked in red X.

4.5.5 Analysis of interaction between colistin and calcium ions

The observations of previous research groups (Sud & Feingold 1970; Chen & Feingold 1972; Newton 1954) suggest that divalent cations may antagonize the bactericidal effect of polymyxin antibiotics. However, the exact mechanism of these antagonism events is not known yet. To exclude the interactions between calcium ions and colistin molecules, the NMR-spectroscopy analysis was carried out. The NMR method is useful for studying the complexation of small molecule ligands, e.g. peptide antibiotics with metal ions by recording the chemical shift of analyzing particles. I started with a NMR spectral profiling of intact colistin followed by measuring NMR spectra of a mixture of colistin and calcium chloride dehydrate. In order to analyse the colistin-calcium interactions, the peptide was dissolved in DMSO-d6 either

separately or along with increasing concentration of CaCl2 x 2H2O. The spectra of colistin in the presence or absence of calcium ions were measured (Figure 4.37). No change in the proton chemical shift of the peptide in presence of calcium was observed, suggesting that colistin complexation by calcium ions did not occur.

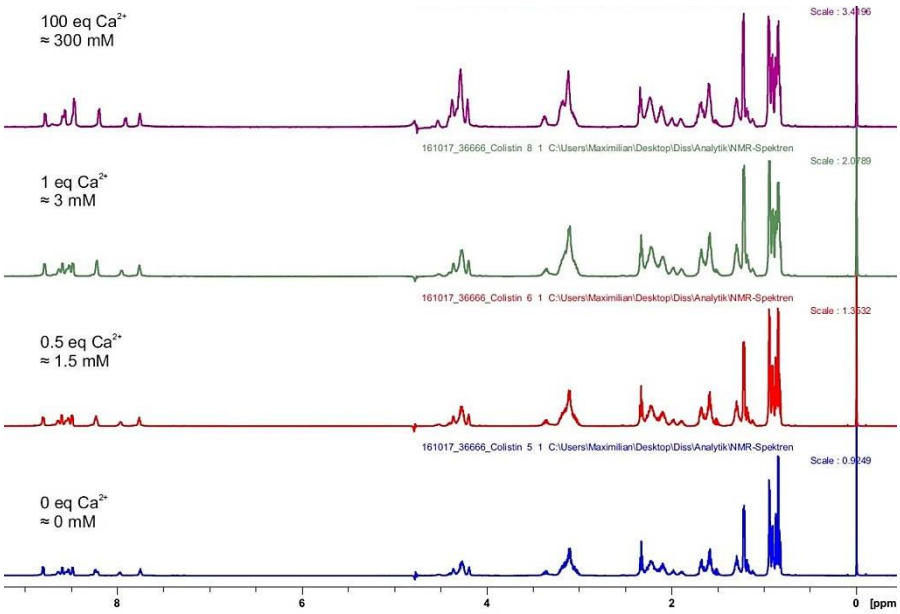

Figure 4.37 **1H-NMR spectra of colistin peptide preincubated with and without different concentration of calcium salt taken at 28°C.** A complexation or binding of colistin by calcium ions would lead to a change in the chemical shift of the side chain signals of the colistin antibiotic but they are identical in the presence/absence of Ca^{2+}. The 1H-NMR analysis of changes in chemical shifts has not identified the sites susceptible to interactions with calcium ions.

4.5.6 Differentiation between MCR-1 and non-MCR-1 producers based on Ca^{2+} deprivation

The discovery that *mcr-1*-mediated resistance to colistin is calcium inducible (see chapter 4.5.4) encourage me to evaluate the effects of calcium depletion on MCR-1 activity *in situ* as measured by growth curve determination for representative *mcr-1*-producing *E. coli* and isolate intrinsically resistant to colistin. Removal of calcium through addition of the increasing concentration of chelating agent selective for Ca^{2+}, EGTA inhibited the growth of *E. coli* isolate expressing *mcr-1* gene in the presence of colistin (Figure 4.38A). Surprisingly, the growth of isolates exhibiting a *mcr-1*-indepentent resistance mechanism to colistin was not repressed by the addition of a chelating agent (Figure 4.38B).

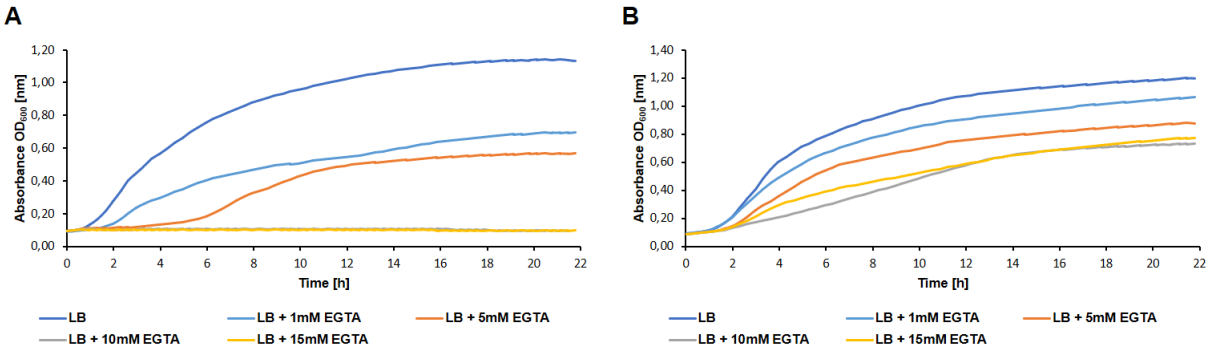

Figure 4.38 **Growth curves of representative MCR-1 and non-MCR-1 producers in the presence of increasing concentration of EGTA and 2 mg/L of colistin. (A)** The growth curves of *mcr-1*-producing *E. coli* and **(B)** *Providencia rettgeri* exhibiting *mcr-1*-independent resistance mechanism to colistin. In the presence of colistin, EGTA inhibits the growth of MCR-1 producers, whereas intrinsically-resistant isolates are not affected. Data are expressed as the mean ± SEM from three independent experiments.

Profound growth inhibition due to EGTA exposure was also observed when MIC values towards colistin were determined for 48 *mcr-1*-expressing *E. coli* (Figure 4.39) supporting the theory for calcium being a requirement in MCR-1 function. These outcomes imply that divalent cations, specifically calcium ions, are important to resistance mediated by MCR-1 mechanism.

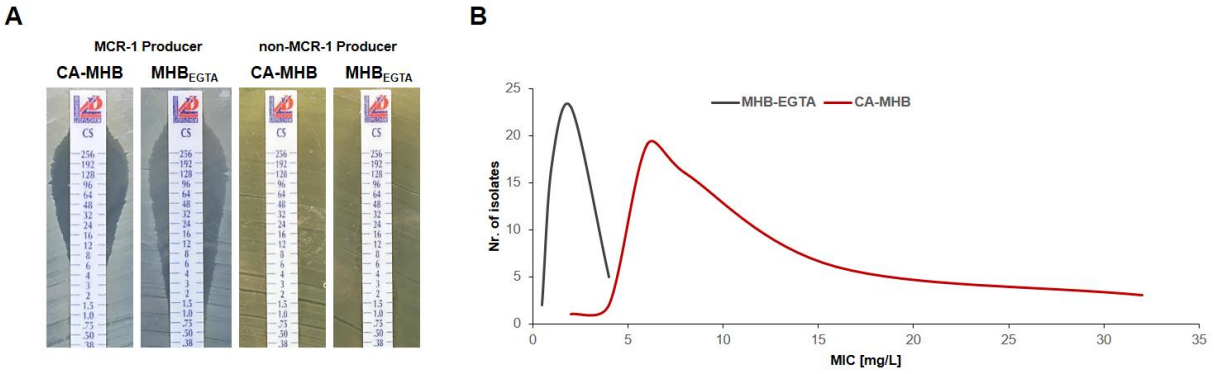

Figure 4.39 **The effect of calcium depletion on the minimum inhibitory concentration (MIC) of colistin for MCR-1 and non-MCR-1 producers. (A)** The colistin MIC values for representative *mcr-1*-producing and intrinsically resistant isolates determined by Etest. **(B)** Colistin susceptibility testing of 48 isolates expressing *mcr-1* gene determined by broth microdilution (BMD). A significant drop in colistin MIC values was observed in Ca^{2+} depleted medium for all tested MCR-1 producers. The colistin MICs were measured in cation-adjusted Mueller Hinton broth (CA-MHB) and Mueller Hinton broth supplemented with 10 mM EGTA (MHB_{EGTA}).

On the basis of the aforementioned results, which are indicating that the *mcr-1*-dependent colistin resistance mechanism requires calcium for its activity, I developed a simple method for differentiation between MCR-1 and non-MCR-1 producers. This test is based on the broth

microdilution (BMD) in MHB supplemented with 10 mM EGTA (MHB_{EGTA}) and standard CA-MHB as recommended by the European Committee on Antimicrobial Susceptibility Testing (EUCAST) and Clinical Laboratory Standard Institute (CLSI) guidelines. For each tested isolate, bacterial suspension was inoculated in parallel into all wells of 2 rows in 96well microplate, including CA-MHB and MHB_{EGTA} (Figure 4.40).

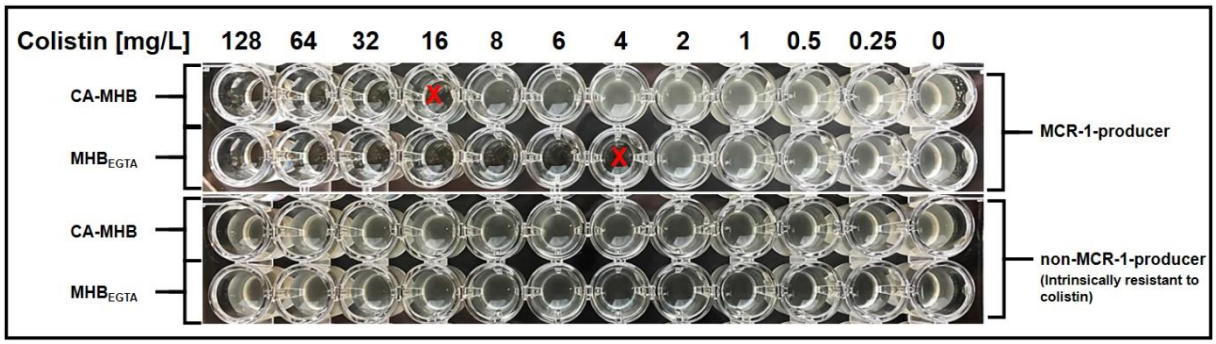

Figure 4.40 **Representative results of the EGTA-based test for distinguishing of MCR-1 and non-MCR-1 producers.** Intrinsically resistant isolates exhibit the same MIC towards colistin in both CA-MHB and MHB_{EGTA}, whereas *mcr-1*-producing *E. coli* have decreased colistin MIC values in MHB_{EGTA} compare to CA-MHB.

The parallel analysis of MIC of colistin in CA-MHB and MHB_{EGTA} allowed for simultaneous colistin susceptibility testing and differentiation between MCR-1 and non-MCR-1 producers. All isolates intrinsically resistant to colistin had the same MIC towards colistin in both CA-MHB and MHB_{EGTA}, whereas MCR-1 producers exhibited a decrease in colistin MICs in MHB_{EGTA} compared to CA-MHB. The mechanisms leading to this effect remain to be elucidated.

The test described here is simple to perform and is based on the requirement of the MCR-1 relating to the presence of Ca^{2+}. It provides not only detection of colistin-resistant *Enterobacteriaceae* but also enable for determination of different types of colistin resistance mechanisms (i.e. intrinsic and transferable) and therefore may contribute to containment of mobile colistin resistance.

4.5.7 LPS modification triggers formation of OMV

Modification of bacterial outer membrane mediated by *mcr-1* gene not only results in increased resistance to cationic antimicrobial peptides, such as colistin but also may contribute to other events important for bacterial survival, colonization and host inception. Recent study have revealed links between remodeling of lipid A domain of LPS and the delivery of proteins and

toxins that are associated with outer membrane vesicles (Elhenawy et al. 2016). Elhenawy at al. discovered that changes in LPS mediated by deacylation of lipid A play a role in OMV biogenesis. Divalent cations intercalate between LPS molecules and stabilize the negatively charged bacterial membranes. Modification of lipopolysaccharides can alert LPS packing order by replacing structurally important cations leading to charge - charge repulsion, and therefore trigger local deformation of outer membrane, causing increase formation of the OMV. Thus, I tested the effect of LPS remodeling mediated by *mcr-1* colistin resistance mechanism on OMV formation employing recombinant *E. coli* DH10β strain expressing *mcr-1* gene as well as transconjugants of *E. coli* J53 carrying different *mcr-1*-encoding plasmids (Figure 4.41). Expression of *mcr-1* in recombinant *E. coli* resulted in 2-fold increase in vesiculation phenotype compare to empty vector control. The same profound augmentation of OMV levels was observed for transconjugants of *E. coli* J53 harboring *mcr-1* in different Inc-type plasmids. Taken together, these results suggest that the *mcr-1* gene can trigger elevated releases of OMVs by modification of outer membrane through addition of phosphoethanolamine group to lipid A domain of LPS.

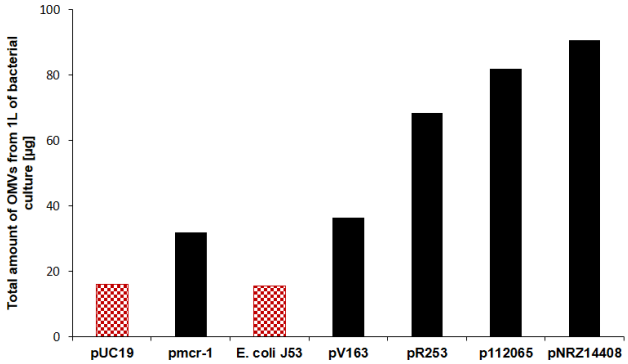

Figure 4.41 **Expression of *mcr-1* gene induces OMV production in *E. coli*.** The *mcr-1* gene cloned into pUC19 vector or encoded on different Inc-type plasmids was transferred into *E. coli* DH10β and *E. coli* J53, respectively. Vesiculation phenotype of *E. coli* was assessed by OMVs isolation followed by vesicular proteins quantification based on Bradford assay. Control strains carrying either the empty vector control or no plasmid are marked in white and red chequers. Bar graph represents data obtained from single trial analysis.

Discussion - Section II

In the second section of this thesis, I investigated the modification of the bacterial membranes at the level of lipopolysaccharides mediated by plasmid-borne colistin resistance mechanism (*mcr-1*). I confirmed that the expression of this gene confers resistance to colistin by catalyzing the addition of phosphoethanolamine (pEtN) group to lipid A. Moreover, full-length MCR-1 protein was purified and characterized in terms of its biochemical properties. Based on discovered conditions required for functionality of MCR-1, I devised a novel calcium-enhanced medium for improved determination of *mcr-1*-producing *Enterobacteriace* as well as a new EGTA-based assay for distinguishing of MCR-1 and non-MCR-1 producers. In the following chapter, the overview of obtained outputs is given to summarize and discuss the data from second section of this thesis.

The effect of membrane remodeling mediated by MCR-1 on resistance to colistin and OMV formation

The increasing occurrence of multidrug-resistant (MDR) Gram-negative bacteria (GNB) is a serious threat to global healthcare system due to the severely limited treatment options. In particular, the ESBL-producing GNB that are resistant to carbapenems pose the greatest challenge for successful therapy (World Health Organization 2017). Progressively, colistin is used as a last-line antibiotic for GNB infections as the spread of plasmids encoding antibiotic resistance led to increased treatment failure rates for carbapenems or third generation cephalosporins (Biswas et al. 2012). However, colistin treatment has resulted in the selection of MDR bacterial isolates with chromosomal mutations leading to polymyxin resistance and, more recently, the appearance of a plasmid-encoded resistance to colistin (*mcr-1*) (Liu et al. 2016). This first transferable colistin resistance mechanism might contribute to an even faster spread of colistin resistance among *Enterobacteriaceae* isolates leading to nosocomial outbreaks of untreatable infections. The *mcr-1* gene codes for phosphoethanolamine (pEtN) transferase enzyme that catalyze the transfer of pEtN group onto the glucosamine-disaccharide of lipid A in the outer leaflet of the bacterial outer membrane (Anandan, Evans, Condic-Jurkic, O'Mara, John, Phillips, G. a. Jarvis, et al. 2017). However, its exact mode of action remains to be understood. One of the objectives of this thesis was to investigate the impact of MCR-1 on bacterial membrane remodeling and consequently resistance to colistin.

Homology modelling of the complete MCR-1 with the RaptorX protein structure prediction server identified the soluble portions of two pEtN transferases, LptA and EptC, as

the closest relatives of known structure. The MCR-1 contains two discretely folded domains: one N-terminal transmembrane (TM) domain and one C-terminal presumably periplasmic-facing catalytic domain (Ma et al. 2016). I experimentally validated that the expression of the complete *mcr-1* gene augments colistin resistance in *E. coli*, as assessed by determination of MIC towards colistin for a recombinant strain expressing *mcr-1* gene, as well as analysis of structural changes in lipid A extracted from a transconjugant of *E. coli* harboring wild type or mutated IncX4 plasmids. This supports the previous findings indicating that *mcr-1* confers resistance to colistin by masking the negative charges of the 1 and 4' phosphate groups on lipid A, thereby reducing its affinity for cationic peptides (Y. Y. Liu et al. 2017; Y. Y. Liu et al. 2017). To get insights into biochemical properties of MCR-1, the *mcr-1* gene was cloned into a pET-28a expression vector, followed by protein overexpression and purification in the presence of the 1% detergent dodecyl-β-D-maltoside (DDM) by a metal-affinity chromatography (IMAC). Furthermore, the purified full-length MCR-1 was found to be enzymatically active, as determined by cleavage of the Acyl-NBD-PE substrate using fluorescence-based thin layer chromatography (TLC) enzyme assay. In addition, the truncated version of MCR-1 (MCR-$1_{\Delta 1\text{-}214}$) was not able to successfully hydrolysis of pEtN group from the lipid substrate, suggesting that membrane anchoring region is essential for proper function of the MCR-1 enzyme. This result is consistent with the previous findings indicating that transmembrane domain may play a key role in substrate and lipid A binding (Gao et al. 2016; Hinchliffe et al. 2017; Hu et al. 2016; Ma et al. 2016; Stojanoski et al. 2016). To the best of my knowledge, this is the first report on purification of complete MCR-1, which is enzymatically active.

The *mcr-1* gene is highly conserved and is capable of conferring resistance to colistin but clearly only under defined conditions. Thus, even though the presence of the *mcr-1* gene results in increased resistance to polymyxin antibiotics, many isolates exhibit an MIC of 2 mg/L towards colistin, just below the clinical breakpoint of EUCAST, and are therefore categorized as sensitive despite harboring the plasmid-borne colistin resistance gene (Chew et al. 2017). An analysis of minimum inhibitory concentration (MIC) towards colistin for *mcr-1*-producing *Enterobacteriaceae* isolates revealed an increased resistance to colistin in the presence of heat-inactivated human serum, which contains high amounts of calcium ions. This led us to the discovery that elevated Ca^{2+} level is required for the functionality of *mcr-1*-mediated resistance. Therefore, I devised a calcium-enhanced medium (CE-MHB) based on MHB that mimics conditions required for the mobile colistin resistance and allows for solving current problems associated with colistin susceptibility testing for isolates exhibiting low MICs towards colistin

(EUCAST 2016). All *mcr-1*-encoding isolates tested in this thesis that grown in CE-MHB exhibited increased MIC values as compared to growth in the reference CA-MHB. There was a clear separation of MIC values between resistant- and susceptible- bacteria when using CE-MHB. Importantly, the isolates that are colistin susceptible or do not carry the *mcr-1* gene remain colistin-sensitive regardless of the presence of increased calcium concentrations in the medium. Additionally, the use of a strain harboring an isogenic IncX4 plasmid lacking *mcr-1* confirms its contribution to calcium-dependent resistance towards colistin. However, the mechanisms leading to this effect remain to be understood, but because there is no increased resistance of colistin-sensitive strains, Ca^{2+} does not antagonize the bactericidal effect of colistin by preventing binding of the peptide to the bacterial cell wall.

In order to exclude the interactions between calcium ions and colistin, which could lead to increased MIC towards colistin, the NMR-spectroscopy analysis was performed. No change in the proton chemical shift of the peptide in presence of calcium was observed, suggesting there is no complexation of colistin by calcium ions. However, the previous reports suggest that divalent cations may antagonize the bactericidal effect of polymyxin antibiotics, but exact mechanism of these antagonism events is not known yet (Sud & Feingold 1970; Chen & Feingold 1972; Newton 1954).

The effects of calcium depletion on MCR-1 activity were evaluated by growth curve analysis as well as determination of MICs towards colistin for *mcr-1*-positive *E. coli*. Removal of calcium through addition of the 5 - 15 mM chelating agent selective for Ca^{2+}, EGTA inhibited the growth of *E. coli* isolates expressing *mcr-1* gene in the presence of colistin. Surprisingly, the growth of isolates intrinsically resistant to colistin has not been suppressed by calcium chelation. These outcomes imply that divalent cations, specifically calcium ions, are important to *mcr-1* mediated colistin resistance and their depletion can be used for simple differentiation between mobile and intrinsic/adaptive colistin resistance mechanisms. Based on my knowledge, there is no existing literature that describes the effect of chelation of calcium ions on *mcr-1* mediated resistance to colistin. However, there are recent publications indicating that use of metalloenzyme chelators, such as EDTA and dipicolinic acids inhibits the MCR-1 by binding zinc ions, which are present in the catalytic side of this enzyme (Esposito et al. 2017; Coppi at al. 2017). From a transmission analysis standpoint, an easy distinguishing of intrinsic and transferable resistance mechanism is an important healthcare parameter, which can prevent form further dissemination of colistin resistance, and consequently promote better treatment options.

In this thesis, I investigated the effect of membrane remodeling on OMV formation by the structural changes in lipid A mediated by *mcr-1* colistin resistance mechanism. To evaluate the involvement of MCR-1 in regulating of bacterial vesiculation phenotype, the *mcr-1* gene was recombinantly expressed in *E. coli* DH10β and OMVs were isolated followed by Bradford quantification assay. Expression of *mcr-1* has led to 2-fold increase in the amounts of OMV, as compared to empty vector control. The same profound increase of OMV levels was noted for transconjugants of *E. coli* J53 harboring *mcr-1* in different Inc-type plasmids. These results suggest that the release of vesicles may depend on net charge/integrity of bacterial membranes. This hypothesis is supported by Elhenawy et al. and Mashburn-Warren et al. who argued that changes in the structure of the lipid A and the loss of divalent cations stabilizing cell wall contribute to generate membrane curvature, and thus OMV production (Elhenawy et al. 2016; Mashburn-Warren et al. 2008). Although there are increasing number of compelling studies on the vesiculation phenomenon occurring in Gram-negative bacteria, the mechanisms of OMV formation remain still enigmatic (Bonnington & Kuehn 2017). Based on the current models for OMV production accepted by the scientific community (Schwechheimer & Kuehn 2015) as well as the aforementioned involvement of *mcr-1* and *hlyF* (which has been investigated in first section of this thesis) in the vesiculation process, it is rational to think that more than one mechanism is responsible for vesicles biogenesis. I agree with the hypothesis proposing that the induction of charge-charge repulsion triggered by the structural changes of lipopolysaccharide can lead to local membrane deformation, and consequently vesicle formation. The existence of such a LPS-dependent OMV formation mechanism, would be a convincing evidence that all Gram-negative bacteria have one unified, evolutionary conserved mode of vesicle biogenesis. In addition, a bilayer-couple model of OMV production is appealing to me as well (Schertzer & Whiteley 2012). It suggests that the increased concentration of an amphiphilic molecules causes expansion of the outer bacterial leaflet relative to the inner leaflet, thus triggering localized membrane curvature and consequently formation of double membranes vesicle. The release of OMVs composed of both outer and inner membranes would explain the presence of DNA and other cytoplasmic molecules, which could be packed into bacterial blebs along with cytoplasmic membrane.

In conclusion, the data in this section of the thesis evaluates the role of *mcr-1* gene with respect to colistin resistance, outer membrane vesicle formation and its involvement in altering the structure of lipid A. This study provides a biochemical analysis of purified full-length MCR-1 and reports on the elevated Ca^{2+} level that is required for *mcr-1*-mediated colistin resistance. The possibility that bacteria utilize the fluctuation in calcium ions to regulate the mobile colistin

resistance has significant implications for currently recommended colistin susceptibility testing. The Ca^{2+}-enhanced medium devised here will make surveillance of *mcr-1*-producing *Enterobacteriaceae* much easier and will improve our understanding of the true prevalence of *mcr-1* expressing isolates. Differentiation between MCR-1 and non-MCR-1 producers based on calcium deprivation will contribute to constrain dissemination of the mobile colistin resistance.

List of Tables

List of Figures

References

Alaniz, R.C. et al., 2007. Membrane vesicles are immunogenic facsimiles of Salmonella typhimurium that potently activate dendritic cells, prime B and T cell responses, and stimulate protective immunity in vivo. *Journal of immunology (Baltimore, Md. : 1950)*, 179(11), pp.7692–7701.

Alekshun, M.N. & Levy, S.B., 2007. Molecular Mechanisms of Antibacterial Multidrug Resistance. *Cell*, 128(6), pp.1037–1050.

Amber L. Schuh and Anjon Audhya, 2014. The ESCRT machinery: From the plasma membrane to endosomes and back again. , 49(3), pp.242–261.

Anandan, A., Evans, G.L., Condic-Jurkic, K., O'Mara, M.L., John, C.M., Phillips, N.J., Jarvis, G.A., et al., 2017. Structure of a lipid A phosphoethanolamine transferase suggests how conformational changes govern substrate binding, *Proc Natl Acad Sci*, 114(9):2218-2223.

Bader, G.D. & Hogue, C.W., 2003. An automated method for finding molecular complexes in large protein interaction networks. *BMC Bioinformatics*, 4(1), p.2.

Bai, J. et al., 2014. Identification and characterization of outer membrane vesicle-associated proteins in Salmonella enterica serovar Typhimurium. *Infection and Immunity*, 82(10), pp.4001–4010.

Barton, B.M., Harding, G.P. & Zuccarelli, A.J., 1995. A general method for detecting and sizing large plasmids. *Anal.Biochem.*, 226(2), pp.235–240.

Bauman, S.J. & Kuehn, M.J., 2006. Purification of outer membrane vesicles from Pseudomonas aeruginosa and their activation of an IL-8 response. *Microbes and Infection*, 8(9–10), pp.2400–2408.

Bernal, P. et al., 2013. Antibiotic adjuvants: Identification and clinical use. *Microbial Biotechnology*, 6(5), pp.445–449.

Biswas, S. et al., 2012. Colistin: an update on the antibiotic of the 21st century. *Expert Review of Anti-infective Therapy*, 10(8), pp.917–934.

Blair, J.M. a. et al., 2015. Molecular mechanisms of antibiotic resistance. *Nature Reviews Microbiology*, 13(1), pp.42–51.

Bohuszewicz, O., Liu, J. & Low, H.H., 2016. Membrane remodelling in bacteria. *Journal of Structural Biology*, 196(1), pp.3–14.

Bomberger, J.M. et al., 2009. Long-distance delivery of bacterial virulence factors by pseudomonas aeruginosa outer membrane vesicles. *PLoS Pathogens*, 5(4).

Bonnington, K. & Kuehn, M., 2017. Breaking the bilayer: OMV formation during environmental transitions. *Microbial Cell*, 4(2), pp.64–66.

Budhani, R.K. & Struthers, J.K., 1998. Interaction of Streptococcus pneumoniae and Moraxella catarrhalis: Investigation of the indirect pathogenic role of β-lactamase-producing moraxellae by use of a continuous-culture biofilm system. *Antimicrobial Agents and Chemotherapy*, 42(10), pp.2521–2526.

Burrows LL, Charter DF, Lam JS., 1996. Molecular characterization of the *Pseudomonas aeruginosa* serotype O5 (PAO1) B-band lipopolysaccharide gene cluster. *Mol Microbiol*, 22, pp.481–495.

Carmen Schwechheimer & Kuehn, M.J., 2015. Outer-membrane vesicles from Gram-negative bacteria: biogenesis and functions. *Nat. Rev. Microbiol*, 13(10), pp.605–619.

Cascales, E. et al., 2002. Pal lipoprotein of *Escherichia coli* plays a major role in outer membrane integrity. *Journal of bacteriology*, 184(3), pp.754–759.

Cascales, E. et al., 2000. Proton motive force drives the interaction of the inner membrane TolA and outer membrane Pal proteins in *Escherichia coli*. *Molecular Microbiology*, 38(4), pp.904–915.

Chatterjee, S.N. & Das, J., 1967. Electron microscopic observations on the excretion of cell-wall material by Vibrio cholerae. *Journal of general microbiology*, 49(4), pp.1–11.

Chen, C.C. & Feingold, D.S., 1972. Locus of divalent cation inhibition of the bactericidal action of polymyxin B. *Antimicrobial Agents and Chemotherapy*, 2(5), pp.331–335.

Chen, H.D. & Groisman, E.A., 2013. The biology of the PmrA/PmrB two-component system: the major regulator of lipopolysaccharide modifications. *Annual review of microbiology*, 67, pp.83–112.

Chew, K.L. et al., 2017. Colistin and polymyxin B susceptibility testing for carbapenem-resistant and *mcr* -positive *Enterobacteriaceae* : Comparison of Sensititre, Microscan, Vitek 2, and Etest with broth microdilution. *Journal of Clinical Microbiology*, (June), p.JCM.00268-17.

Choi, D.-S. et al., 2011. Proteomic analysis of outer membrane vesicles derived from Pseudomonas aeruginosa. *Proteomics*, 11(16), pp.3424–3429.

Ciofu, O. et al., 2000. Chromosomal beta-lactamase is packaged into membrane vesicles and secreted from Pseudomonas aeruginosa. *The Journal of antimicrobial chemotherapy*, 45(1), pp.9–13.

Conly, J.M. & Johnston, B.L., 2006. Colistin: The phoenix arises. *Canadian Journal of Infectious Diseases and Medical Microbiology*, 17(5), pp.267–269.

Dauros Singorenko, P. et al., 2017. Isolation of membrane vesicles from prokaryotes: a technical and biological comparison reveals heterogeneity. *Journal of Extracellular Vesicles*, 6(1), p.1324731.

Davin-Regli, A. & Pagès, J.M., 2015. Enterobacter aerogenes and Enterobacter cloacae; Versatile bacterial pathogens confronting antibiotic treatment. *Frontiers in Microbiology*, 6(MAY), pp.1–10.

Davtyan, A., Simunovic, M. & Voth, G.A., 2016. Multiscale simulations of protein-facilitated membrane remodeling. *Journal of Structural Biology*, 196(1), pp.57–63.

DE, S.N. et al., 1959. Enterotoxicity of bacteria-free culture-filtrate of Vibrio cholerae. *Nature*, 183(4674), pp.1533–4.

Deatheragea, B.L. & Cooksona, B.T., 2012. Membrane vesicle release in bacteria, eukaryotes, and archaea: A conserved yet underappreciated aspect of microbial life. *Infection and Immunity*, 80(6), pp.1948–1957.

Dijkshoorn, L., Nemec, a & Seifert, H., 2007. An increasing threat in hospitals: multidrug-resistant Acinetobacter baumannii. *Nat Rev Microbiol*, 5(12), pp.939–951.

Dorward, D.W., Garon, C.F. & Judd, R.C., 1989. Export and intercellular transfer of DNA via membrane blebs of Neisseria gonorrhoeae. *Journal of Bacteriology*, 171(5), pp.2499–2505.

Dubey, G.P. et al., 2016. Architecture and Characteristics of Bacterial Nanotubes. *Developmental Cell*, 36(4), pp.453–461.

Duncan, L. et al., 2004. Loss of lipopolysaccharide receptor CD14 from the surface of human

macrophage-like cells mediated by Porphyromonas gingivalis outer membrane vesicles. *Microbial Pathogenesis*, 36(6), pp.319–325.

Elhenawy, W. et al., 2016. LPS remodeling triggers formation of outer membrane vesicles in salmonella. *mBio*, 7(4), pp.1–12.

Ellis, T.N. & Kuehn, M.J., 2010. Virulence and immunomodulatory roles of bacterial outer membrane vesicles. *Microbiology and molecular biology reviews : MMBR*, 74(1), pp.81–94.

Eucast, 2016. Recommendations for MIC determination of colistin (polymyxin E) As recommended by the joint CLSI-EUCAST Polymyxin Breakpoints Working Group Available_from: http://www.eucast.org/fileadmin/src/media/PDFs/EUCAST_files/General_documents/Recommendations, (March, 22), p.2016.

Falagas, M.E. et al., 2006. The use of intravenous and aerosolized polymyxins for the treatment of infections in critically ill patients: A review of the recent literature. *Clinical Medicine and Research*, 4(2), pp.138–146.

Falagas, M.E. & Kasiakou, S.K., 2005. Colistin: the revival of polymyxins for the management of multidrug-resistant gram-negative bacterial infections. *Clinical Infectious Diseases*, 40(9), pp.1333–1341.

Falgenhauer, L. et al., 2017. Genome analysis of the carbapenemand colistin-resistant Escherichia coli isolate NRZ14408 reveals horizontal gene transfer pathways towards panresistance and enhanced virulence. *Antimicrobial Agents and Chemotherapy*, 61(4), pp.1–6.

Frias, A. et al., 2010. Membrane vesicles: A common feature in the extracellular matter of cold-adapted antarctic bacteria. *Microbial Ecology*, 59(3), pp.476–486.

Fulsundar, S. et al., 2014. Gene transfer potential of outer membrane vesicles of Acinetobacter baylyi and effects of stress on vesiculation. *Applied and Environmental Microbiology*, 80(11), pp.3469–3483.

Gaibani, P. et al., 2013. Outbreak Of citrobacter freundii carrying Vim-1 in an italian hospital, identified during the carbapenemases screening actions, June 2012. *International Journal of Infectious Diseases*, 17(9), pp.e714-e717.

Gao, R. et al., 2016. Dissemination and Mechanism for the MCR-1 Colistin Resistance. *PLoS Pathogens*, 12(11), pp.1–19.

Gurung, M. et al., 2011. Staphylococcus aureus produces membrane-derived vesicles that induce host cell death. *PLoS ONE*, 6(11): e27958.

Hancock, R.E., 1997. Peptide antibiotics. *The Lancet*, 349(9049), pp.418–422.

Hinchliffe, P. et al., 2017. Insights into the Mechanistic Basis of Plasmid-Mediated Colistin Resistance from Crystal Structures of the Catalytic Domain of MCR-1. *Scientific Reports*, 7(September 2016), p.39392.

Hu, M. et al., 2016. Crystal Structure of Escherichia coli originated MCR-1, a phosphoethanolamine transferase for Colistin Resistance. *Scientific Reports*, 6(September), p.38793.

Irving, A.T. et al., 2014. The immune receptor NOD1 and kinase RIP2 interact with bacterial peptidoglycan on early endosomes to promote autophagy and inflammatory signaling. *Cell Host and Microbe*, 15(5), pp.623–635.

Jan, A.T., 2017. Outer Membrane Vesicles (OMVs) of gram-negative bacteria: A perspective update. *Frontiers in Microbiology*, 8(JUN), pp.1–11.

Jang, K.-S. et al., 2014. Comprehensive proteomic profiling of outer membrane vesicles from Campylobacter jejuni. *Journal of proteomics*, 98, pp.90–8.

Johnson, J.R. et al., 2010. Escherichia coli sequence type ST131 as the major cause of serious multidrug-resistant E. coli infections in the United States. *Clinical Infectious Diseases*, 51(3), pp.286–294.

Johnson, T.J., Johnson, S.J. & Nolan, L.K., 2006. Complete DNA sequence of a ColBM plasmid from avian pathogenic Escherichia coli suggests that it evolved from closely related ColV virulence plasmids. *Journal of Bacteriology*, 188(16), pp.5975–5983.

Jones, C.L. et al., 2015. Fatal Outbreak of an Emerging Clone of Extensively Drug-Resistant Acinetobacter baumannii with Enhanced Virulence. *Clinical Infectious Diseases*, 61(2), pp.145–154.

Kadurugamuwa, J.L. & Beveridge, T.J., 1995. Virulence factors are released from Pseudomonas aeruginosa in association with membrane vesicles during normal growth and exposure to gentamicin: A novel mechanism of enzyme secretion. *Journal of Bacteriology*, 177(14), pp.3998–4008.

Källberg, M. et al., 2012. Template-based protein structure modeling using the RaptorX web server. *Nature protocols*, 7(8), pp.1511–22.

Kallberg, Y. et al., 2002. Short-chain dehydrogenases/reductases (SDRs). Coenzyme-based functional assignments in completed genomes. *European Journal of Biochemistry*, 269(18), pp.4409–4417.

Kamada, N. et al., 2013. Control of pathogens and pathobionts by the gut microbiota. *Nature immunology*, 14(7), pp.685–90.

Kaparakis-Liaskos, M. & Ferrero, R.L., 2015. Immune modulation by bacterial outer membrane vesicles. *Nature Reviews Immunology*, 15(6), pp.375–387.

Kaper, J.B., Nataro, J.P. & Mobley, H.L.T., 2004. Pathogenic Escherichia coli. *Nature Reviews Microbiology*, 2(2), pp.123–140.

Kavanagh, K.L. et al., 2008. Medium- and short-chain dehydrogenase/reductase gene and protein families: The SDR superfamily: Functional and structural diversity within a family of metabolic and regulatory enzymes. *Cellular and Molecular Life Sciences*, 65(24), pp.3895–3906.

Kempke, A.P. et al., 2016. Antibiotic strategies in the era of multidrug resistance. *Journal of intensive care medicine*, 20(1), pp.164–176.

Klieve, A. V et al., 2005. Naturally Occurring DNA Transfer System Associated with Membrane Vesicles in Cellulolytic. *Society*, 71(8), pp.4248–4253.

Klimentová, J. & Stulík, J., 2015. Methods of isolation and purification of outer membrane vesicles from gram-negative bacteria. *Microbiological Research*, 170, pp.1–9.

Kristensen, D.M. et al., 2010. A low-polynomial algorithm for assembling clusters of orthologous groups from intergenomic symmetric best matches. *Bioinformatics*, 26(12), pp.1481–1487.

Kulkarni, H.M. & Jagannadham, M. V., 2014. Biogenesis and multifaceted roles of outer membrane vesicles from Gram-negative bacteria. *Microbiology (United Kingdom)*, 160(2014), pp.2109–2121.

Kulp, A. & Kuehn, M.J., 2010. Biological functions and biogenesis of secreted bacterial outer membrane vesicles. *Annual review of microbiology*, 64, pp.163–184.

Kumar, K. et al., 2011. NIH Public Access., 2(8), pp.1305–1323.

Kwon, S.O. et al., 2009. Proteome analysis of outer membrane vesicles from a clinical Acinetobacter baumannii isolate. *FEMS Microbiology Letters*, 297(2), pp.150–156.

Laurent Poirel, Aurélie Jayol, P.N., 2017. Polymyxins: Antibacterial Activity, Susceptibility Testing, and Resistance Mechanisms Encoded by Plasmids or Chromosomes., 30(2), pp.557–596.

Lee, E.Y. et al., 2007. Global proteomic profiling of native outer membrane vesicles derived from Escherichia coli. *Proteomics*, 7(17), pp.3143–3153.

Lee, E.Y. et al., 2009. Gram-positive bacteria produce membrane vesicles: Proteomics-based characterization of Staphylococcus aureus-derived membrane vesicles. *Proteomics*, 9(24), pp.5425–5436.

Lee, J.-C.J.H. et al., 2013. Transcription factor σB plays an important role in the production of extracellular membrane-derived vesicles in Listeria monocytogenes. *PLoS ONE*, 8(8), p.e73196.

Li, Y. et al., 2012. LPS remodeling is an evolved survival strategy for bacteria. *Proceedings of the National Academy of Sciences*, 109(22), pp.8716–8721.

Ligon, B.L., 2004. Penicillin: Its Discovery and Early Development. *Seminars in Pediatric Infectious Diseases*, 15(1), pp.52–57.

Lim, S. & Yoon, H., 2015. Roles of outer membrane vesicles (OMVs) in bacterial virulence. *Journal of Bacteriology and Virology*, 45(1), pp.1–10.

Liu, Y.-Y. et al., 2015. Emergence of plasmid-mediated colistin resistance mechanism MCR-1 in animals and human beings in China: a microbiological and molecular biological study. *The Lancet Infectious Diseases*, 3099(15), pp.1–8.

Liu, Y.-Y. et al., 2017. Structural Modification of Lipopolysaccharide Conferred by *mcr-1* in Gram-Negative ESKAPE Pathogens. *Antimicrobial Agents and Chemotherapy*.

Ma, G. et al., 2016. High resolution crystal structure of the catalytic domain of MCR-1. *Scientific Reports*, 6(1), p.39540.

Magiorakos, a et al., 2011. Bacteria : an International Expert Proposal for Interim Standard Definitions for Acquired Resistance. *Microbiology*, 18(3), pp.268–281.

Mashburn-Warren, L. et al., 2008. Interaction of quorum signals with outer membrane lipids: Insights into prokaryotic membrane vesicle formation. *Molecular Microbiology*, 69(2), pp.491–502.

Mashburn-Warren, L.M. & Whiteley, M., 2006. Special delivery: Vesicle trafficking in prokaryotes. *Molecular Microbiology*, 61(4), pp.839–846.

McBroom, A.J. & Kuehn, M.J., 2007. Release of outer membrane vesicles by Gram-negative bacteria is a novel envelope stress response. *Molecular Microbiology*, 63(2), pp.545–558.

McBroom, a. J. et al., 2006. Outer Membrane Vesicle Production by Escherichia coli Is Independent of Membrane Instability. *Journal of Bacteriology*, 188(15), pp.5385–5392.

McMahon, H.T. & Gallop, J.L., 2005. Membrane curvature and mechanisms of dynamic cell membrane remodelling. *Nature*, 438(7068), pp.590–596.

Mellata, M., 2013. Human and Avian Extraintestinal Pathogenic *Escherichia coli* : Infections,

Zoonotic Risks, and Antibiotic Resistance Trends. *Foodborne Pathogens and Disease*, 10(11), pp.916–932.

Mellata, M., Touchman, J.W. & Curtis, R., 2009. Full sequence and comparative analysis of the plasmid pAPEC-1 of avian pathogenic E. coli chi7122 (O78:k80:H9). *PLoS ONE*, 4(1):e4232.

Mitra, S. et al., 2015. Immunomodulatory role of outer membrane vesicles of Shigella in mouse model. *Trials in Vaccinology*, 4, pp.56–60.

Momen-Heravi, F. et al., 2013. Current methods for the isolation of extracellular vesicles. *Biological Chemistry*, 394(10), pp.1253–1262.

Morales, C. et al., 2004. Detection of a novel virulence gene and a Salmonella virulence homologue among Escherichia coli isolated from broiler chickens. *Foodborne pathogens and disease*, 1(3), pp.160–165.

Mukherjee, K. et al., 2010. Galleria mellonella as a model system for studying Listeria pathogenesis. *Applied and Environmental Microbiology*, 76(1), pp.310–317.

Munita, J.M. et al., 2016. Mechanisms of Antibiotic Resistance. *Microbiol Spectr.*, 4(2), pp.1–37.

Murase, K. et al., 2016. HlyF produced by extraintestinal pathogenic Escherichia coli is a virulence factor that regulates outer membrane vesicle biogenesis. *Journal of Infectious Diseases*, 212(11), pp.856–865.

Needham, B.D. & Trent, M.S., 2013. Fortifying the barrier: the impact of lipid A remodelling on bacterial pathogenesis. *Nature Reviews Microbiology*, 11(7), pp.467–481.

Newton, B.A., 1954. Site of action of Polymyxin on Pseudomonas aeruginosa: Antagonism by Cations. *Journal of General Microbiology*, 10(3), pp.491–499.

Nho, J.S. et al., 2015. Acinetobacter nosocomialis secretes outer membrane vesicles that induce epithelial cell death and host inflammatory responses. *Microbial Pathogenesis*, 81, pp.39–45.

Nurk, S. et al., 2013. Assembling genomes and mini-metagenomes from highly chimeric reads. In *Lecture Notes in Computer Science (including subseries Lecture Notes in Artificial Intelligence and Lecture Notes in Bioinformatics)*. pp. 158–170.

Olaitan, A.O., Morand, S. & Rolain, J.-M., 2014. Mechanisms of polymyxin resistance: acquired and intrinsic resistance in bacteria. *Frontiers in Microbiology*, 5(November), p.643.

Pande, S. et al., 2015. Metabolic cross-feeding via intercellular nanotubes among bacteria. *Nature Communications*, 6, p.6238.

Panigraphy, R., 2015. Serratia marcescens Causing Pneumonia - A Rare Case Report. *J. Pulm. Respir. Med.*, 5(2), pp.254–255.

de Pedro, M.A. & Cava, F., 2015. Structural constraints and dynamics of bacterial cell wall architecture. *Frontiers in Microbiology*, 6(MAY), pp.1–10.

Pepperell, C. et al., 2002. Low-virulence Citrobacter species encode resistance to multiple antimicrobials. *Antimicrobial Agents and Chemotherapy*, 46(11), pp.3555–3560.

Pérez-Cruz, C. et al., 2013. New type of outer membrane vesicle produced by the gram-negative bacterium Shewanella vesiculosa M7T: Implications for DNA content. *Applied and Environmental Microbiology*, 79(6), pp.1874–1881.

Pérez-Cruz, C. et al., 2015. Outer-inner membrane vesicles naturally secreted by gram-negative

pathogenic bacteria. *PLoS ONE*, 10(1), pp.1–18.

Raetz, C.R.H. et al., 2007. Lipid A modification systems in gram-negative bacteria. *Annual review of biochemistry*, 76, pp.295–329.

Rajagopala, S. V. et al., 2014. The binary protein-protein interaction landscape of Escherichia coli. *Nature Biotechnology*, 32(3), pp.285–290.

Renelli, M. et al., 2004. DNA-containing membrane vesicles of Pseudomonas aeruginosa PAO1 and their genetic transformation potential. *Microbiology*, 150(7), pp.2161–2169.

Rivera, J. et al., 2010. Bacillus anthracis produces membrane-derived vesicles containing biologically active toxins. *Proceedings of the National Academy of Sciences of the United States of America*, 107(44), pp.19002–7.

Roier, S. et al., 2016. A novel mechanism for the biogenesis of outer membrane vesicles in Gram-negative bacteria. *Nature communications*, 7, p.10515.

Rumbo, C. et al., 2011. Horizontal transfer of the OXA-24 carbapenemase gene via outer membrane vesicles: A new mechanism of dissemination of carbapenem resistance genes in Acinetobacter baumannii. *Antimicrobial Agents and Chemotherapy*, 55(7), pp.3084–3090.

Sambrook, J., Russell, D.W. & Laboratory., C.S.H., 2012. Molecular cloning : a laboratory manual. *Cold Spring Harbor Laboratory, Cold Spring Harbor, N.Y.:, 4th.*

Schaar, V. et al., 2011. Moraxella catarrhalis outer membrane vesicles carry β-lactamase and promote survival of Streptococcus pneumoniae and Haemophilus influenzae by inactivating amoxicillin. *Antimicrobial Agents and Chemotherapy*, 55(8), pp.3845–3853.

Schembri, M.A., Dalsgaard, D. & Klemm, P., 2004. Capsule Shields the Function of Short Bacterial Adhesins. *Journal of Bacteriology*, 186(5), pp.1249–1257.

Schertzer, J. & Whiteley, M., 2012. A Bilayer-Couple Model of Bacterial Outer Membrane Vesicle. *MBio*, 3(2), pp.e00297-11.

Schouler, C. et al., 2012. Diagnostic strategy for identifying avian pathogenic Escherichia coli based on four patterns of virulence genes. *Journal of Clinical Microbiology*, 50(5), pp.1673–1678.

Schwechheimer, C. & Kuehn, M.J., 2015. Outer-membrane vesicles from Gram-negative bacteria: biogenesis and functions. *Nature reviews. Microbiology*, 13(10), pp.605–19.

Sharpe, S.W., Kuehn, M.J. & Mason, K.M., 2011. Elicitation of epithelial cell-derived immune effectors by outer membrane vesicles of nontypeable haemophilus influenzae. *Infection and Immunity*, 79(11), pp.4361–4369.

Shetty, A. et al., 2011. Nanopods: A new bacterial structure and mechanism for deployment of outer membrane vesicles. *PLoS ONE*, 6(6).

Sonnhammer, E.L.L., von Heijne, G. & Krogh, A., 1998. A hidden Markov model for predicting transmembrane helices in protein sequences. *Proc Int Conf Intell Syst Mol Biol.*,6, pp.175-82.

Southern, S.J. et al., 2016. Survival protein A is essential for virulence in Yersinia pestis. *Microbial Pathogenesis*, 92, pp.50–53.

Stojanoski, V. et al., 2016. Structure of the catalytic domain of the colistin resistance enzyme MCR-1. *BMC Biology*, 14(1), p.81.

Strand, M.R., 2008. Insect Hemocytes and Their Role in Immunity. *Insect Immunology*, 32, pp.25–47.

Sud, I.J. & Feingold, D.S., 1970. Mechanism of polymyxin B resistance in Proteus mirabilis. *Journal of Bacteriology*, 104(1), pp.289–294.

Tan, I.S. & Ramamurthi, K.S., 2013. Membrane remodeling: FisB will do in a pinch. *Current Biology*, 23(6), pp.R251–R253.

Thomas, C.M. & Nielsen, K.M., 2005. Mechanisms of, and barriers to, horizontal gene transfer between bacteria. *Nature reviews. Microbiology*, 3(9), pp.711–721.

Toyofuku, M. et al., 2012. Identification of proteins associated with the Pseudomonas aeruginosa biofilm extracellular matrix. *J Proteome Res*, 11(10), pp.4906–4915.

Ungar, D. & Hughson, F.M., 2003. SNARE protein structure and function. *Annual review of cell and developmental biology*, 19, pp.493–517.

Vollmer, W. & Bertsche, U., 2008. Murein (peptidoglycan) structure, architecture and biosynthesis in Escherichia coli. *Biochimica et Biophysica Acta - Biomembranes*, 1778(9), pp.1714–1734.

World Health Organization, 2017. WHO publishes list of bacteria for which new antibiotics are urgently needed. Available at:

http://www.who.int/mediacentre/news/releases/2017/bacteria-antibiotics-needed/en/.

Wright, G.D., 2010. Q&A: Antibiotic resistance: where does it come from and what can we do about it? *BMC biology*, 8, p.123.

Wu, E.L. et al., 2013. Molecular dynamics and NMR spectroscopy studies of E. coli lipopolysaccharide structure and dynamics. *Biophysical Journal*, 105(6), pp.1444–1455.

Wu, G. et al., 2014. Priming Galleria mellonella (Lepidoptera: Pyralidae) Larvae With Heat-Killed Bacterial Cells Induced an Enhanced Immune Protection Against Photorhabdus luminescens TT01 and the Role of Innate Immunity in the Process. *Journal of Economic Entomology*, 107(2), pp.559–569.

Yáñez-Mó, M. et al., 2015. Biological properties of extracellular vesicles and their physiological functions. *Journal of extracellular vesicles*, 4, p.27066.

Yaron, S. et al., 2000. Vesicle-Mediated Transfer of Virulence Genes from Escherichia coli O157:H7 to Other Enteric Bacteria. *Applied and environmental microbiology*, 66(10), pp.4414–4420.

Yu, N.Y. et al., 2010. PSORTb 3.0: Improved protein subcellular localization prediction with refined localization subcategories and predictive capabilities for all prokaryotes. *Bioinformatics*, 26(13), pp.1608–1615.

Zong, Z., 2013. Complete sequence of pJIE186-2, a plasmid carrying multiple virulence factors from a sequence type 131 Escherichia coli O25 strain. *Antimicrobial Agents and Chemotherapy*, 57(1), pp.597–600.

Zurfluh, K., Tasara, T., et al., 2016. Draft Genome Sequence of *Escherichia coli* S51, a Chicken Isolate Harboring a Chromosomally Encoded *mcr-1* Gene. *Genome Announcements*, 4(4), pp.e00796-16.

Zurfluh, K., Kieffer, N., et al., 2016. Features of the mcr-1 cassette respect to colistin resistance. *Antimicrobial agents and chemotherapy*, (August), pp.1–7.

Zybailov, B. et al., 2006. Statistical analysis of membrane proteome expression changes in Saccharomyces cerevisiae. *J Proteome Res*, 5(9), pp.2339–2347.

Acknowledgements

I am really grateful to everyone who has supported me through my PhD study and made it a memorable experience. I would like to start with thanking my supervisor, Prof. Trinad Chakraborty, for his support and guidance throughout this process. Most of all, I would like to thank Dr. Linda Falgenhauer for her encouragement and support from my first days at the Institute of Medical Microbiology and Dr. Can Imirzalioglu, for his invaluable help and care.

I would like to say a huge thank you to all of the Chakraborty lab members, past and present, who have made the Institute of Medical Microbiology a great place to work and learn. I would particularly like to thank Martina Hudel, Dr. Mobarak Abu Mraheil, Dr. Martin Leustik for all of their valuable input, and Alexandra Amend, Christina Gerstman and Saina Azarderakhsh for their invaluable help as well as for always managing to make friendly and pleasant atmosphere in the laboratory. Thanks to all of my friends in the BFS and ECCPS who have celebrated and commiserated with me throughout the past four years.

An extra special thank you must go to Prof. Manfred Rohde and Dr. Ursula Sommer, who have provided me with a fantastic support and assistance during electron microscopy study, it has been greatly appreciated.

Finally, I would like to thank my wife Paulina, for her love and support. I would also like to thank my parents for teaching me that I can achieve anything I put my mind to, none of this would have been possible without them.

Declaration

I declare that I have completed this dissertation single-handedly without the unauthorized help of a second party and only with the assistance acknowledged therein. I have appropriately acknowledged and referenced all text passages that are derived literally from or are based on the content of published or unpublished work of others, and all information that relates to verbal communications. I have abided by the principles of good scientific conduct laid down in the charter of the Justus Liebig University of Giessen in carrying out the investigations described in the dissertation.

Konrad Gwozdzinski

Curriculum vitae

The curriculum vitae was removed from the electronic version of the paper.

Appendix

Appendix A - Colistin MIC values for *mcr-1*-producing isolates

Table A-1 The list of isolates and their properties used in the MCR-1 study (Chapter 4.5). Colistin MIC values were determined by Etest in cation-adjusted Mueller-Hinton broth (CA-MHB) and calcium-enhanced Mueller-Hinton broth (CE-MHB).

Species	**Source**	**Incompatibility group of the *mcr-1*-positive plasmids**	**Colistin MIC [mg/L]**	
			CA-MHB	**CE-MHB**
*E. coli*_001	Human	IncHI2	2	24
*E. coli*_002	Pig	IncX4	2	12
*E. coli*_003	Pig	IncHI2	4	16
*E. coli*_004	Pig	IncHI2	4	24
*E. coli*_005	food (beef)	IncX4	2	16
*E. coli*_006	food (poultry)	IncX4	2	16/24
*E. coli*_013	Cattle	IncHI2	4	32
*E. coli*_018	food (poultry)	chromosomal	2	16
*E. coli*_020	food (poultry)	IncHI2	3	12
*E. coli*_021	Pig	IncX4	6	32
*E. coli*_022	Pig	IncX4	3	16
*E. coli*_023	Pig	IncX4	3	24
*E. coli*_024	Pig	ND	3	24
*E. coli*_025	Pig	IncHI2	4	24
*E. coli*_026	Pig	IncHI2	3	24
*E. coli*_027	Pig	IncX4	3	24
*E. coli*_028	Pig	IncHI2	3	12
*E. coli*_029	Pig	IncX4	3	24
*E. coli*_030	Pig	IncX4	4	16
*E. coli*_031	food (poultry)	IncHI2	4	16
*E. coli*_032	food (poultry)	IncHI2	4	16
*E. coli*_033	food (poultry)	IncX4	3	16
*E. coli*_034	food (poultry)	ND	4	24
*E. coli*_035	food (poultry)	ND	4	24
*E. coli*_037	pig	IncX4	3	6
*E. coli*_038	pig	IncX4	4	24
*E. coli*_039	pig	IncHI2	3	16
*E. coli*_040	pig	IncX4	4	12
*E. coli*_041	pig	IncX4	4	16
*E. coli*_042	pig	IncX4	4	24
*E. coli*_043	pig	IncHI2	4	12
*E. coli*_044	pig	IncHI2	4	24
*E. coli*_045	pig	ND	6	24
*E. coli*_046	pig	IncX4	3	16
*E. coli*_047	pig	IncX4	4	16
*E. coli*_048	pig	IncX4	3	24
*E. coli*_049	pig	IncX4	4	16

*E. coli*_050	pig	IncX4/IncN	4	16
*E. coli*_051	pig	IncX4	4	16
*E. coli*_052	pig	IncX4	6	24
*E. coli*_053	pig	ND	4	24
*E. coli*_054	poultry	IncHI2	4	16
*E. coli*_055	poultry	ND	4	24
*E. coli*_056	poultry	IncX4	6	24
*E. coli*_057	poultry	IncX4	4	24
*E. coli*_058	poultry	ND	6	32/48
*E. coli*_059	poultry	IncX4	4	24
*E. coli*_060	poultry	IncHI2	4	16
*K. pneumoniae*_002	poultry	ND	>128	>128
*E. coli*_010*	poultry	NA	2	2
*E. coli*_017*	companion animal	NA	1.5	1.5
E. coli CAE02*	cattle	NA	1.5	1.5
E. coli CAE07*	cattle	NA	1.5	1.5
E. coli CAE13*	cattle	NA	2	2
E. coli CLO28*	poultry	NA	1.5	1.5
E. coli CLO29*	poultry	NA	2	1.5
E. coli CLO47*	cattle	NA	2	2
E. coli DO14*	companion animal	NA	1.5	1.5
E. coli DO21*	companion animal	NA	1.5	1.5
E. coli DH10β*	laboratory strain	NA	2	2
p002/DH10β	transconjugant	IncX4	4	32
p002 Δ*mcr-1*	Δ*mcr-1* of p002 in *E. coli* DH10β	IncX4	2	2
t004/J53	transconjugant of *E. coli* J53 harboring p004	IncHI2	2	16
t002/J53	transconjugant of *E. coli* J53 harboring p002	IncX4	2	24
t003/J53	transconjugant of *E. coli* J53 harboring p003	IncHI2	2	12
t001/J53	transconjugant of *E. coli* J53 harboring p001	IncHI2	2	12

* *mcr-1*-negative isolates; ND - not determined; NA - not applicable

Table 3.1 The equipment used in this study.

Instrument	Manufacturer
Analytical balance	Mettler, Giessen, Germany
Autoclave	Getinge, Getinge, Sweden
Biological safety cabinets	Thermo scientific, USA
CHEF-DR II System	Bio-Rad, USA
Cell-counting chamber	Brand, Wertheim, Germany
Centrifuges	Eppendorf, Hamburg, Germany
CO_2-incubator	Thermo scientific, USA
Cross flow filtration system	Spectrum labs, USA
Electroblotting apparatus	Construction of the institute
Electrophoresis apparatus (agarose gel electrophoresis)	Construction of the institute
Electrophoresis apparatus (SDS-PAGE)	Biometra, Goettingen, Germany
Electroporator	Bio-Rad, USA
Field emission scanning electron microscope	Carl Zeiss, Germany
Film developer for Western blots	Agfa Healthcare, Mortsel, Belgium
Fluorescence microscope	Keyence, Japan
Freezer (-20°C)	Bosch, Stuttgart, Germany
Freezer (-80°C)	Thermo Scientific, USA
Freezing chamber for eukaryotic cells	Nalgene Sigma Aldrich, St. Louis, USA
Fridge (4°C)	Bosch, Stuttgart, Germany
Gel Imaging Systems	Bio-Rad, USA
Hypercassette for film development	Amersham Biosciences, Little Chalfont, Buckinghamshire, UK
Ice machine	Ziegra, Isernhagen, Germany
Incubator	Thermo Scientific, USA
Light microscope	Hund, Wetzlar, Germany
Magnetic stirrer	IKA, Staufen, Germany
Mass spectrometer	Thermo Scientific, USA
Microliter pipettes	Eppendorf, Hamburg, Germany
Microplate reader	Tecan, Maennedorf, Switzerland
Microwave oven	Sharp, Japan
MiSeq sequencer	Illumina, USA
Multi-channel pipette	Biozym, Hessisch Oldendorf, Germany
Microapplicator	
NanoDrop Spectrophotometer	Thermo Scientific, USA
pH-Meter	Knick, Berlin, Germany
Pipetboy	Integra Biosciences, Zizers, Switzerland
Plate shaker	IKA, Staufen, Germany
Shaking-incubator	Infors, Basel, Switzerland
Tangential Flow Filtration system	Pall, USA
Thermal cycler	Applied Biosystems, USA
Thermomixer	Eppendorf, Hamburg, Germany
Transmission electron microscopy	Carl Zeiss, Germany
Ultracentrifuge	Beckman, USA
Vortex mixer	VWR, Radnor, PA, USA

Water bath	Grant Instruments, UK
Milli-Q water purification system	Merck, Germany

Table 3.2 The consumables used in this study.

Item	Manufacturer
96-well plates flat-bottom	Greiner, Frickenhausen, Germany
96-well plates U-bottom	Greiner, Frickenhausen, Germany
96-well plates V-bottom	Greiner, Frickenhausen, Germany
Bottle top filters	VWR, Radnor, PA, USA
Cell scraper	Greiner, Frickenhausen, Germany
Cover slips	R. Langenbrinck, Germany
Cryovials	Sarstedt, Nuembrecht, Germany
Cuvettes	Ratiolab, Dreieich, Germany
Disposable pipettes	Greiner, Frickenhausen, Germany
Disposable scalpels	Feather, Osaka, Japan
Disposable syringes	Braun, Melsungen, Germany
ECL films	Amersham Biosciences, UK
Electron microscopy grids	Merck, Germany
Electroporation cuvettes	Thermo Scientific, USA
Examination gloves	Ansell, Richmond, VIC, Australia
Films for 96-well plates	Thermo Scientific, USA
Glass slides	R. Langenbrinck, Germany
Glassware	Schott, Mainz, Germany
Hollow Fiber Filters	Spectrum labs, USA
Inoculating loops	Nunc Sigma Aldrich, St. Louis, USA
Microcentrifuge tubes, 1.5 ml	Eppendorf, Hamburg, Germany
Multiwell tissue culture plates	Becton Dickinson; Franklin Lakes, USA
Paper towels	Kimberly Clark, Irwing, USA
Parafilm	Pechiney Plastic Packaging, USA
Petri dishes	Greiner, Frickenhausen, Germany
Pipette tips	Greiner, Frickenhausen, Germany
Pipette tips (with filter)	Nerbe Plus, Winsen/Luke, Germany
Plastic tubes 50 ml, 15 ml	Greiner, Frickenhausen, Germany
PVDF membrane	Roche, Basel, Switzerland
Syringe filters	Merck, Germany
Tangential flow filtration membranes	Pall, USA
Tissue culture dishes	Becton Dickinson, Franklin Lakes, USA
Density gradient medium (OptiPrep)	Sigma Aldrich, Germany

Table 3.3 Chemicals used in this study.

Chemical	Supplier
1 kb plus DNA ladder	Thermo Scientific, USA
Acetone	Sigma Aldrich, Germany
Acid Hydrolysate of Casein	Sigma Aldrich, Germany
Agar	Sigma Aldrich, Germany
Agarose	Sigma Aldrich, Germany
Ammonium peroxidisulphate (APS)	Merck, Germany
Ampicillin	Sigma Aldrich, Germany
Beef Extract	Sigma Aldrich, Germany

Boric acid	Sigma Aldrich, Germany
Bovine serum albumin (BSA)	Sigma Aldrich, Germany
Bradford protein assay	Bio-Rad, Germany
Bromophenol blue	Serva, Germany
Calcium chloride dihydrate	Sigma Aldrich, Germany
Cefotaxime	Sigma Aldrich, Germany
Colistin	Sigma Aldrich, Germany
Deoxycholic acid	Sigma Aldrich, Germany
Dimethyl sulphoxide (DMSO)	Merck, Germany
Dithiothreitol (DTT)	Serva, Germany
DMEM medium	Thermo Scientific, USA
ECL detection system	Thermo Scientific, USA
EDTA	Merck, Germany
EPON Resin	Pelco, USA
Ethanol	Sigma Aldrich, Germany
Ethidium bromide	Roth, Germany
Fetal bovine serum (FBS)	PAA Laboratories, Germany
Ficoll	GE Healthcare Life Sciences, Germany
Film developer solution for Western blots (Unimatic D)	Calbe Chemie; Calbe, Germany
Film fixer solution for Western blots (Unimatic F)	Calbe Chemie; Calbe, Germany
Formaldehyde	Merck, Germany
Formic acid	Sigma Aldrich, Germany
Glucose	Sigma Aldrich, Germany
Glutaraldehyde	Sigma Aldrich, Germany
Glycerol	Merck, Germany
Glycine	Merck, Germany
Hanks´ balanced salt solution (HBSS)	Roth; Karlsruhe, Germany
Isopropanol	Merck, Germany
Isopropyl β-D-1-thiogalactopyranoside (IPTG)	Sigma Aldrich, Germany
Kanamycin	Sigma Aldrich, Germany
Lambda PFG Ladder	New england biolabs, UK
Lipofectamine 2000	Thermo Scientific, USA
Low Range PFG Marker	New england biolabs, UK
Magnesium chloride hexahydrate	Sigma Aldrich, Germany
Methanol	Sigma Aldrich, Germany
Nitrocefin	Thermo Scientific, USA
N-lauroylsarcosine	Sigma Aldrich, Germany
Opti-MEM I medium	Thermo Scientific, USA
Osmium tetroxide	Sigma Aldrich, Germany
Page ruler plus pre-stained protein Ladder	Thermo Scientific, USA
Paraformaldehyde	Sigma Aldrich, Germany
Phosphate-buffered saline (PBS)	Biochrom AG; Berlin, Germany
Polyacrylamide	Roth, Germany
Potassium chloride	Sigma Aldrich, Germany
Potassium dihydrogen phosphate	Sigma Aldrich, Germany
ProLong Gold Antifade with 4',6-diamidino-2-phenylindole (DAPI)	Thermo Scientific, USA

Protease inhibitor cocktail III	Merck, Germany
SDS	Sigma Aldrich, Germany
Skimmed milk powder	Sigma Aldrich, Germany
Sodium Cacodylate	Sigma Aldrich, Germany
Sodium chloride	Roth, Germany
Sodium hydrogen phosphate	Merck, Germany
Sodium phosphate	Sigma Aldrich, Germany
Starch	Sigma Aldrich, Germany
TEMED	Roth, Germany
Tris	Roth, Germany
Triton X-100	Serva, Germany
Trypsin/EDTA	PAA Laboratories, Germany
Tryptone	Becton Dickinson; Franklin Lakes, NJ,
Tween-20	Serva; Heidelberg, Germany
Uranyl acetate	Sigma Aldrich, Germany
X-gal	Sigma Aldrich, Germany
Yeast extract	Becton Dickinson, USA
β-mercaptoethanol	Sigma Aldrich, Germany

Table 3.4 Enzymes used in this study.

Enzyme	Manufacturer
DNAse I	Thermo Scientific, USA
Lysozyme	Sigma Aldrich, Germany
Q5 high fidelity DNA polymerase	New England Biolabs, UK
Restiction Endonucleases	Thermo Scientific, USA, New England Biolabs, UK
T4 DNA Ligase	Thermo Scientific, USA
Taq DNA Polymerase	Thermo Scientific, USA
Tfl DNA Polymerase	Promega, USA

Table 3.5 Kits used in this study.

Kit	Manufacturer
Gibson Assembly® Cloning Kit	New England Biolabs, UK
Maxi plasmid isolation Kit	Qiagen, Germany
Mini plasmid isolation Kit	Qiagen, Germany
PureLink Genomic DNA isolation kit	Thermo Scientific, USA
QIAquick PCR Purification Kit	Qiagen, Germany

Table 3.6 Buffers, media and solutions used in this study.

Buffers, media and solutions	Components
0.2 M Sodium Cacodylate Stock Buffer	42.8g/l Sodium Cacodylate Set pH to 7.2
1.5 M Tris, pH 6.8 (Stock buffer for stacking gels)	181.65 g Tris base dissolved in Milli-Q water to 1 L pH set to 6.8
1.5 M Tris, pH 8.8 (Stock buffer for separating gels)	181.65 g Tris base

	dissolved in Milli-Q water 1 L pH set to 8.8
10x TBE buffer	121.1 g/l Tris base 61.8 g/l Boric acid 7.4 g/l EDTA
10x PBS	27 mM KCl 1.4 M NaCl 81 mM Na2HPO4 15 mM KH2PO4 dissolved in Milli-Q water pH set to 7.4
10x SDS-PAGE running buffer	250 mM tris 1.92 M glycine 1% (w/v) SDS dissolved in Milli-Q water
10x Transfer buffer:	30 g/l Tris base 144 g/l glycine
1x TBS with Tween-20	10 mM tris-HCl (pH 8) 150 mM NaCl 0.1% (v/v) Tween-20
1x TE buffer	10mM tris-HCl (pH 8) 1 mM EDTA
5X loading buffer (agarose gel electrophoresis)	25% (w/v) ficoll type 400 0.25% (w/v) bromophenol blue in 1x TE buffer
5x SDS-PAGE loading buffer	62.5 mM tris-HCl (pH 6.8) 2% (w/v) SDS 20% (v/v) gycerol 5% (v/v) β-mercaptoethanol 0.125 % (w/v) bromophenol blue dissolved in Milli-Q water
Antibiotic stock solutions	Ampicillin: 100 mg/ml in mQ water Colistin: 50 mg/ml in mQ water Cefotaxime: 50 mg/ml in mQ water Kanamycin: 50 mg/ml in mQ water
CCMB80 buffer	80mM Calcium Chloride 20mM Manganese Chloride 10mM Magnesium Chloride 10mM Potassium Acetate 10% Glycerol
Cell Lysis Buffer (PFGE)	50 mM Tris-HCl 1M NaCl 100 mM EDTA 0,5% N-lauroylsarcosine Set pH to 7.6

Coomassie Blue stock solution	250 mg Coomassie Brilliant Blue per 100 mL of fixing solution
Destaining solution for Coomassie brilliant blue	400 mL methanol 100 mL glacial acetic acid 500 ml Milli-Q water
Fixing solution for Coomassie brilliant blue	600 mL methanol 75 mL glacial acetic acid 325 ml Milli-Q water
GES solution	5 M guanidinium thiocyanate 100 mM EDTA 0.5% (v/v) Sarkosyl
Lysogeny broth (LB)	5 g/l yeast extract 10 g/l tryptone 5 g/l NaCl
Mueller Hinton medium	17.5 g/l Acid Hydrolysate of Casein 3.0 g/l Beef Extract 1.5 g/l Starch
Super optimal catabolite medium (SOC)	5 g/l yeast extract 20 g/l tryptone 0.584 g/l NaCl 0.186 g/l KCl 2.4 g/l $MgSO_4$ 200 g/l Glucose

Appendix B - Vesicular proteins identified in *C. freundii* OMVs

Table A-2 Proteins identified in *Citrobacter freundii*-derived OMVs.

UniProtKB/TrEMBL accession number	Protein name	Function*	Trial		
			I	II	III
Outer membrane					
A0A023V1S4	Capsular biosynthesis protein	Function unknown	+	+	+
A0A023V2V4	Uncharacterized protein	Cell wall/membrane/envelope biogenesis	+	+	+
A0A023V3K6	Phospholipase A	Cell wall/membrane/envelope biogenesis	+	+	+
A0A023V726	Maltoporin	Carbohydrate transport and metabolism	+	+	+
A0A023V7G6	Vitamin B12 transporter BtuB	Coenzyme transport and metabolism	+	+	+
A0A023V7S0	Ferrichrome transporter	Inorganic ion transport and metabolism	+	+	+
A0A023V7V2	Outer membrane protein assembly factor BamA	Cell wall/membrane/envelope biogenesis	+	+	+
A0A023V8L6	Outer membrane receptor protein	Inorganic ion transport and metabolism	+	+	+
A0A023V950	LPS-assembly protein LptD	Cell wall/membrane/envelope biogenesis	+	+	+
A0A023V9K1	Membrane protein	Cell wall/membrane/envelope biogenesis	+	+	+
A0A023V9L0	Membrane protein	Cell wall/membrane/envelope biogenesis	+	+	+
A0A023V9Q9	Membrane protein	Cell wall/membrane/envelope biogenesis	+	+	+
A0A023VAA1	MltA-interacting protein MipA	Cell wall/membrane/envelope biogenesis	+	+	+
A0A023VAB7	Ion channel protein Tsx	Cell wall/membrane/envelope biogenesis	+	+	+
A0A023VAN4	Lipid A palmitoyltransferase PagP	Not in COG genes	-	+	+
A0A023VBV0	Membrane protein	Cell wall/membrane/envelope biogenesis	+	+	+
A0A023VC38	Porin	Cell wall/membrane/envelope biogenesis	-	+	+
A0A023VCF7	Membrane protein	Cell wall/membrane/envelope biogenesis	+	+	+
A0A023VD55	Porin	Cell wall/membrane/envelope biogenesis	+	+	+
A0A023VFD9	Outer membrane siderophore receptor	Inorganic ion transport and metabolism	+	+	+
A0A023VFQ1	Membrane protein	Cell wall/membrane/envelope biogenesis	+	+	+
A0A023VG07	Long-chain fatty acid outer membrane transporter	Lipid transport and metabolism	+	+	+
A0A023V3J5	Biofilm formation protein HmsH	General function prediction only	+	+	+
A0A023V4N3	Phospholipid ABC transporter substrate	Cell wall/membrane/envelope biogenesis	+	+	+
A0A023V4Y1	Uroporphyrin-III methyltransferase	Function unknown	+	+	+
A0A023V5D4	Uncharacterized protein	Cell wall/membrane/envelope biogenesis	+	+	+
A0A023V6A0	Membrane protein	Cell wall/membrane/envelope biogenesis	+	+	+
A0A023V6Z2	Cell division protein FtsI	Cell cycle control, cell division, chr. partitioning	+	+	+
A0A023V8B4	Uncharacterized protein	General function prediction only	-	+	+
A0A023V8F6	Cell division protein FtsH	Posttran. modifi., protein turnover, chaperones	+	+	+
A0A023VB08	RND transporter	Cell wall/membrane/envelope biogenesis	+	+	+
A0A023VCT1	Membrane protein	Cell wall/membrane/envelope biogenesis	+	+	+
A0A023VDY1	Membrane protein	Not in COG genes	+	+	+
A0A023V1M8	Membrane protein	Cell wall/membrane/envelope biogenesis	+	+	+
A0A023V1V9	Murein hydrolase effector LrgB	Cell wall/membrane/envelope biogenesis	+	+	+
A0A023V236	Uncharacterized protein	Energy production and conversion	+	+	+
A0A023V2H3	Membrane-bound lytic murein transglycosylase C	Cell wall/membrane/envelope biogenesis	+	+	+
A0A023V2R7	Uncharacterized protein	Posttran. modifi., protein turnover, chaperones	+	+	+
A0A023V367	Membrane protein	Cell wall/membrane/envelope biogenesis	+	+	+
A0A023V3F5	Membrane-bound lytic murein transglycosylase A	Cell wall/membrane/envelope biogenesis	+	+	+
A0A023V467	Uncharacterized protein	Cell wall/membrane/envelope biogenesis	+	+	+
A0A023V4B0	Lipoprotein NlpD	Cell wall/membrane/envelope biogenesis	+	+	+
A0A023V4B9	Metalloprotease	Posttran. modifi., protein turnover, chaperones	+	+	+
A0A023V4I0	Outer membrane N-deacetylase	Carbohydrate transport and metabolism	+	+	+

A0A023V4K7	Lipoprotein NlpI	Cell wall/membrane/envelope biogenesis	+	+	+
A0A023V552	Membrane protein	Function unknown	+	+	+
A0A023V5T8	Membrane protein	Cell wall/membrane/envelope biogenesis	+	+	+
A0A023V6D6	Uncharacterized protein	Function unknown	+	+	+
A0A023V7B4	Outer membrane lipoprotein RcsF	Not in COG genes	+	+	+
A0A023V7E3	Membrane protein	Not in COG genes	+	+	+
A0A023V827	Membrane protein	Cell wall/membrane/envelope biogenesis	+	+	+
A0A023V828	Uncharacterized protein	General function prediction only	+	+	+
A0A023V8V0	LPS-assembly lipoprotein LptE	Cell wall/membrane/envelope biogenesis	+	+	+
A0A023V986	Copper homeostasis protein	Cell wall/membrane/envelope biogenesis	+	+	+
A0A023V9B2	Lipoprotein	Cell wall/membrane/envelope biogenesis	+	+	+
A0A023VAE2	Uncharacterized protein	Function unknown	+	+	+
A0A023VAG4	Uncharacterized protein	Function unknown	+	+	+
A0A023VAY3	Peptidoglycan-associated outer membrane lipoprotein	Cell wall/membrane/envelope biogenesis	+	+	+
A0A023VAZ1	Curli production assembly/transport protein CsgG	Cell wall/membrane/envelope biogenesis	+	+	+
A0A023VAZ9	Acyl-CoA thioesterase	Carbohydrate transport and metabolism	+	+	+
A0A023VB21	Lipoprotein	Not in COG genes	+	+	+
A0A023VB83	Penicillin-binding protein activator LpoB	Cell wall/membrane/envelope biogenesis	+	+	+
A0A023VB86	Murein lipoprotein	Cell wall/membrane/envelope biogenesis	+	+	+
A0A023VBP7	Uncharacterized protein	Function unknown	+	+	+
A0A023VBT7	Endopeptidase	Cell wall/membrane/envelope biogenesis	+	+	+
A0A023VCE6	Transcriptional regulator	Cell wall/membrane/envelope biogenesis	+	+	+
A0A023VCV6	Lipoprotein	Not in COG genes	+	+	+
A0A023VD27	Membrane protein	Cell wall/membrane/envelope biogenesis	+	+	+
A0A023VDB8	Outer-membrane lipoprotein LolB	Cell wall/membrane/envelope biogenesis	+	+	+
A0A023VDF1	Membrane-bound lytic murein transglycosylase A	Cell wall/membrane/envelope biogenesis	+	+	+
A0A023VEG2	Membrane protein	Cell wall/membrane/envelope biogenesis	+	+	+
A0A023VEX2	Outer membrane protein assembly factor BamD	Cell wall/membrane/envelope biogenesis	+	+	+
A0A023VF30	Outer membrane protein assembly factor BamB	Cell wall/membrane/envelope biogenesis	+	+	+
A0A023VF93	Lipoprotein	General function prediction only	+	+	+
A0A023VFG1	Membrane protein	Cell wall/membrane/envelope biogenesis	+	+	+
A0A023VG72	RpoE-regulated lipoprotein	Mobilome: prophages, transposons	+	+	+
A0A023VG87	ABC transporter permease	Cell wall/membrane/envelope biogenesis	+	+	+
A0A023VGJ5	Outer membrane protein assembly factor BamC	Function unknown	+	+	+
A0A023VGX7	Membrane protein	Cell wall/membrane/envelope biogenesis	+	+	+
	Inner membrane				
A0A023V5B6	Formate dehydrogenase	Energy production and conversion	-	-	+
A0A023V7X6	Lipoprotein	Inorganic ion transport and metabolism	+	+	+
A0A023VA60	Multidrug transporter	Cell wall/membrane/envelope biogenesis	+	+	+
A0A023V3J4	Sec-independent protein translocase protein TatA	Intracellular trafficking, secr., vesicular transport	+	+	+
A0A023V4V4	Sec-independent protein translocase protein TatB	Intracellular trafficking, secr., vesicular transport	+	+	+
A0A023V578	D-alanyl-D-alanine carboxypeptidase	Cell wall/membrane/envelope biogenesis	-	+	+
A0A023V5D0	Sulfoxide reductase catalytic subunit YedY	Energy production and conversion	+	+	+
A0A023V5Q8	ATP synthase subunit b	Energy production and conversion	+	+	+
A0A023V7G2	Protein HflC	Posttran. modifi., protein turnover, chaperones	+	+	+
A0A023V869	Cell division protein FtsL	Cell cycle control, cell division, chr. partitioning	+	+	+
A0A023V8T8	D-alanyl-D-alanine carboxypeptidase	Cell wall/membrane/envelope biogenesis	-	+	+
A0A023V946	Membrane protein	Cell wall/membrane/envelope biogenesis	+	+	+

A0A023VAB2	Colicin uptake protein TolR	Intracellular trafficking, secr., vesicular transport	+	+	+
A0A023VBI8	Peptidase M15	Cell wall/membrane/envelope biogenesis	+	+	+
A0A023VBJ3	Sulfoxide reductase catalytic subunit YedY	Energy production and conversion	+	+	+
A0A023VDF8	Formate dehydrogenase	Energy production and conversion	+	+	+
A0A023V304	Mechanosensitive ion channel protein MscS	Cell wall/membrane/envelope biogenesis	-	+	+
A0A023V3D7	Serine/threonine protein kinase	Amino acid transport and metabolism	+	+	+
A0A023V3L6	Protoheme IX biogenesis protein	Function unknown	+	+	+
A0A023V5J6	Preprotein translocase subunit SecG	Intracellular trafficking, secr., vesicular transport	+	+	+
A0A023V5K7	ATP-dependent zinc metalloprotease FtsH	Posttran. modifi., protein turnover, chaperones	+	+	+
A0A023V5N9	Membrane protein insertase YidC	Cell wall/membrane/envelope biogenesis	+	+	+
A0A023V5V2	Magnesium transport protein CorA	Inorganic ion transport and metabolism	-	+	+
A0A023V622	Uncharacterized protein	Cell wall/membrane/envelope biogenesis	+	+	+
A0A023V649	Cell division protein FtsX	Cell cycle control, cell division, chr. partitioning	+	+	+
A0A023V6Q2	Fumarate reductase subunit C	Energy production and conversion	+	+	+
A0A023V6Y2	PTS system mannitol-specific transporter sub. IICBA	Carbohydrate transport and metabolism	+	+	+
A0A023V6Z9	Topoisomerase II	Not in COG genes	+	+	+
A0A023V792	Zinc metalloprotease	Posttran. modifi., protein turnover, chaperones	-	+	+
A0A023V7Y3	Uncharacterized protein	Function unknown	+	+	-
A0A023V8A6	PTS system trehalose(Maltose)-specific transporter	Carbohydrate transport and metabolism	+	+	+
A0A023V8D1	Anaerobic C4-dicarboxylate transporter	Carbohydrate transport and metabolism	+	+	+
A0A023V9B5	Protein translocase subunit SecD	Intracellular trafficking, secr., vesicular transport	+	+	+
A0A023V9D6	Cell division protein FtsK	Cell cycle control, cell division, chr. partitioning	+	+	+
A0A023VAA8	Cytochrome d terminal oxidase subunit 1	Energy production and conversion	+	+	+
A0A023VAL1	Membrane protein	Not in COG genes	+	+	+
A0A023VAS5	Apolipoprotein N-acyltransferase	Cell wall/membrane/envelope biogenesis	+	+	+
A0A023VBB3	Colicin uptake protein TolQ	Intracellular trafficking, secr., vesicular transport	+	+	+
A0A023VCB6	PTS mannose transporter subunit IID	Carbohydrate transport and metabolism	+	+	+
A0A023VCW8	Protease HtpX	Posttran. modifi., protein turnover, chaperones	+	+	+
A0A023VDS3	UPF0259 membrane protein CFNIH1_18960	Not in COG genes	-	-	+
A0A023VDX7	sn-glycerol-3-phosphate transporter	Carbohydrate transport and metabolism	+	+	+
A0A023VFQ8	Amino acid transporter	Amino acid transport and metabolism	+	+	+
A0A023VG42	NADH-quinone oxidoreductase subunit A	Energy production and conversion	+	+	+
A0A023VGL0	Signal peptidase I	Intracellular trafficking, secr., vesicular transport	+	+	+
	Periplasmic				
A0A023V241	N-acetylmuramoyl-L-alanine amidase	Cell wall/membrane/envelope biogenesis	+	+	+
A0A023V2G7	Uncharacterized protein	Not in COG genes	+	+	+
A0A023V2P0	LacI family transcriptional regulator	Carbohydrate transport and metabolism	+	+	+
A0A023V2X6	Protein-disulfide isomerase	Posttran. modifi., protein turnover, chaperones	-	+	+
A0A023V337	Capsular biosynthesis protein	Cell wall/membrane/envelope biogenesis	+	+	+
A0A023V360	Glycine/betaine ABC transporter substrate	Amino acid transport and metabolism	+	+	+
A0A023V3B2	Cell division protein FtsB	Cell cycle control, cell division, chr. partitioning	+	+	+
A0A023V3C2	Hydrogenase 2 large subunit	Energy production and conversion	-	+	+
A0A023V3F9	Protease	Posttran. modifi., protein turnover, chaperones	-	+	+
A0A023V3G2	UPF0441 protein CFNIH1_02420	Function unknown	+	+	+
A0A023V3H3	Uncharacterized protein	Function unknown	+	+	+
A0A023V3S2	L-asparaginase II	Translation, ribosomal structure and biogenesis	+	+	+

A0A023V3Y3	Lipopolysaccharide export system protein LptA	Cell wall/membrane/envelope biogenesis	+	+	+
A0A023V4C4	CTP synthase	Nucleotide transport and metabolism	+	+	+
A0A023V4I4	Uncharacterized protein	Not in COG genes	+	+	+
A0A023V4J7	Penicillin-binding protein activator LpoA	Cell wall/membrane/envelope biogenesis	+	+	+
A0A023V4J9	Peptidyl-prolyl cis-trans isomerase	Posttran. modifi., protein turnover, chaperones	+	+	+
A0A023V4Q2	Cell division protein FtsP	Cell cycle control, cell division, chr. partitioning	+	+	+
A0A023V4S1	Uncharacterized protein	Not in COG genes	-	+	+
A0A023V4S6	Glycerol-3-phosphate ABC transporter substrate	Carbohydrate transport and metabolism	+	+	+
A0A023V4U5	Copper resistance protein	Not in COG genes	+	+	+
A0A023V4V8	DNA recombination protein RmuC	Replication, recombination and repair	+	+	+
A0A023V4X6	Membrane protein	Function unknown	+	+	+
A0A023V582	Thiol:disulfide interchange protein	Posttran. modifi., protein turnover, chaperones	+	+	+
A0A023V5F8	Beta-lactamase	Defense mechanisms	+	+	+
A0A023V5L8	ABC transporter substrate-binding protein	Lipid transport and metabolism	+	+	+
A0A023V5P5	Serine endoprotease DegQ	Posttran. modifi., protein turnover, chaperones	+	+	+
A0A023V5S0	D-ribose transporter subunit RbsB	Carbohydrate transport and metabolism	+	+	+
A0A023V5T5	Maltose-binding protein	Not in COG genes	+	+	+
A0A023V5X8	Uncharacterized protein	Signal transduction mechanisms	+	+	+
A0A023V656	Peptidyl-prolyl cis-trans isomerase	Posttran. modifi., protein turnover, chaperones	+	+	+
A0A023V657	Uncharacterized protein	Not in COG genes	+	+	+
A0A023V689	Peptidase	Amino acid transport and metabolism	+	+	+
A0A023V6C8	Uncharacterized protein	General function prediction only	+	+	+
A0A023V6D5	C4-dicarboxylate ABC transporter	Carbohydrate transport and metabolism	+	+	+
A0A023V6D8	Peptide ABC transporter substrate-binding protein	Amino acid transport and metabolism	+	+	+
A0A023V6G8	Leucine ABC transporter substrate-binding protein	Amino acid transport and metabolism	+	+	+
A0A023V7D7	Phosphate-binding protein PstS	Inorganic ion transport and metabolism	+	+	-
A0A023V7I5	2', 3'-cyclic nucleotide 2'-phosphodiesterase	Nucleotide transport and metabolism	+	+	+
A0A023V7J5	Sugar ABC transporter substrate-binding protein	Carbohydrate transport and metabolism	+	+	+
A0A023V7M8	Uncharacterized protein	Not in COG genes	-	+	+
A0A023V7Q0	Sugar ABC transporter substrate-binding protein	Carbohydrate transport and metabolism	+	+	+
A0A023V7U4	Cytochrome c-552	Inorganic ion transport and metabolism	+	+	+
A0A023V7W4	Transcriptional regulator	Carbohydrate transport and metabolism	+	+	+
A0A023V7X5	Uncharacterized protein	Function unknown	+	+	+
A0A023V7Y4	Lytic murein transglycosylase	Cell wall/membrane/envelope biogenesis	+	+	+
A0A023V7Y9	Protein CreA	Signal transduction mechanisms	+	+	+
A0A023V802	VirG	Posttran. modifi., protein turnover, chaperones	+	-	+
A0A023V817	Transpeptidase	Cell wall/membrane/envelope biogenesis	-	+	+
A0A023V850	Biofilm stress and motility protein A	Function unknown	+	+	+
A0A023V8F2	N-acetylmuramoyl-l-alanine amidase II	Cell wall/membrane/envelope biogenesis	+	+	+
A0A023V8F8	Vitamin B12-binding protein	Inorganic ion transport and metabolism	-	+	-
A0A023V8F9	Peptidyl-prolyl cis-trans isomerase	Posttran. modifi., protein turnover, chaperones	-	-	+
A0A023V8K4	Endopeptidase	Not in COG genes	+	+	+
A0A023V8U3	Chaperone SurA	Posttran. modifi., protein turnover, chaperones	+	+	+
A0A023V8Z6	Fimbrial protein FimI	Cell motility	+	+	+
A0A023V915	Multicopper oxidase	Cell cycle control, cell division, chr. partitioning	+	+	+
A0A023V949	Serine endoprotease	Posttran. modifi., protein turnover, chaperones	+	+	+
A0A023V968	Disulfide isomerase	Posttran. modifi., protein turnover, chaperones	+	+	+
A0A023V969	Chaperone protein skp	Cell wall/membrane/envelope biogenesis	+	+	+
A0A023V984	Uncharacterized protein	Not in COG genes	-	+	+
A0A023V997	L,D-transpeptidase	Cell wall/membrane/envelope biogenesis	+	+	+
A0A023V9B7	Uncharacterized protein	Cell wall/membrane/envelope biogenesis	+	+	+

A0A023V9C8	Amino acid transporter	Amino acid transport and metabolism	+	+	+
A0A023V9J5	5'-nucleotidase	Nucleotide transport and metabolism	+	+	+
A0A023V9J6	Lipoprotein	Function unknown	+	+	+
A0A023V9K9	Protein TolB	Intracellular trafficking, secr., vesicular transport	+	+	+
A0A023V9Q0	Adhesin	Cell motility	+	+	+
A0A023V9S7	Glutathione ABC transporter substrate-binding protein	Amino acid transport and metabolism	+	+	+
A0A023V9T4	Glucans biosynthesis protein G	Cell wall/membrane/envelope biogenesis	+	+	+
A0A023V9W6	Outer-membrane lipoprotein carrier protein	Cell wall/membrane/envelope biogenesis	+	+	+
A0A023VAA5	Uncharacterized protein	Cell motility	+	+	+
A0A023VAK6	Putrescine-binding periplasmic protein	Amino acid transport and metabolism	+	+	+
A0A023VAQ2	Murein L,D-transpeptidase	Cell wall/membrane/envelope biogenesis	+	+	+
A0A023VAV2	Lysozyme inhibitor	Cell wall/membrane/envelope biogenesis	+	+	+
A0A023VAV8	Glucose-1-phosphatase	Not in COG gene	+	+	+
A0A023VAW8	Ferrous iron transporter	Inorganic ion transport and metabolism	+	+	+
A0A023VAZ4	Molybdate transporter	Defense mechanisms	+	+	+
A0A023VB05	Uncharacterized protein	Intracellular trafficking, secr., vesicular transport	+	+	+
A0A023VBB6	Tol-pal system protein	General function prediction only	+	+	+
A0A023VBF1	Spermidine/putrescine ABC transporter substrate	Amino acid transport and metabolism	+	+	+
A0A023VBG4	Glutamine ABC transporter substrate-bindnig protein	Amino acid transport and metabolism	+	+	+
A0A023VBI6	Uncharacterized protein	Carbohydrate transport and metabolism	+	+	+
A0A023VBM5	Sulfurtransferase	Inorganic ion transport and metabolism	+	+	+
A0A023VBW6	Peptide ABC transporter substrate-binding protein	Amino acid transport and metabolism	-	+	+
A0A023VC10	UPF0312 protein CFNIH1_15285	General function prediction only	-	+	+
A0A023VC24	Nickel ABC transporter substrate-binding protein	Amino acid transport and metabolism	+	+	+
A0A023VC75	Probable thiol peroxidase	Posttran. modifi., protein turnover, chaperones	+	+	+
A0A023VC81	Peptigoglycan-binding protein LysM	Cell wall/membrane/envelope biogenesis	+	+	+
A0A023VCB5	Uncharacterized protein	General function prediction only	-	+	+
A0A023VCD2	Peptide ABC transporter substrate-binding protein	Amino acid transport and metabolism	+	+	+
A0A023VCD3	Conjugal transfer protein TrbG	Intracellular trafficking, secr., vesicular transport	+	-	+
A0A023VCF4	Formate dehydrogenase	Energy production and conversion	-	+	+
A0A023VCR7	Uncharacterized protein	Posttran. modifi., protein turnover, chaperones	-	+	+
A0A023VCR9	Periplasmic trehalase	Carbohydrate transport and metabolism	+	+	+
A0A023VCU3	Uncharacterized protein	Function unknown	+	+	+
A0A023VCZ2	Spermidine dehydrogenase	Sec. metabo. biosynthe., transp. and catabo.	-	+	+
A0A023VD12	Peptide ABC transporter substrate-binding protein	Amino acid transport and metabolism	-	+	+
A0A023VDI9	Lipoprotein	Translation, ribosomal structure and biogenesis	+	+	+
A0A023VDM6	Glucans biosynthesis protein D	Cell wall/membrane/envelope biogenesis	+	+	+
A0A023VDV0	Peptide ABC transporter substrate-binding protein	Amino acid transport and metabolism	+	+	+
A0A023VDX8	Peptide ABC transporter substrate-binding protein	Amino acid transport and metabolism	+	+	+
A0A023VE03	Vancomycin high temperature exclusion protein	Cell wall/membrane/envelope biogenesis	+	+	+
A0A023VE85	Carboxy-terminal protease	Posttran. modifi., protein turnover, chaperones	+	+	+
A0A023VEB4	Nitrate reductase	Energy production and conversion	+	+	+
A0A023VEF0	N-acetylmuramoyl-l-alanine amidase I	Cell wall/membrane/envelope biogenesis	+	+	+
A0A023VEK0	N-acetylmuramoyl-L-alanine amidase amid	Cell wall/membrane/envelope biogenesis	+	+	+
A0A023VEK2	Arginine ABC transporter substrate-binding protein	Amino acid transport and metabolism	+	+	+
A0A023VEM3	Osmoprotectant uptake system substrate	Cell wall/membrane/envelope biogenesis	+	+	+
A0A023VER5	Zinc ABC transporter substrate-binding protein	Inorganic ion transport and metabolism	+	+	+

A0A023VET1	LacI family transcriptional regulator	Carbohydrate transport and metabolism	+	+	+
A0A023VEV9	Anti-sigma E factor	Signal transduction mechanisms	+	+	+
A0A023VEW3	L-arabinose-binding periplasmic protein	Carbohydrate transport and metabolism	+	+	+
A0A023VEZ0	Ecotin	Posttran. modifi., protein turnover, chaperones	+	+	+
A0A023VEZ3	Cystine transporter subunit	Amino acid transport and metabolism	+	+	+
A0A023VF06	Uncharacterized protein	Cell wall/membrane/envelope biogenesis	+	+	+
A0A023VF11	Beta-barrel assembly-enhancing protease	General function prediction only	+	+	+
A0A023VF13	Glycerophosphodiester phosphodiesterase	Lipid transport and metabolism	+	+	+
A0A023VF38	L,D-transpeptidase	Cell wall/membrane/envelope biogenesis	+	+	+
A0A023VF68	Histidine ABC transporter substrate HisJ	Amino acid transport and metabolism	+	+	+
A0A023VFA2	Thiosulfate reductase PhsA	Energy production and conversion	+	+	+
A0A023VFD6	Sugar ABC transporter substrate-binding protein	Carbohydrate transport and metabolism	+	+	+
A0A023VFF9	Acyl-CoA thioesterase	Amino acid transport and metabolism	+	+	+
A0A023VG28	Beta-lactamase	Defense mechanisms	+	+	+
A0A023VGE9	Thiosulfate transporter subunit	Inorganic ion transport and metabolism	+	+	-
A0A023VFF5	zipA	Cell division protein ZipA homolog	+	+	+
A0A023VFN3	ccmE	Cytochrome c-type biogenesis protein CcmE	+	+	+
	Cytoplasmic				
A0A023V248	Thymidylate synthase	Nucleotide transport and metabolism	+	+	+
A0A023V2B2	6-phospho-beta-glucosidase	Carbohydrate transport and metabolism	-	+	+
A0A023V2F0	S-adenosylmethionine synthase	Coenzyme transport and metabolism	+	+	+
A0A023V2H1	Alanine--tRNA ligase	Translation, ribosomal structure and biogenesis	+	+	+
A0A023V2W4	Uncharacterized protein	Inorganic ion transport and metabolism	-	+	+
A0A023V311	Transketolase	Carbohydrate transport and metabolism	+	+	+
A0A023V325	Uronate isomerase	Carbohydrate transport and metabolism	+	+	+
A0A023V369	Uncharacterized protein	Coenzyme transport and metabolism	-	-	+
A0A023V376	5-keto-4-deoxy-D-glucarate aldolase	Carbohydrate transport and metabolism	+	-	+
A0A023V397	Polyribonucleotide nucleotidyltransferase	Translation, ribosomal structure and biogenesis	+	+	+
A0A023V3A1	Transcription termination NusA	Transcription	+	+	+
A0A023V3C3	UDP-N-acetylglucosamine 1-carboxyvinyltransferase	Cell wall/membrane/envelope biogenesis	-	+	+
A0A023V3D9	Aldehyde reductase	Energy production and conversion	+	+	+
A0A023V3E3	Cytosine deaminase	Nucleotide transport and metabolism	-	+	+
A0A023V3E5	L-fucose isomerase	Carbohydrate transport and metabolism	+	+	+
A0A023V3F0	50S ribosomal protein L13	Translation, ribosomal structure and biogenesis	+	+	+
A0A023V3F4	Malate dehydrogenase	Energy production and conversion	+	+	+
A0A023V3H0	Acetyl-CoA carboxylase	Lipid transport and metabolism	+	+	+
A0A023V3I0	4-deoxy-L-threo-5-hexosulose-uronate-isomerase	Carbohydrate transport and metabolism	+	+	+
A0A023V3I5	Xaa-Pro dipeptidase	Amino acid transport and metabolism	+	+	+
A0A023V3I9	3-octaprenyl-4-hydroxybenzoate carboxy-lyase	Coenzyme transport and metabolism	+	+	+
A0A023V3J8	Uridine phosphorylase	Nucleotide transport and metabolism	+	+	+
A0A023V3N2	Cell division protein ZapA	Cell cycle control, cell division, chr. partitioning	+	+	+
A0A023V3N5	Uncharacterized protein	Translation, ribosomal structure and biogenesis	+	+	+
A0A023V3Q9	50S ribosomal protein L17	Translation, ribosomal structure and biogenesis	+	+	+
A0A023V3R0	Serine dehydratase	Amino acid transport and metabolism	-	+	+
A0A023V3R1	Glycine/betaine ABC transporter ATP-binding protein	Inorganic ion transport and metabolism	+	+	+
A0A023V3R2	Ribosomal RNA small subunit methyltransferase E	Translation, ribosomal structure and biogenesis	-	-	+
A0A023V3R7	Glutamate--cysteine ligase	Coenzyme transport and metabolism	+	+	+
A0A023V3R9	50S ribosomal protein L18	Translation, ribosomal structure and biogenesis	+	+	+
A0A023V3S4	50S ribosomal protein L24	Translation, ribosomal structure and biogenesis	-	+	+
A0A023V3S9	30S ribosomal protein S3	Translation, ribosomal structure and biogenesis	-	+	+

A0A023V3T5	50S ribosomal protein L4	Translation, ribosomal structure and biogenesis	+	+	+
A0A023V3V6	Elongation factor Tu	Translation, ribosomal structure and biogenesis	+	+	+
A0A023V3W6	Phosphoglucosamine mutase	Carbohydrate transport and metabolism	+	+	+
A0A023V3X2	Enolase	Carbohydrate transport and metabolism	+	+	+
A0A023V3X9	ABC transporter ATP-binding protein	Cell wall/membrane/envelope biogenesis	+	-	-
A0A023V3Y9	1,2-propanediol oxidoreductase	Energy production and conversion	+	+	+
A0A023V407	Ribulose-phosphate 3-epimerase	Carbohydrate transport and metabolism	+	+	+
A0A023V419	Aldo/keto reductase	General function prediction only	+	+	+
A0A023V421	DNA-binding protein Fis	Transcription	+	+	+
A0A023V422	Phosphoenolpyruvate carboxykinase [ATP]	Energy production and conversion	+	+	+
A0A023V461	DNA-binding protein	Transcription	+	+	+
A0A023V471	Transcriptional repressor MprA	Transcription	-	+	+
A0A023V478	Protein RecA	Replication, recombination and repair	+	+	+
A0A023V485	ATP-dependent RNA helicase RhlB	Replication, recombination and repair	+	+	+
A0A023V487	Glycine dehydrogenase (decarboxylating)	Amino acid transport and metabolism	+	+	+
A0A023V493	Proline aminopeptidase P II	Amino acid transport and metabolism	+	+	+
A0A023V494	Putative reductase CFNIH1_03990	Lipid transport and metabolism	-	+	+
A0A023V498	Ribose-5-phosphate isomerase A	Carbohydrate transport and metabolism	+	+	+
A0A023V4A3	30S ribosomal protein S21	Translation, ribosomal structure and biogenesis	+	+	+
A0A023V4A8	Fructose-bisphosphate aldolase	Carbohydrate transport and metabolism	+	+	+
A0A023V4B8	DNA-directed RNA polymerase subunit alpha	Transcription	+	+	+
A0A023V4D0	50S ribosomal protein L6	Translation, ribosomal structure and biogenesis	+	+	+
A0A023V4D2	50S ribosomal protein L14	Translation, ribosomal structure and biogenesis	+	+	+
A0A023V4D5	LOG family protein	General function prediction only	+	+	+
A0A023V4D6	Oligopeptidase A	Amino acid transport and metabolism	+	+	+
A0A023V4D9	50S ribosomal protein L22	Translation, ribosomal structure and biogenesis	+	+	+
A0A023V4E3	50S ribosomal protein L3	Translation, ribosomal structure and biogenesis	+	+	+
A0A023V4G2	Elongation factor G	Translation, ribosomal structure and biogenesis	+	+	+
A0A023V4G4	Methionine gamma-lyase	Amino acid transport and metabolism	+	+	+
A0A023V4I5	Tartronate semialdehyde reductase	Lipid transport and metabolism	+	+	+
A0A023V4I9	Glycine--tRNA ligase alpha subunit	Translation, ribosomal structure and biogenesis	+	-	+
A0A023V4J4	Crp/Fnr family transcriptional regulator	Signal transduction mechanisms	+	+	+
A0A023V4K2	Lysine--tRNA ligase	Translation, ribosomal structure and biogenesis	+	+	+
A0A023V4K5	Siroheme synthase	Coenzyme transport and metabolism	-	+	+
A0A023V4K8	Translation initiation factor IF-2	Translation, ribosomal structure and biogenesis	+	+	+
A0A023V4M3	Ribosomal RNA large subunit methyltransferase E	Translation, ribosomal structure and biogenesis	-	+	+
A0A023V4N1	Phosphoglycerate kinase	Carbohydrate transport and metabolism	+	+	+
A0A023V4P1	Glutathione S-transferase	Posttran. modifi., protein turnover, chaperones	+	+	+
A0A023V4Q1	Protein-export protein SecB	Intracellular trafficking, secr., vesicular transport	+	+	+
A0A023V4Q4	N-acetylneuraminate lyase	Amino acid transport and metabolism	+	-	-
A0A023V4Q6	30S ribosomal protein S9	Translation, ribosomal structure and biogenesis	+	+	+
A0A023V4R5	3',5'-cyclic adenosine monophosphate phosphodiester.	Signal transduction mechanisms	+	+	+
A0A023V4S4	Uncharacterized protein	Function unknown	+	+	+
A0A023V4S5	Rod shape-determining protein MreB	Cell cycle control, cell division, chr. partitioning	+	+	+
A0A023V4Z6	Transcription termination factor Rho	Transcription	+	+	+
A0A023V529	30S ribosomal protein S13	Translation, ribosomal structure and biogenesis	+	+	+
A0A023V533	30S ribosomal protein S5	Translation, ribosomal structure and biogenesis	+	+	+
A0A023V536	DNA gyrase subunit B	Replication, recombination and repair	+	+	+
A0A023V537	50S ribosomal protein L5	Translation, ribosomal structure and biogenesis	+	+	+

A0A023V542	50S ribosomal protein L16	Translation, ribosomal structure and biogenesis	+	+	+
A0A023V544	Bifunctional protein HldE	Cell wall/membrane/envelope biogenesis	+	+	+
A0A023V546	50S ribosomal protein L23	Translation, ribosomal structure and biogenesis	+	+	+
A0A023V553	Bifunctional protein GlmU	Cell wall/membrane/envelope biogenesis	+	+	+
A0A023V581	50S ribosomal protein L21	Translation, ribosomal structure and biogenesis	+	+	+
A0A023V589	Glycerol dehydrogenase	Energy production and conversion	+	-	+
A0A023V5B4	Uncharacterized protein	Function unknown	+	+	+
A0A023V5D3	Transcription accessory protein	Transcription	-	+	+
A0A023V5E8	Protoporphyrinogen oxidase	Coenzyme transport and metabolism	-	+	+
A0A023V5F1	Glycerol-3-phosphate dehydrogenase	Energy production and conversion	+	+	+
A0A023V5J2	Ribosome-binding factor A	Translation, ribosomal structure and biogenesis	+	+	+
A0A023V5K8	50S ribosomal protein L11	Translation, ribosomal structure and biogenesis	+	+	+
A0A023V5L1	Deoxyribose mutarotase	Carbohydrate transport and metabolism	+	-	+
A0A023V5L3	DNA-directed RNA polymerase subunit beta'	Transcription	+	+	+
A0A023V5L4	Octaprenyl diphosphate synthase	Coenzyme transport and metabolism	+	+	-
A0A023V5N2	Membrane protein	Signal transduction mechanisms	+	+	+
A0A023V5N6	Bifunctional purine biosynthesis protein PurH	Nucleotide transport and metabolism	+	+	+
A0A023V5P0	Stringent starvation protein A	Posttran. modifi., protein turnover, chaperones	+	+	+
A0A023V5P1	30S ribosomal protein S4	Translation, ribosomal structure and biogenesis	+	+	+
A0A023V5P7	50S ribosomal protein L15	Translation, ribosomal structure and biogenesis	+	+	+
A0A023V5Q2	30S ribosomal protein S8	Translation, ribosomal structure and biogenesis	+	+	+
A0A023V5Q3	Protease TldD	General function prediction only	-	+	+
A0A023V5Q7	30S ribosomal protein S17	Translation, ribosomal structure and biogenesis	+	+	+
A0A023V5R7	30S ribosomal protein S10	Translation, ribosomal structure and biogenesis	+	+	+
A0A023V5T2	Ferroxidase	Inorganic ion transport and metabolism	+	+	+
A0A023V5T6	30S ribosomal protein S7	Translation, ribosomal structure and biogenesis	+	+	+
A0A023V5T9	Ubiquinone/menaquinone biosynthesis C-methyltrans.	Coenzyme transport and metabolism	+	+	+
A0A023V5U1	Uncharacterized protein	Transcription	+	+	+
A0A023V5U4	Glyoxylate/hydroxypyruvate reductase B	Energy production and conversion	+	-	+
A0A023V5X7	Cell division protein DamX	Cell cycle control, cell division, chr. partitioning	-	+	+
A0A023V5Z2	Osmolarity response regulator	Signal transduction mechanisms	+	+	+
A0A023V5Z7	Mannitol-1-phosphate 5-dehydrogenase	Carbohydrate transport and metabolism	+	+	+
A0A023V600	ATP-dependent protease ATPase subunit HslU	Posttran. modifi., protein turnover, chaperones	+	+	+
A0A023V607	30S ribosomal protein S11	Translation, ribosomal structure and biogenesis	+	+	+
A0A023V609	ADP-L-glycero-D-manno-heptose-6-epimerase	Cell wall/membrane/envelope biogenesis	+	+	+
A0A023V610	Aspartate kinase	Amino acid transport and metabolism	+	+	-
A0A023V611	50S ribosomal protein L30	Translation, ribosomal structure and biogenesis	-	+	+
A0A023V613	Glucose-1-phosphate adenylyltransferase	Carbohydrate transport and metabolism	+	-	+
A0A023V625	50S ribosomal protein L2	Translation, ribosomal structure and biogenesis	+	+	+
A0A023V626	Argininosuccinate lyase	Amino acid transport and metabolism	+	+	+
A0A023V647	50S ribosomal protein L1	Translation, ribosomal structure and biogenesis	+	+	+
A0A023V663	Uncharacterized protein	Not in COG genes	+	+	-
A0A023V686	30S ribosomal protein S6	Translation, ribosomal structure and biogenesis	+	+	+
A0A023V695	Tryptophan--tRNA ligase	Translation, ribosomal structure and biogenesis	+	+	+
A0A023V697	Universal stress protein	Signal transduction mechanisms	+	+	+
A0A023V6A3	Glutathione reductase	Energy production and conversion	+	+	+
A0A023V6B2	Glucose-6-phosphate isomerase	Carbohydrate transport and metabolism	+	+	+
A0A023V6F1	Probable cytosol aminopeptidase	Amino acid transport and metabolism	+	+	+
A0A023V6F7	Glutamine--fructose-6-phosphate aminotransferase	Cell wall/membrane/envelope biogenesis	+	+	+
A0A023V6G1	ATP synthase subunit alpha	Energy production and conversion	+	+	+

A0A023V6H2	Cell division protein FtsE	Cell cycle control, cell division, chr. partitioning	+	+	+
A0A023V6I9	GTP-binding protein TypA	Signal transduction mechanisms	+	+	+
A0A023V6L3	Uncharacterized protein	Inorganic ion transport and metabolism	+	+	+
A0A023V6L7	L-threonine 3-dehydrogenase	Amino acid transport and metabolism	+	+	+
A0A023V6M5	Dihydrodipicolinate synthase	Amino acid transport and metabolism	+	+	+
A0A023V6N4	Fumarate hydratase	Energy production and conversion	+	+	+
A0A023V6N6	Thymidine phosphorylase	Nucleotide transport and metabolism	+	+	+
A0A023V6R6	Transaldolase	Carbohydrate transport and metabolism	+	+	+
A0A023V6R7	Adenylosuccinate synthetase	Nucleotide transport and metabolism	+	+	+
A0A023V6S5	Fructose-6-phosphate aldolase	Carbohydrate transport and metabolism	+	+	+
A0A023V6S7	30S ribosomal protein S20	Translation, ribosomal structure and biogenesis	+	+	+
A0A023V6T8	Peptidyl-prolyl cis-trans isomerase	Posttran. modifi., protein turnover, chaperones	+	+	+
A0A023V6U5	Transcription termination NusG	Transcription	+	+	+
A0A023V6V0	DNA-directed RNA polymerase subunit beta	Transcription	+	+	+
A0A023V6V7	Ribosomal RNA small subunit methyltransferase A	Translation, ribosomal structure and biogenesis	+	+	+
A0A023V6W8	DNA-binding protein	Replication, recombination and repair	+	+	+
A0A023V6Y1	Trehalose-6-phosphate hydrolase	Carbohydrate transport and metabolism	+	+	+
A0A023V6Y8	Serine acetyltransferase	Amino acid transport and metabolism	+	+	+
A0A023V6Z1	Phosphoglycerate mutase	Carbohydrate transport and metabolism	+	+	+
A0A023V6Z3	Arginine deiminase	Amino acid transport and metabolism	+	+	+
A0A023V6Z6	2-amino-3-ketobutyrate coenzyme A ligase	Coenzyme transport and metabolism	+	+	+
A0A023V704	Cell division protein ftsA	Cell cycle control, cell division, chr. partitioning	-	+	+
A0A023V706	50S ribosomal protein L28	Translation, ribosomal structure and biogenesis	+	+	+
A0A023V709	DNA polymerase III subunit beta	Replication, recombination and repair	+	+	+
A0A023V710	Orotate phosphoribosyltransferase	Nucleotide transport and metabolism	-	+	+
A0A023V727	Pyruvate dehydrogenase E1 component	Energy production and conversion	+	+	+
A0A023V730	ATP synthase subunit beta	Energy production and conversion	+	+	+
A0A023V750	Single-stranded DNA-binding protein	Replication, recombination and repair	+	+	+
A0A023V758	Dihydrofolate reductase	Coenzyme transport and metabolism	+	+	+
A0A023V762	Penicillin-binding protein 1B	Cell wall/membrane/envelope biogenesis	+	+	+
A0A023V768	Glutamate-1-semialdehyde 2,1-aminomutase	Coenzyme transport and metabolism	+	+	+
A0A023V773	5'-methylthioadenosine nucleosidase	Nucleotide transport and metabolism	+	+	+
A0A023V781	Succinyltransferase	Amino acid transport and metabolism	+	+	+
A0A023V787	Uridylate kinase	Nucleotide transport and metabolism	+	+	+
A0A023V799	Phosphopentomutase	Carbohydrate transport and metabolism	+	+	+
A0A023V7A2	Lysine decarboxylase LdcC	Amino acid transport and metabolism	+	-	+
A0A023V7A4	Superoxide dismutase	Inorganic ion transport and metabolism	+	+	+
A0A023V7B0	ATP-dependent 6-phosphofructokinase	Carbohydrate transport and metabolism	+	+	+
A0A023V7B6	Triosephosphate isomerase	Carbohydrate transport and metabolism	+	+	+
A0A023V7B7	Small heat shock protein IbpA	Posttran. modifi., protein turnover, chaperones	+	+	+
A0A023V7B9	Molybdenum cofactor biosynthesis protein MogA	Coenzyme transport and metabolism	+	+	+
A0A023V7C1	Glycerol kinase	Energy production and conversion	+	+	+
A0A023V7C4	Chaperone protein DnaK	Posttran. modifi., protein turnover, chaperones	+	+	+
A0A023V7D2	ATP-dependent protease subunit HslV	Posttran. modifi., protein turnover, chaperones	+	+	+
A0A023V7E0	Aspartate ammonia-lyase	Amino acid transport and metabolism	+	+	+
A0A023V7E2	ATP synthase gamma chain	Energy production and conversion	+	+	-
A0A023V7F2	Catalase-peroxidase	Inorganic ion transport and metabolism	+	+	+
A0A023V7F7	Phosphoenolpyruvate carboxylase	Energy production and conversion	+	+	+
A0A023V7G7	Probable GTP-binding protein EngB	Cell cycle control, cell division, chr. partitioning	+	+	+
A0A023V7H2	Glutamine synthetase	Amino acid transport and metabolism	+	+	+
A0A023V7H6	50S ribosomal protein L10	Translation, ribosomal structure and biogenesis	+	+	+

A0A023V7J4	UDP-diaminopimelate ligase	Cell wall/membrane/envelope biogenesis	-	+	+
A0A023V7K6	Cell division protein FtsZ	Cell cycle control, cell division, chr. partitioning	+	+	+
A0A023V7N2	Acetyltransferase component of pyruvate dehydrogen.	Energy production and conversion	+	+	+
A0A023V7N5	Aspartate carbamoyltransferase regulatory chain	Nucleotide transport and metabolism	+	+	+
A0A023V7P0	Ornithine carbamoyltransferase	Amino acid transport and metabolism	+	+	+
A0A023V7P3	Cell division protein FtsN	Cell cycle control, cell division, chr. partitioning	+	+	+
A0A023V7S2	Soluble pyridine nucleotide transhydrogenase	Energy production and conversion	+	+	+
A0A023V7T0	Uncharacterized protein	Energy production and conversion	+	+	+
A0A023V7U0	50S ribosomal protein L7/L12	Translation, ribosomal structure and biogenesis	+	+	+
A0A023V7U5	Ribosome-recycling factor	Translation, ribosomal structure and biogenesis	-	+	+
A0A023V7X8	Deoxyribose-phosphate aldolase	Nucleotide transport and metabolism	+	+	+
A0A023V814	4-hydroxy-tetrahydrodipicolinate reductase	Amino acid transport and metabolism	+	+	+
A0A023V820	DNA helicase	Replication, recombination and repair	+	+	+
A0A023V821	10 kDa chaperonin	Posttran. modifi., protein turnover, chaperones	+	+	+
A0A023V824	Elongation factor P	Translation, ribosomal structure and biogenesis	+	+	+
A0A023V830	Succinate dehydrogenase iron-sulfur subunit	Energy production and conversion	+	+	+
A0A023V834	Phosphatidylserine decarboxylase proenzyme	Lipid transport and metabolism	-	+	+
A0A023V841	GTPase HflX	Translation, ribosomal structure and biogenesis	-	+	+
A0A023V855	Trigger factor	Posttran. modifi., protein turnover, chaperones	+	+	+
A0A023V860	Peptidylprolyl isomerase	Posttran. modifi., protein turnover, chaperones	+	+	+
A0A023V862	30S ribosomal protein S18	Translation, ribosomal structure and biogenesis	+	+	+
A0A023V880	Cell division protein FtsQ	Cell cycle control, cell division, chr. partitioning	+	+	+
A0A023V885	Peptidase PmbA	General function prediction only	+	+	+
A0A023V892	GMP reductase	Nucleotide transport and metabolism	+	+	+
A0A023V8C1	Uncharacterized protein	Posttran. modifi., protein turnover, chaperones	+	+	+
A0A023V8D4	60 kDa chaperonin	Posttran. modifi., protein turnover, chaperones	+	+	+
A0A023V8E4	Fumarate reductase flavoprotein subunit	Energy production and conversion	+	+	+
A0A023V8F7	Beta-galactosidase	Carbohydrate transport and metabolism	+	+	+
A0A023V8G0	Ribonuclease R	Transcription	+	+	+
A0A023V8G4	Uncharacterized protein	Energy production and conversion	+	+	+
A0A023V8G5	UPF0325 protein CFNIH1_10505	Cell wall/membrane/envelope biogenesis	+	+	+
A0A023V8H3	Elongation factor Ts	Translation, ribosomal structure and biogenesis	+	+	+
A0A023V8H5	50S ribosomal protein L9	Translation, ribosomal structure and biogenesis	+	+	+
A0A023V8I6	3-hydroxyacyl-[acyl-carrier-protein] dehydratase Fab	Lipid transport and metabolism	+	+	+
A0A023V8I8	Inorganic pyrophosphatase	Energy production and conversion	+	+	+
A0A023V8J2	Acetyl-coenzyme A carboxylase carboxyl transferase	Lipid transport and metabolism	+	+	+
A0A023V8J4	D-alanine--D-alanine ligase	Cell wall/membrane/envelope biogenesis	+	+	+
A0A023V8M7	Purine nucleoside phosphorylase DeoD-type	Nucleotide transport and metabolism	+	+	+
A0A023V8M9	Riboflavin biosynthesis protein RibD	Coenzyme transport and metabolism	+	+	-
A0A023V8N8	Valine--tRNA ligase	Translation, ribosomal structure and biogenesis	+	+	+
A0A023V8N9	Probable phosphoglycerate mutase GpmB	Carbohydrate transport and metabolism	+	+	+
A0A023V8P2	Uncharacterized protein	Replication, recombination and repair	+	+	+
A0A023V8Q4	Phosphoheptose isomerase	Carbohydrate transport and metabolism	+	+	+
A0A023V8Q8	Chaperone protein DnaJ	Posttran. modifi., protein turnover, chaperones	+	+	+
A0A023V8R2	Isoleucine--tRNA ligase	Translation, ribosomal structure and biogenesis	+	+	+
A0A023V8R3	Tyrosine phenol-lyase	Amino acid transport and metabolism	+	+	+
A0A023V8R6	Amino acid dehydrogenase	Energy production and conversion	+	+	+
A0A023V8R7	Citrate lyase subunit alpha	Energy production and conversion	+	+	+
A0A023V8V2	UPF0255 protein frsA	Signal transduction mechanisms	-	+	+
A0A023V8W8	Transcriptional regulator MraZ	Translation, ribosomal structure and biogenesis	+	+	+

A0A023V8X8	Nucleoside triphosphate hydrolase	Signal transduction mechanisms	+	-	+
A0A023V8Y4	ABC transporter ATP-binding protein	General function prediction only	+	+	+
A0A023V8Y7	Cell division protein ZapD	Cell cycle control, cell division, chr. partitioning	+	+	+
A0A023V8Z0	Cysteine--tRNA ligase	Translation, ribosomal structure and biogenesis	+	+	+
A0A023V8Z3	TorR family transcriptional regulator	Signal transduction mechanisms	+	+	+
A0A023V904	Dihydrolipoyl dehydrogenase	Energy production and conversion	+	+	+
A0A023V906	Negative modulator of initiation of replication	Replication, recombination and repair	+	+	+
A0A023V927	Succinate dehydrogenase flavoprotein subunit	Energy production and conversion	+	+	+
A0A023V928	3-methyl-2-oxobutanoate hydroxymethyltransferase	Coenzyme transport and metabolism	-	-	+
A0A023V930	Succinyl-CoA ligase [ADP-forming] subunit alpha	Energy production and conversion	+	+	+
A0A023V956	Transcriptional regulator	Transcription	-	+	+
A0A023V9B0	Peroxiredoxin	Defense mechanisms	+	+	+
A0A023V9E2	Pyruvate formate-lyase	Energy production and conversion	+	+	+
A0A023V9E3	Transcriptional regulator HU subunit alpha	Replication, recombination and repair	+	+	-
A0A023V9E6	tRNA-dimethylallyladenosine synthase	Translation, ribosomal structure and biogenesis	+	+	+
A0A023V9F9	30S ribosomal protein S2	Translation, ribosomal structure and biogenesis	+	+	+
A0A023V9G0	N-acetylglucosamine-6-phosphate deacetylase	Carbohydrate transport and metabolism	+	+	+
A0A023V9G8	Ferric uptake regulator	Inorganic ion transport and metabolism	+	+	+
A0A023V9H2	Phosphoglucomutase	Carbohydrate transport and metabolism	+	+	+
A0A023V9H6	Aminoacyl-histidine dipeptidase	Amino acid transport and metabolism	+	+	+
A0A023V9H8	Asparagine--tRNA ligase	Translation, ribosomal structure and biogenesis	+	+	+
A0A023V9H9	Glutamate 5-kinase	Amino acid transport and metabolism	+	+	+
A0A023V9J0	Succinate dehydrogenase iron-sulfur subunit	Energy production and conversion	+	+	+
A0A023V9J9	Proline--tRNA ligase	Translation, ribosomal structure and biogenesis	+	+	+
A0A023V9L2	Ribosomal RNA large subunit methyltransferase I	Translation, ribosomal structure and biogenesis	+	+	+
A0A023V9L7	Galactokinase	Carbohydrate transport and metabolism	+	+	+
A0A023V9L9	Uncharacterized protein	Mobilome: prophages, transposons	+	+	+
A0A023V9N0	Urocanate hydratase	Amino acid transport and metabolism	+	+	+
A0A023V9Q7	Peptidase T	Amino acid transport and metabolism	+	+	+
A0A023V9R4	ABC transporter ATP-binding protein	General function prediction only	-	+	+
A0A023V9V5	Nicotinamidase	Coenzyme transport and metabolism	+	+	+
A0A023V9W7	Pyrroline-5-carboxylate reductase	Amino acid transport and metabolism	+	+	+
A0A023V9Y0	Cytidylate kinase	Nucleotide transport and metabolism	+	+	+
A0A023V9Z2	Queuine tRNA-ribosyltransferase	Translation, ribosomal structure and biogenesis	-	+	+
A0A023VA33	ATP-dependent Clp protease ATP-binding ClpX	Posttran. modifi., protein turnover, chaperones	+	+	+
A0A023VA47	Acyl-CoA thioesterase	Lipid transport and metabolism	+	+	+
A0A023VA64	UMP phosphatase	Nucleotide transport and metabolism	+	+	+
A0A023VA66	NAD(P)H dehydrogenase (quinone)	Energy production and conversion	+	+	+
A0A023VA70	Chaperone protein HtpG	Posttran. modifi., protein turnover, chaperones	+	+	+
A0A023VA72	Glutamine--tRNA ligase	Translation, ribosomal structure and biogenesis	+	+	+
A0A023VA74	Delta-aminolevulinic acid dehydratase	Coenzyme transport and metabolism	+	+	+
A0A023VA94	Recombination-associated protein RdgC	Replication, recombination and repair	-	+	+
A0A023VAA0	Succinyl-CoA ligase [ADP-forming] subunit beta	Energy production and conversion	+	+	+
A0A023VAB3	Preprotein translocase subunit YajC	Intracellular trafficking, secr., vesicular transport	+	+	+
A0A023VAB8	Phosphoglycerate mutase	Carbohydrate transport and metabolism	+	+	+
A0A023VAE3	Ribonuclease E	Translation, ribosomal structure and biogenesis	+	+	+
A0A023VAF6	3-oxoacyl-[acyl-carrier-protein] synthase 2	Lipid transport and metabolism	+	+	+
A0A023VAG2	DNA protection during starvation protein	Inorganic ion transport and metabolism	+	+	+
A0A023VAJ3	Adenylate kinase	Nucleotide transport and metabolism	+	+	+
A0A023VAJ7	Alkyl hydroperoxide reductase	Defense mechanisms	+	+	+

A0A023VAL3	Leucine-responsive transcriptional regulator	Transcription	+	+	+
A0A023VAL4	Translation initiation factor IF-3	Translation, ribosomal structure and biogenesis	+	+	+
A0A023VAL6	Universal stress protein UspG	Signal transduction mechanisms	+	+	+
A0A023VAL7	Integration host factor subunit alpha	Replication, recombination and repair	+	+	+
A0A023VAM7	Phosphoserine aminotransferase	Coenzyme transport and metabolism	+	+	+
A0A023VAN8	3-deoxy-manno-octulosonate cytidylyltransferase	Cell wall/membrane/envelope biogenesis	+	+	+
A0A023VAP6	Aromatic amino acid aminotransferase	Amino acid transport and metabolism	+	+	+
A0A023VAQ8	Pyrimidine-specific ribonucleoside hydrolase RihA	Nucleotide transport and metabolism	+	+	+
A0A023VAU0	Glucosamine-6-phosphate deaminase	Carbohydrate transport and metabolism	+	+	+
A0A023VAU1	Superoxide dismutase	Inorganic ion transport and metabolism	+	+	+
A0A023VAW1	Citrate synthase	Energy production and conversion	+	+	+
A0A023VAW4	Alkyl hydroperoxide reductase	Defense mechanisms	+	+	+
A0A023VAX7	Oxidoreductase	Energy production and conversion	+	+	+
A0A023VAZ0	Galactose-1-phosphate uridylyltransferase	Carbohydrate transport and metabolism	+	-	-
A0A023VB12	Molybdenum cofactor biosynthesis protein B	Coenzyme transport and metabolism	+	+	+
A0A023VB41	Uncharacterized protein	Carbohydrate transport and metabolism	+	+	+
A0A023VB54	3-ketoacyl-ACP reductase	Lipid transport and metabolism	+	+	+
A0A023VB59	Phosphoenolpyruvate synthase	Carbohydrate transport and metabolism	+	+	+
A0A023VB85	Putative GTP cyclohydrolase 1 type 2	Coenzyme transport and metabolism	+	+	+
A0A023VB93	Uncharacterized protein	Coenzyme transport and metabolism	+	+	+
A0A023VB97	2-oxoglutarate dehydrogenase complex	Energy production and conversion	+	+	+
A0A023VB98	Uncharacterized protein	Translation, ribosomal structure and biogenesis	+	+	+
A0A023VBA3	30S ribosomal protein S1	Translation, ribosomal structure and biogenesis	-	+	+
A0A023VBA9	Phenylacetaldehyde dehydrogenase	Energy production and conversion	+	+	+
A0A023VBB2	4-aminobutyrate aminotransferase	Amino acid transport and metabolism	+	+	+
A0A023VBC7	High frequency lysogenization protein HflD homolog	Mobilome: prophages, transposons	+	+	+
A0A023VBD4	Aminopeptidase N	Amino acid transport and metabolism	+	+	+
A0A023VBF0	3-hydroxydecanoyl-[acyl-carrier-protein] dehydratase	Lipid transport and metabolism	+	+	+
A0A023VBI5	Glyceraldehyde-3-phosphate dehydrogenase	Carbohydrate transport and metabolism	+	+	+
A0A023VBL3	Serine--tRNA ligase	Translation, ribosomal structure and biogenesis	+	+	+
A0A023VBL4	DeoR faimly transcriptional regulator	Transcription	+	-	+
A0A023VBM2	Glutamate dehydrogenase	Amino acid transport and metabolism	+	+	+
A0A023VBP8	UPF0502 protein CFNIH1_15335	Function unknown	+	+	+
A0A023VBR5	Dihydroorotate dehydrogenase (quinone)	Nucleotide transport and metabolism	+	-	+
A0A023VBS5	3-oxoacyl-[acyl-carrier-protein] synthase 3	Lipid transport and metabolism	+	+	+
A0A023VBT0	Threonine--tRNA ligase	Translation, ribosomal structure and biogenesis	+	+	+
A0A023VBT4	Phenylalanine--tRNA ligase beta subunit	Translation, ribosomal structure and biogenesis	+	+	+
A0A023VBV5	Enoyl-[acyl-carrier-protein] reductase [NADH]	Lipid transport and metabolism	+	+	+
A0A023VBX2	Gamma-aminobutyraldehyde dehydrogenase	Energy production and conversion	-	-	+
A0A023VC14	Riboflavin synthase subunit alpha	Coenzyme transport and metabolism	+	+	+
A0A023VC16	Dihydroorotase	Nucleotide transport and metabolism	+	-	+
A0A023VC23	Lactoylglutathione lyase	Sec. metabo. biosynthe., transp. and catabo.	+	+	+
A0A023VC46	Malonyl CoA-acyl carrier protein transacylase	Lipid transport and metabolism	+	+	-
A0A023VC47	Nitrate reductase	Energy production and conversion	+	-	+
A0A023VC57	X-Pro aminopeptidase	Amino acid transport and metabolism	-	+	+
A0A023VC58	Fumarate hydratase	Energy production and conversion	-	+	+
A0A023VC74	Peptidase M32	Amino acid transport and metabolism	+	+	+
A0A023VC77	NADH dehydrogenase	Energy production and conversion	+	+	+
A0A023VC94	Malonic semialdehyde reductase	Energy production and conversion	+	+	+
A0A023VCA6	Adenylosuccinate lyase	Nucleotide transport and metabolism	-	+	+
A0A023VCB2	Isocitrate dehydrogenase [NADP]	Energy production and conversion	+	+	+

A0A023VCB3	Serine dehydratase	Amino acid transport and metabolism	+	+	+
A0A023VCG5	50S ribosomal protein L20	Translation, ribosomal structure and biogenesis	+	+	+
A0A023VCK1	Pyruvate kinase	Carbohydrate transport and metabolism	-	+	+
A0A023VCL3	Pyruvate kinase	Carbohydrate transport and metabolism	+	+	+
A0A023VCL6	DNA-binding protein	Transcription	+	+	+
A0A023VCP3	Ribose-phosphate pyrophosphokinase	Nucleotide transport and metabolism	+	+	+
A0A023VCQ3	Glutaredoxin	Posttran. modifi., protein turnover, chaperones	+	+	+
A0A023VCR2	Transcriptional regulator SlyA	Transcription	+	+	-
A0A023VCR8	Tyrosine--tRNA ligase	Translation, ribosomal structure and biogenesis	+	+	+
A0A023VCS6	Ferritin	Inorganic ion transport and metabolism	+	+	+
A0A023VCT5	Phenylalanine--tRNA ligase alpha subunit	Translation, ribosomal structure and biogenesis	+	+	+
A0A023VCU1	Site-determining protein	Cell cycle control, cell division, chr. partitioning	+	+	+
A0A023VCW5	Uncharacterized protein	Not in COG genes	-	+	+
A0A023VD11	Cobalt-precorrin-3B C(17)-methyltransferase	Coenzyme transport and metabolism	+	+	+
A0A023VD31	Propanediol dehydratase	Sec. metabo. biosynthe., transp. and catabo.	-	-	+
A0A023VD33	Pyridoxamine kinase	Coenzyme transport and metabolism	+	-	+
A0A023VD54	Aspartyl-tRNA synthetase	Translation, ribosomal structure and biogenesis	+	+	+
A0A023VD93	Bifunctional D-altronate/D-mannonate dehydratase	Cell wall/membrane/envelope biogenesis	+	+	+
A0A023VD94	Aldehyde-alcohol dehydrogenase	Energy production and conversion	+	+	+
A0A023VDA0	Nitrate reductase	Energy production and conversion	+	+	+
A0A023VDA7	6-phosphogluconate dehydrogenase, decarboxylating	Carbohydrate transport and metabolism	+	+	+
A0A023VDC3	Diaminobutyrate--2-oxoglutarate aminotransferase	Amino acid transport and metabolism	-	+	+
A0A023VDF2	NAD-dependent malic enzyme	Energy production and conversion	+	+	+
A0A023VDH0	Methionine--tRNA ligase	Translation, ribosomal structure and biogenesis	+	+	+
A0A023VDH8	Beta-D-glucoside glucohydrolase	Carbohydrate transport and metabolism	+	+	+
A0A023VDJ2	Transcriptional regulator	Transcription	+	+	+
A0A023VDJ5	Precorrin-8X methylmutase	Coenzyme transport and metabolism	+	+	+
A0A023VDJ8	GTP cyclohydrolase 1	Coenzyme transport and metabolism	+	+	+
A0A023VDP0	Histidine biosynthesis bifunctional protein HisB	Amino acid transport and metabolism	+	+	+
A0A023VDQ6	Universal stress protein F	Signal transduction mechanisms	+	+	+
A0A023VDS0	Probable transcriptional regulatory protein	Transcription	+	+	+
A0A023VDT2	Arginine-tRNA ligase	Translation, ribosomal structure and biogenesis	+	-	+
A0A023VDX0	Ribonucleotide-diphosphate reductase subunit beta	Nucleotide transport and metabolism	+	+	+
A0A023VDY2	UTP--glucose-1-phosphate uridylyltransferase	Cell wall/membrane/envelope biogenesis	+	+	+
A0A023VE02	Peptide chain release factor 1	Translation, ribosomal structure and biogenesis	+	-	+
A0A023VE10	Peptidyl-tRNA hydrolase	Translation, ribosomal structure and biogenesis	+	+	+
A0A023VE23	Aconitate hydratase	Energy production and conversion	+	+	+
A0A023VE26	Bifunctional PTS system fructose-specific transporter	Signal transduction mechanisms	+	+	+
A0A023VE49	Protein MtfA	Signal transduction mechanisms	+	+	+
A0A023VE81	Uncharacterized protein	Function unknown	+	+	+
A0A023VE90	Propanediol dehydratase	Sec. metabo. biosynthe., transp. and catabo.	+	+	+
A0A023VEA3	Aldehyde dehydrogenase	Energy production and conversion	-	+	+
A0A023VEA5	Transcriptional regulator NarL	Signal transduction mechanisms	+	+	+
A0A023VEB3	2-dehydro-3-deoxyphosphooctonate aldolase	Cell wall/membrane/envelope biogenesis	+	+	+
A0A023VEC6	Ribosome-binding ATPase YchF	Translation, ribosomal structure and biogenesis	+	+	+
A0A023VEE0	Glycerol-3-phosphate dehydrogenase	Energy production and conversion	+	+	+
A0A023VEE1	Dihydroxyacetone kinase	Carbohydrate transport and metabolism	+	+	+
A0A023VEH1	PTS mannose transporter subunit IIAB	Carbohydrate transport and metabolism	+	+	+
A0A023VEH4	NADH-quinone oxidoreductase subunit C/D	Energy production and conversion	+	+	+
A0A023VEI5	RNA chaperone ProQ	Signal transduction mechanisms	+	+	+
A0A023VEI7	Acetate kinase	Energy production and conversion	+	+	+

A0A023VEK7	Fructose-bisphosphate aldolase	Carbohydrate transport and metabolism	+	+	+
A0A023VEL0	Acetyl-coenzyme A carboxylase carboxyl transferase	Lipid transport and metabolism	+	+	+
A0A023VEL2	Uracil phosphoribosyltransferase	Nucleotide transport and metabolism	+	+	+
A0A023VEL7	Antiporter	Cell cycle control, cell division, chr. partitioning	+	-	-
A0A023VEM7	GMP synthase [glutamine-hydrolyzing]	Nucleotide transport and metabolism	-	+	+
A0A023VEN8	Dihydropyrimidine dehydrogenase	Nucleotide transport and metabolism	+	+	+
A0A023VEN9	Cytoskeleton protein RodZ	Cell cycle control, cell division, chr. partitioning	+	+	+
A0A023VEP5	Sulfurtransferase	Inorganic ion transport and metabolism	-	+	-
A0A023VER1	Glucose-6-phosphate 1-dehydrogenase	Carbohydrate transport and metabolism	+	+	+
A0A023VER7	Glutamate--tRNA ligase	Translation, ribosomal structure and biogenesis	+	+	+
A0A023VES9	Cysteine synthase	Amino acid transport and metabolism	+	+	+
A0A023VEU6	Nitrogen regulatory protein P-II 1	Signal transduction mechanisms	+	+	+
A0A023VEV1	Cobalt-precorrin-2 C(20)-methyltransferase	Coenzyme transport and metabolism	+	+	+
A0A023VEV4	Peroxidase	Inorganic ion transport and metabolism	+	+	+
A0A023VEV8	Cobalt-precorrin-4 C(11)-methyltransferase	Coenzyme transport and metabolism	+	+	+
A0A023VEW5	Methyltransferase	Translation, ribosomal structure and biogenesis	+	+	+
A0A023VEW9	Propanediol utilization protein	Amino acid transport and metabolism	+	-	+
A0A023VEX0	Uncharacterized protein	Carbohydrate transport and metabolism	+	+	+
A0A023VEZ1	UPF0265 protein CFNIH1_21290	Function unknown	+	+	+
A0A023VF01	Transcriptional regulatory protein RcsB	Signal transduction mechanisms	+	+	+
A0A023VF05	Thiol peroxidase	Posttran. modifi., protein turnover, chaperones	+	-	+
A0A023VF09	Ribonucleoside-diphosphate reductase	Nucleotide transport and metabolism	+	+	+
A0A023VF26	Inosine-5'-monophosphate dehydrogenase	Nucleotide transport and metabolism	+	+	+
A0A023VF41	NADH dehydrogenase	Energy production and conversion	+	+	+
A0A023VF51	UPF0304 protein CFNIH1_23015	Function unknown	+	+	+
A0A023VF65	Propanediol dehydratase	Sec. metabo. biosynthe., transp. and catabo.	+	+	+
A0A023VF71	Restriction endonuclease	Not in COG genes	+	+	+
A0A023VF72	Cell division protein DedD	Cell cycle control, cell division, chr. partitioning	+	+	-
A0A023VF79	Semialdehyde dehydrogenase	Amino acid transport and metabolism	+	+	+
A0A023VF86	3-oxoacyl-ACP synthase	Lipid transport and metabolism	+	+	+
A0A023VF95	Ribonuclease 3	Transcription	+	+	+
A0A023VFB4	Uncharacterized protein	Function unknown	+	+	+
A0A023VFC2	Protein GrpE	Posttran. modifi., protein turnover, chaperones	+	+	+
A0A023VFG2	PTS system glucose-specific transporter subunit IIA	Carbohydrate transport and metabolism	+	+	+
A0A023VFH5	Short-chain dehydrogenase	Lipid transport and metabolism	+	+	+
A0A023VFI8	Acetyltransferase CFNIH1_23620	Translation, ribosomal structure and biogenesis	-	+	+
A0A023VFL3	Malic enzyme	Energy production and conversion	+	+	+
A0A023VFM9	4-hydroxy-tetrahydrodipicolinate synthase	Amino acid transport and metabolism	+	+	+
A0A023VFN2	Dihydropyrimidine dehydrogenase	Amino acid transport and metabolism	+	+	+
A0A023VFR1	DNA gyrase subunit A	Replication, recombination and repair	+	+	+
A0A023VFR4	flavodoxin	Lipid transport and metabolism	+	+	+
A0A023VFR6	Nucleoid-associated protein CFNIH1_22255	Function unknown	+	+	+
A0A023VFT4	1,4-dihydroxy-2-naphthoyl-CoA synthase	Coenzyme transport and metabolism	+	+	+
A0A023VFU6	Cysteine desulfurase IscS	Amino acid transport and metabolism	+	+	+
A0A023VFV3	NADH-quinone oxidoreductase subunit B	Energy production and conversion	+	+	+
A0A023VFV6	Ribulokinase	Carbohydrate transport and metabolism	+	+	+
A0A023VFW4	Phosphate acetyltransferase	Energy production and conversion	+	+	+
A0A023VFZ7	Ubiquinone biosynthesis O-methyltransferase	Coenzyme transport and metabolism	+	+	+
A0A023VG00	50S ribosomal protein L19	Translation, ribosomal structure and biogenesis	+	+	+
A0A023VG33	Glucokinase	Carbohydrate transport and metabolism	+	+	+
A0A023VG37	NADH dehydrogenase	Energy production and conversion	+	+	+

A0A023VG74	Aminoglycoside adenylyltransferase	General function prediction only	+	+	+
A0A023VGB2	Phosphoribosylaminoimidazole-synthase	Nucleotide transport and metabolism	+	+	+
A0A023VGD7	Phosphoenolpyruvate-protein phosphotransferase	Carbohydrate transport and metabolism	+	+	+
A0A023VGE8	Membrane protein	Signal transduction mechanisms	+	+	+
A0A023VGF3	Nucleoside diphosphate kinase	Nucleotide transport and metabolism	+	+	+
A0A023VGG8	Peptidase B	Amino acid transport and metabolism	+	+	+
A0A023VGJ9	Membrane protein	Cell motility	+	+	+
A0A023VGM3	Chaperone protein ClpB	Posttran. modifi., protein turnover, chaperones	+	+	+
A0A023VGN0	Histidine--tRNA ligase	Translation, ribosomal structure and biogenesis	+	+	+
A0A023VGN1	30S ribosomal protein S16	Translation, ribosomal structure and biogenesis	+	+	+
A0A023VGT7	Serine hydroxymethyltransferase	Amino acid transport and metabolism	+	+	+
A0A023VGU8	Pyridoxine 5'-phosphate synthase	Coenzyme transport and metabolism	+	+	+
A0A023VGV2	Dihydropteroate synthase	Coenzyme transport and metabolism	+	+	+
A0A023VGV9	Autonomous glycyl radical cofactor	Coenzyme transport and metabolism	+	+	+
A0A023VGX8	StdB protein	Cell motility	+	+	+
A0A023VGX9	Signal recognition particle protein	Intracellular trafficking, secr., vesicular transport	+	+	+
		Secreted			
A0A023V5C2	Penicillin-binding protein 1A	Cell wall/membrane/envelope biogenesis			
A0A023V8E2	Beta-lactamase	Defense mechanisms			
A0A023V8G6	Type-1 fimbrial protein subunit A	Cell motility			

***** COG functional class

Appendix C - Map of *mcr-1*-encoding IncX4 plasmids

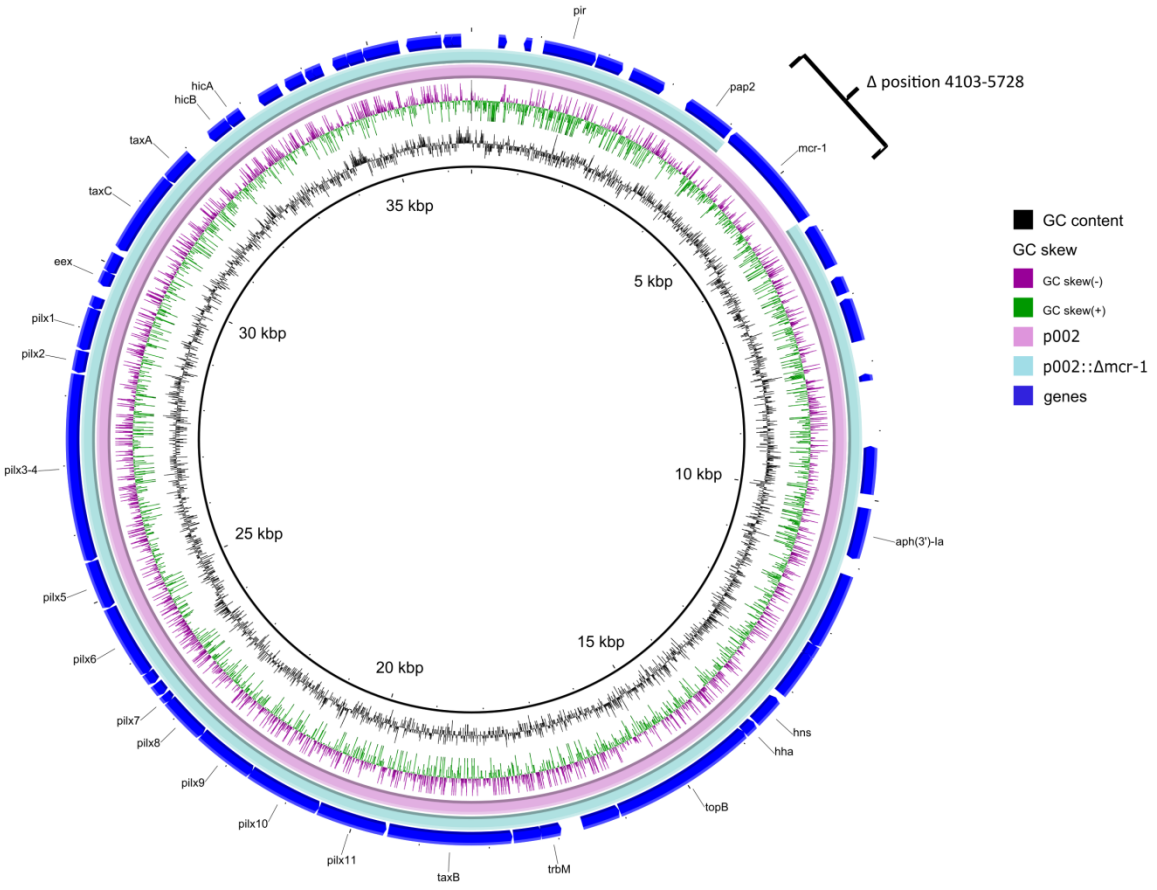

Figure A-0.1 **Map of *mcr-1*-encoding IncX4 plasmids used in the study.** p002 and p002::Δ*mcr-1* have identical sequences apart from the absence of the *mcr-1* gene in the latter plasmid (marked with the bracket)